Enhancements to Generic Disposal System Modeling Capabilities

Fuel Cycle Research & Development

Prepared for
U.S. Department of Energy
Used Fuel Disposition

G. Freeze, W.P. Gardner, P. Vaughn,
S.D. Sevougian, P. Mariner,
V. Mousseau, G. Hammond
Sandia National Laboratories

November 2013

FCRD-UFD-2014-000062
SAND2013-10532P

Sandia National Laboratories is a multi-program laboratory managed and operated by Sandia Corporation, a wholly owned subsidiary of Lockheed Martin Corporation, for the U.S. Department of Energy's National Nuclear Security Administration under contract DE-AC04-94AL85000.

APPENDIX E

FCT DOCUMENT COVER SHEET [1]

Name/Title of Deliverable/ Milestone/Revision No.	Enhancements to Generic Disposal System Modeling Capabilities, M2FT-14SN0808033
Work Package Title and Number	Generic Disposal System Analysis, FT-14SN080803
Work Package WBS Number	1.02.08.08
Responsible Work Package Manager	Geoff Freeze (Name/Signature)
Date Submitted	

Quality Rigor Level for Deliverable/Milestone[2]	☐ QRL-3	☐ QRL-2	☐ QRL-1 Nuclear Data	☒ Lab/Participant QA Program (no additional FCT QA requirements)

This deliverable was prepared in accordance with Sandia National Laboratories
(Participant/National Laboratory Name)

QA program which meets the requirements of

☒ DOE Order 414.1 ☐ NQA-1-2000 ☐ Other

This Deliverable was subjected to:

☒ Technical Review ☐ Peer Review

Technical Review (TR)
Review Documentation Provided

☐ Signed TR Report or,

☐ Signed TR Concurrence Sheet or,

☒ Signature of TR Reviewer(s) below

Peer Review (PR)
Review Documentation Provided

☐ Signed PR Report or,

☐ Signed PR Concurrence Sheet or,

☐ Signature of PR Reviewer(s) below

Name and Signature of Reviewers

Bill Arnold Bill W. Arnold

Robert MacKinnon Robert J MacKinnon

NOTE 1: *Appendix E should be filled out and submitted with the deliverable. Or, if the PICS:NE system permits, completely enter all applicable information in the PICS:NE Deliverable Form. The requirement is to ensure that all applicable information is entered either in the PICS:NE system or by using the FCT Document Cover Sheet.*

NOTE 2: *In some cases there may be a milestone where an item is being fabricated, maintenance is being performed on a facility, or a document is being issued through a formal document control process where it specifically calls out a formal review of the document. In these cases, documentation (e.g., inspection report, maintenance request, work planning package documentation or the documented review of the issued document through the document control process) of the completion of the activity, along with the Document Cover Sheet, is sufficient to demonstrate achieving the milestone. If QRL 1, 2, or 3 is not assigned, then the Lab / Participant QA Program (no additional FCT QA requirements) box must be checked, and the work is understood to be performed and any deliverable developed in conformance with the respective National Laboratory / Participant, DOE or NNSA-approved QA Program.*

ACKNOWLEDGEMENTS

The independent peer reviewers, Bill Arnold and Bob MacKinnon, provided comments that greatly improved the quality of the document. Helpful comments were also provided by DOE reviewers Mark Tynan and coworkers from the Office of Used Nuclear Fuel Disposition Research and Development.

Section 4 of this report summarizes work that was performed by Shaoping Chu, Dylan Harp, Terry Miller, and Scott Painter of Los Alamos National Laboratory. Section 5 summarizes work that was performed by Marco Bianchi, Hui-Hai Liu, and Jens Birkholzer of Lawrence Berkeley National Laboratory.

EXECUTIVE SUMMARY

The Used Fuel Disposition Campaign (UFDC) of the U.S. Department of Energy (DOE) Office of Nuclear Energy (NE) is conducting research and development (R&D) on generic deep geologic disposal systems (i.e., repositories) for high-activity nuclear wastes (i.e., used nuclear fuel (UNF) and high-level radioactive waste (HLW)) that exist today or that could be generated under future fuel cycles.

This report describes specific activities performed in FY2013 contributing to the development of an enhanced disposal system modeling and analysis capability that takes advantage of high-performance computing (HPC) environments to simulate the important multi-physics phenomena and couplings associated with a geologic repository for UNF and HLW. The enhanced disposal system analysis capability employs the HPC-capable PFLOTRAN multi-physics code to support (1) the evaluation of disposal system performance, including uncertainty, for a range of disposal options (e.g., salt, granite, clay, and deep borehole disposal); and (2) the prioritization of UFDC R&D activities in terms of importance to system performance.

The enhanced PA modeling capability was demonstrated with deterministic and probabilistic analyses of a bedded salt repository reference case. The PFLOTRAN-based multi-physics included representations of the coupled processes of waste degradation, radionuclide mobilization, fluid flow, and radionuclide transport (advection, dispersion, diffusion, sorption, and radionuclide decay and ingrowth) through the engineered barriers and the bedded salt formation to a groundwater sample well location in the aquifer.

The simulation results provide preliminary insights into the important multi-physics processes and couplings controlling long-term performance for the generic reference case salt repository. However, the salt repository simulations only represent a preliminary, demonstration-scale problem. Further salt PA model refinement would be prudent before drawing strong conclusions regarding the relative importance of various parameters.

The HPC environment enabled reasonable run times for the set of 100 probabilistic simulations of the coupled radionuclide source term and flow and transport equations. The application of HPC solutions to the modeling of these integrated phenomena is a significant advancement in PA modeling capability in that it allows the important multi-physics couplings to be represented directly, rather than through simplified abstractions. It also allows for complex representations of the source term; the demonstration problem included explicit representation of 80 individual waste packages (i.e., meter-scale detail of an entire waste emplacement drift).

In addition to the enhanced PA model demonstration for the salt repository, reference cases were also developed for generic granite and clay repositories. Far-field flow and transport simulations were performed for these reference cases as a preliminary demonstration of their compatibility with an enhanced PA model.

This report addresses Generic Disposal System Analysis Work Package Level 2 Milestone – Generic Disposal System Modeling Report (M2FT-14SN0808033).

CONTENTS

CONTENTS (cont.)

FIGURES

FIGURES (cont.)

TABLES

ACRONYMS

ANDRA	Agence Nationale pour la gestion des Déchets Radioactifs (French National Radioactive Waste Management Agency)
BOL	beginning of life
BWR	boiling water reactor
CFR	Code of Federal Regulations
DAKOTA	Design Analysis toolKit for Optimization and Terascale Applications
DOE	U.S. Department of Energy
DPC	dual-purpose canister
DRZ	disturbed rock zone
EBS	engineered barrier system
EDZ	excavation disturbed zone
EOL	end of life
EPA	U.S. Environmental Protection Agency
ERB	example reference biosphere
FEP	feature, event, and process
FY	fiscal year
GDSA	generic disposal system analysis
GWd	gigawatt-day
HDF5	hierarchical data format, version 5
HLW	high-level radioactive waste
HPC	high-performance computing
IAEA	International Atomic Energy Agency
LHS	latin hypercube sampling
LIME	Lightweight Integrating Multi-Physics Environment
MPI	message passing interface
MTHM	metric tons heavy metal
MTIHM	metric tons initial heavy metal
MTU	metric tons uranium

ACRONYMS (cont.)

Nagra	Nationale Genossenschaft für die Lagerung Radioaktiver Abfälle (Swiss National Cooperative for the Disposal of Radioactive Waste)
NBS	natural barrier system
NE	Office of Nuclear Energy
NEA	Nuclear Energy Agency
NRC	U.S. Nuclear Regulatory Commission
NWTRB	U.S. Nuclear Waste Technical Review Board
OoR	(age) out-of-reactor
PETSc	Portable Extensible Toolkit for Scientific Computation
PWR	pressurized water reactor
QA	quality assurance
THC	thermal-hydrologic-chemical
THCM	thermal-hydrologic-chemical-mechanical
THCMBR	thermal-hydrologic-chemical-mechanical-biological-radiological
PA	performance assessment
R&D	research and development
SKB	Svensk Kämbränslehantering AB (Swedish Nuclear Fuel and Waste Management Company)
SNL	Sandia National Laboratories
TRU	transuranic
UFDC	Used Fuel Disposition Campaign
UNF	used nuclear fuel
V&V	verification and validation
WIPP	Waste Isolation Pilot Plant
WF	waste form
WP	waste package
1D, 2D, 3D	one-, two-, and three-dimensional

1. INTRODUCTION

The Used Fuel Disposition Campaign (UFDC) of the U.S. Department of Energy (DOE) Office of Nuclear Energy (NE) is conducting research and development (R&D) on generic deep geologic disposal systems (i.e., repositories) for high-activity nuclear wastes that exist today or that could be generated under future fuel cycles. The term high-activity waste (NWTRB 2011) refers collectively to both used nuclear fuel (UNF) from nuclear reactors and high-level radioactive waste (HLW) from reprocessing of UNF, and from other sources.

Generic Disposal System Modeling and Advanced Disposal System Modeling Work Package activities completed in Fiscal Year (FY) 2012 and prior years demonstrated the capability to perform generic disposal system simulations for salt, granite, clay/shale, and deep borehole disposal options. These capabilities are documented in Clayton et al. (2011), Freeze and Vaughn (2012), and Vaughn et al. (2013a).

This report describes specific activities performed in FY2013 contributing to the development of an enhanced disposal system modeling and analysis capability that can:

- directly integrate conceptual models of subsystem processes and couplings into the system model where necessary;
- leverage existing computational capabilities (e.g., meshing, visualization, high-performance computing (HPC)) where appropriate; and
- be developed and distributed in an open source environment.

The enhanced disposal system analysis capability supports (1) the evaluation of disposal system performance, including uncertainty, for a range of disposal options; and (2) the prioritization of UFDC R&D activities in terms of importance to system performance.

This report addresses Generic Disposal System Analysis (GDSA) Work Package Level 2 Milestone – Generic Disposal System Modeling Report (M2FT-14SN0808033). It incorporates information from the following supporting Milestones: M4FT-13LA0808021 (Chu 2013); M4FT-13LB0808032 (Bianchi et al. 2013); M4FT-13SN0808045 (Freeze et al. 2013a); and M3FT-13SN0808062 (Freeze et al. 2013b). Section 1.1 describes the range of UFDC disposal options. Section 2 describes the enhanced generic disposal system modeling and analysis capabilities, including a conceptual model framework and a PFLOTRAN-based computational framework. Section 3 presents a demonstration of the enhanced modeling and analysis capabilities through application to a generic salt disposal system. The demonstration problem includes a description of a generic bedded salt repository reference case and deterministic and probabilistic system-level simulations using PFLOTRAN. Sections 4 and 5 provide preliminary descriptions of generic disposal system reference cases for granite and clay/shale, respectively. These two sections also describe preliminary process-level model applications that provide a basis for future system-level granite and clay repository demonstration problems for the PFLOTRAN-based enhanced modeling and analysis capability. Section 6 presents a summary and conclusions.

1.1 Disposal Options

Generic UNF and HLW disposal system simulations were conducted by the UFDC in prior years (Clayton et al. 2011; Vaughn et al. 2013a) for salt, clay/shale, granite, and deep borehole disposal options. Hardin et al. (2012) have recently provided more detailed descriptions of potential disposal options for UNF and HLW, including a distinction between “open” modes, where extended ventilation can remove heat for many years after waste emplacement underground, and “enclosed” modes, where waste emplacement is in direct or close contact with natural or engineered materials (e.g., buffer or backfill) and

which may have temperature limits that constrain thermal loading. Specific disposal options proposed by Hardin et al. (2012) include:

- **Salt (enclosed)** – A repository in bedded salt in which individual, carbon steel waste packages are placed on the floor in drifts or alcoves, and immediately covered (backfilled) with run-of-mine salt. All repository openings are backfilled at closure, and shafts are sealed (Hardin et al. 2012, Section 1.4.5.2).
- **Granite/Crystalline (enclosed)** - A repository in crystalline rock (e.g., granite). Vertical borehole emplacement is used with a copper waste package (e.g., Swedish KBS-3 concept), with a clay buffer installed at emplacement. Access and service drifts are backfilled with low-permeability clay-based swelling backfill at closure. Access shafts are sealed at closure (Hardin et al. 2012, Section 1.4.5.1).
- **Clay/Shale (enclosed)** – Waste is emplaced in blind, steel-lined horizontal borings constructed from horizontal access drifts. UNF is emplaced in carbon steel packages with a clay buffer. HLW glass is emplaced in stainless steel pour canisters, within a steel liner. Access and service drifts are backfilled with low permeability clay-based backfill at closure. Access shafts and ramps are sealed at closure (Hardin et al. 2012, Section 1.4.5.3).
- **Deep Borehole (enclosed)** – Ongoing studies are assessing the feasibility of drilling large-diameter holes to 5 km in low-permeability crystalline basement rock. Waste packages would contain single UNF assemblies, or reduced quantities of HLW glass, and would be stacked in the lower 2 km of each hole. The upper section would be sealed (Brady et al. 2009; Arnold et al. 2011).
- **Shale Unbackfilled (open)** – A repository in a clay/shale environment constructed such that ventilation is maintained for at least 50 to 100 years after waste emplacement and before the repository is closed. At repository closure, the access and service drifts (shafts) are backfilled, but not the disposal drift segments where waste packages are emplaced (Hardin et al. 2012, Section 1.5.1).
- **Sedimentary Backfilled (open)** – A repository in unsaturated soft rock constructed such that ventilation is maintained for at least 50 to 100 years after waste emplacement and before the repository is closed. The waste emplacement, access, and service drifts are backfilled at the time of repository closure (Hardin et al., Section 1.5.2).
- **Hard Rock, Unsaturated (open)** – A repository in competent, indurated rock (e.g., igneous or metamorphic) using in-drift emplacement and forced ventilation for 50 to 100 years after waste emplacement. The hydrologic setting is unsaturated, so the emplacement drifts are not backfilled at closure, but other engineered barriers may be installed such as corrosion resistant metallic barriers to water movement (DOE 2008).

This report presents reference case conceptual models demonstration simulations of generic repositories for the salt enclosed (Section 3), granite enclosed (Section 4), and clay enclosed (Section 5) disposal options.

2. GENERIC DISPOSAL SYSTEM MODELING CAPABILITIES

In FY2012, the requirements for an enhanced performance assessment (PA) modeling and analysis capability were identified (Freeze and Vaughn 2012; Vaughn et al. 2013a, Section 2). Enhanced PA modeling capabilities that are responsive to these requirements are documented in this section.

The following definitions are provided to ensure consistent understanding of terminology used throughout the report:

- **Conceptual model –** "A representation of the behavior of a real-world process, phenomenon, or object as an aggregation of scientific concepts, so as to enable predictions about its behavior. Such a model consists of concepts related to geometrical elements of the object (size and shape); dimensionality (one-, two-, or three-dimensional (1D, 2D, or 3D)); time dependence (steady-state or transient); applicable conservation principles (mass, momentum, energy); applicable constitutive relations; significant processes; boundary conditions; and initial conditions." (NRC 1999, Appendix C)
- **Mathematical model –** "A representation of a conceptual model of a system, subsystem, or component through the use of mathematics. Mathematical models can be mechanistic, in which the causal relations are based on physical conservation principles and constitutive equations. In empirical models, causal relations are based entirely on observations." (NRC 1999, Appendix C).
- **Numerical model –** An approximate representation of a mathematical model that is constructed using a numerical description method such as finite volumes, finite differences, or finite elements. A numerical model is typically represented by a series of program statements that are executed on a computer (NRC 2003, Glossary).
- **Computer code –** "An implementation of a mathematical model on a digital computer generally in a higher-order computer language …" (NRC 1999, Appendix C).
- **Safety case –** "An integration of arguments and evidence that describe, quantify and substantiate the safety of the geological disposal facility and the associated level of confidence. In a safety case, the results of safety assessment – i.e. the calculated numerical results for safety indicators – are supplemented by a broader range of evidence that gives context to the conclusions or provides complementary safety arguments, either quantitative or qualitative." (NEA 2012, Section 3.1).
- **Safety assessment** – "A systematic analysis of the hazards associated with geological disposal facility and the ability of the site and designs to provide the safety functions and meet technical requirements. The task involves developing an understanding of how, and under what circumstances, radionuclides might be released from a repository, how likely such releases are, and what would be the consequences of such releases to humans and the environment." (NEA 2012, Section 3.1).

  "Safety assessment … considers the performance of the repository system in terms of radiological impact or some other global measure(s) of impact on safety." … "The time frames over which the safety indicators have to be evaluated vary considerably between national regulations and sometimes have to be determined and justified by the proponent." … "Ultimately, it is necessary to establish a boundary delineating events that lie outside the scope of safety assessment – in order to limit the complexity and uncertainty in safety assessment, as well to encourage attention on those aspects most relevant to safety. This may be done on the basis of probability cut-offs or other criteria, which raises the issue of uncertainties regarding the nature and probability of occurrence of key events and processes. There are several approaches available to do this type of uncertainty evaluation, usually employing a mix of probabilistic and deterministic approaches." (NEA 2012, Section 3.3).

  A safety assessment considers all aspects relevant to protection and safety, including siting, design and operation of the facility (IAEA 2007) and therefore includes elements of both preclosure and postclosure safety.

- **Performance assessment (PA)** – The steps of a PA Methodology (Figure 2-1) are described in Meacham et al. (2011, Section 1). A complete PA includes quantification of the long-term, postclosure performance of the disposal system using a computational system-level PA model, analysis of the associated uncertainties in this prediction of performance, and comparison with the relevant design requirements and safety standards. A PA requires conceptual and computational models based on the relevant features, events, and processes (FEPs), scenarios, and associated uncertainties, that are or could be important to safety. (Sevougian et al. 2012, Section 2). The term "performance assessment" is often used interchangeably with "safety assessment". In this report, "performance assessment" is used to refer to a quantitative postclosure analysis with a PA model.
- **Performance assessment (PA) model** – A PA model is the integrated mathematical and numerical implementation of the conceptual description of the disposal system components and their interactions. To perform calculations with a PA model, a computer code that implements the numerical model must be utilized. A PA model may incorporate deterministic or probabilistic analyses (see Section 2.2.1).

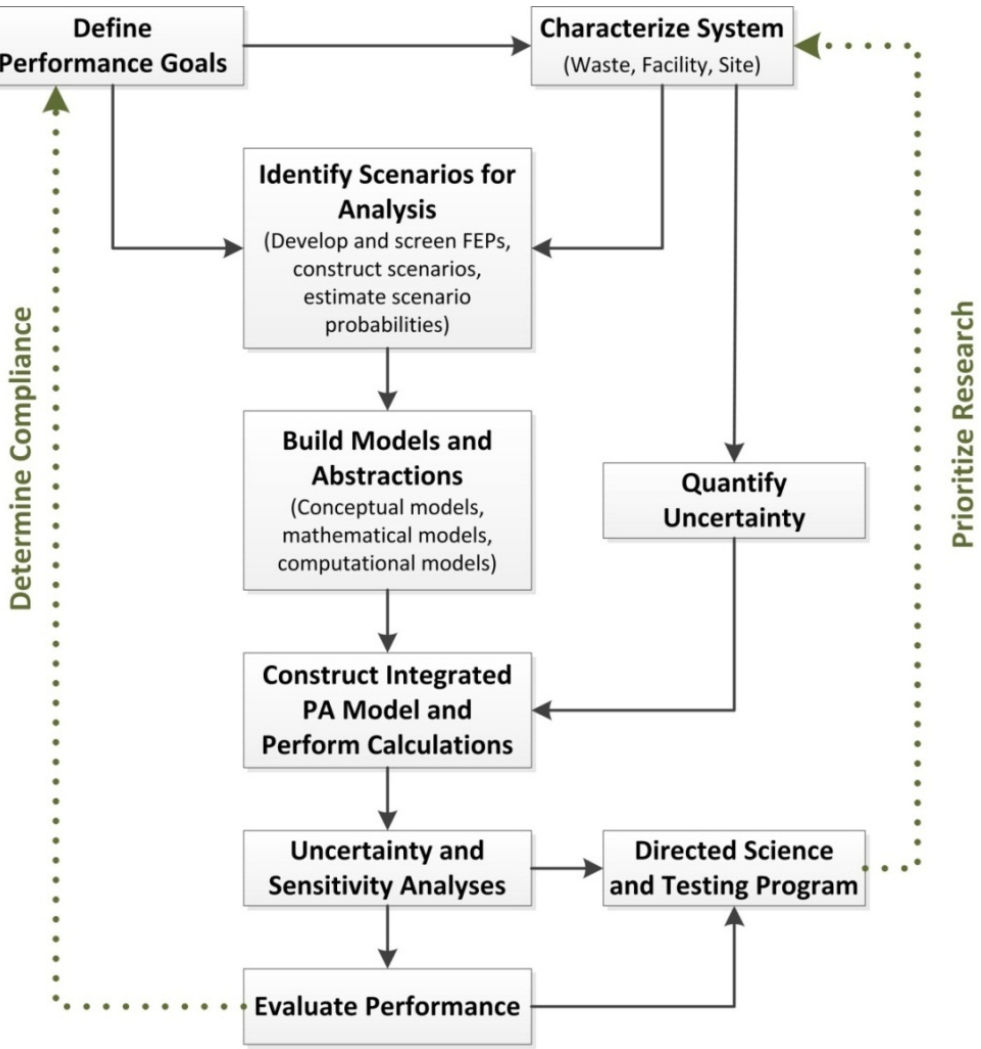

from Meacham et al. (2011, Figure 2)

Figure 2-1. PA Methodology

Consistent with these definitions, the enhanced PA modeling capability described in this section is focused on providing a numerical representation of the integrated multi-physics processes that contribute to the postclosure evolution and performance of the disposal system and a quantitative assessment of the potential impact to human health. The PA model results, in turn, can be used to provide quantitative support for a safety case.

Internationally, there is also a trend towards the development and application of more complex PA models, due to both more powerful computers and to an improved understanding of the multi-physics processes. In general, the use of more complex models with fewer model simplifications provides for greater completeness and transparency, which can eliminate some uncertainty over the results. (NEA 2012, Section 6.3).

The enhanced PA modeling capability supporting generic disposal system modeling includes two main components (Freeze and Vaughn 2012, Section 2):

- A conceptual multi-physics model framework that facilitates development of
  - a conceptual model of the important FEPs and scenarios that describe the multi-physics phenomena of a specific disposal system and its subsystem components, and
  - a mathematical model (e.g., governing equations) that implements the representations of the important FEPs and their couplings.
- A computational framework that facilitates integration of
  - the system analysis workflow (e.g., input pre-processing, integration and numerical solution of the mathematical representations of the conceptual model components, and output post-processing), and
  - the supporting capabilities (e.g., mesh generation, input parameter specification and traceability, matrix solvers, visualization, uncertainty quantification and sensitivity analysis, file configuration management including verification and validation (V&V) and quality assurance (QA) functions, and compatibility with HPC environments).

The conceptual multi-physics model framework supports conceptual model development and integration of the various submodels describing each of the disposal system components. The conceptual model framework is described in Section 2.1. The computational framework supports the numerical model and computer code implementation, including complex modeling and HPC considerations. The computational framework is described in Section 2.2.

2.1 Conceptual Model Framework

This section describes the development of a generic repository conceptual model applicable to a range of disposal options, such as those outlined in Section 1.1. The regions of a generic repository are shown in Figure 2-2. They include: the Engineered Barrier System (EBS); the Natural Barrier System (NBS) or Geosphere; and the Biosphere. Figure 2-2 also illustrates the nested 3D nature of the disposal system. The NBS completely surrounds the EBS (which encompasses the waste and emplacement tunnels, shown in red in the figure); radionuclides can be transported from the waste through the EBS and the NBS to the biosphere along multiple flow pathways. The figure also illustrates the presence of shafts and wells, shown in green. Shafts have the potential to provide a direct connection from the EBS to overlying NBS or to the biosphere. Wells have the potential to provide a direct connection from the NBS to the biosphere.

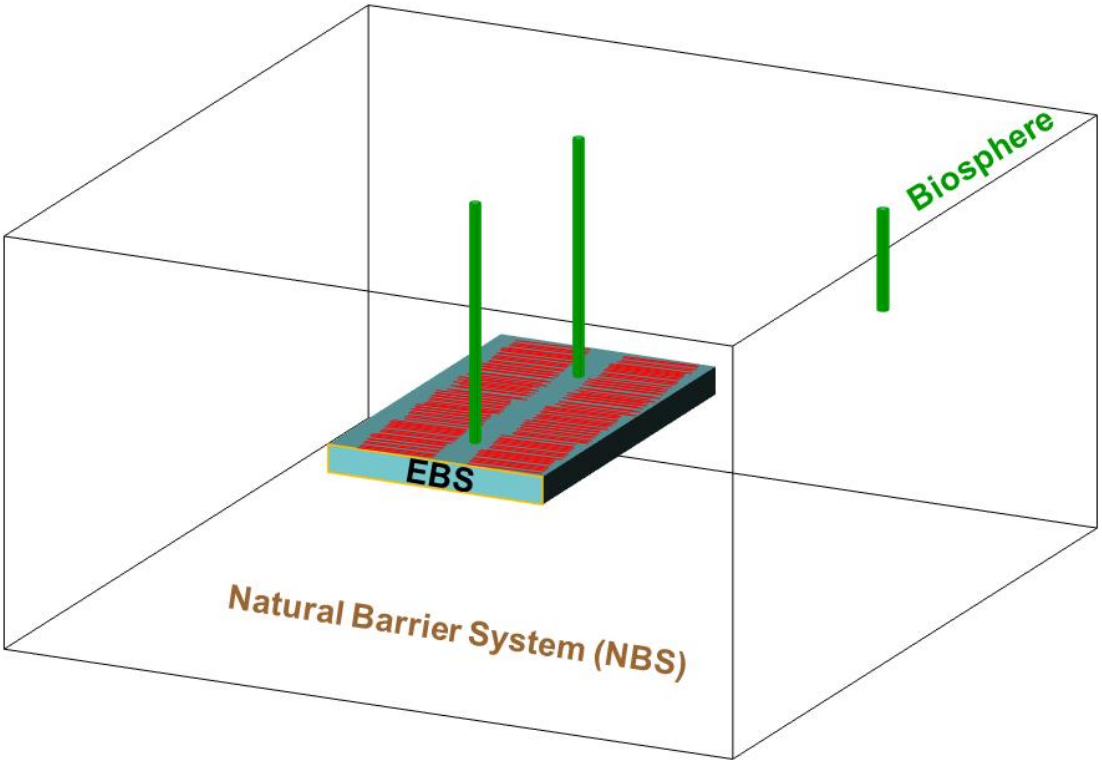

Figure 2-2. Regions of a Generic Disposal System

The features of each of the regions of a generic repository are shown schematically in 1D in Figure 2-3. The features of the EBS include the wastes (e.g., inventory and waste forms) and engineered features (e.g., waste package, buffer and/or backfill, and seals/liner); the features of the NBS include the disturbed rock zone (DRZ), host rock, and other geological units (e.g., overlying or underlying aquifers); and the features of the biosphere include the surface environment and receptor characteristics. The DRZ is the portion of the host rock adjacent to the EBS that experiences durable (but not necessarily permanent) changes due to the presence of the repository. Immediately adjacent to the EBS, these repository-induced changes are more likely to be permanent (e.g., mechanical alteration due to excavation), whereas further from the EBS the repository-induced changes are more likely to be time-dependent but not permanent (e.g., thermal effects due to radioactive decay of waste). The DRZ is sometimes referred to as the excavation disturbed zone (EDZ). However, in this report, DRZ is preferred because it more accurately represents the fact that the disturbed zone includes effects from both excavation and waste emplacement. Alternate terms that are commonly used to describe a disposal system, “near field” and “far field”, are also shown in Figure 2-3. The near field encompasses the EBS and the DRZ (i.e., the components influenced by the presence of the repository). The far field encompasses the remainder of the NBS (i.e., beyond the influence of the repository).

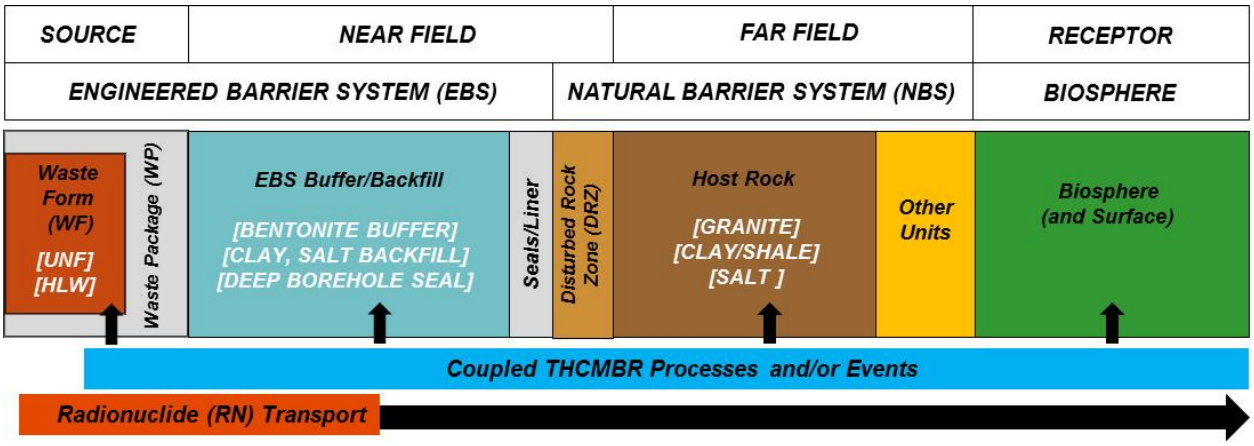

Figure 2-3. Features and Phenomena of a Generic Disposal System

Figure 2-3 also illustrates schematically how radionuclide movement from the waste form to the receptor is influenced by multi-physics phenomena that can act upon and within each of the regions and/or features. These multi-physics phenomena include, at a high level, the thermal-hydrologic-chemical-mechanical-biological-radiological (THCMBR) processes and external events (e.g., seismicity) that describe (1) waste form and waste package degradation, (2) radionuclide mobilization from the waste form and radionuclide release from the waste package (identified as the radionuclide source in), (3) radionuclide transport through the near field and far field, and (4) radionuclide transport, uptake, and health effects in the biosphere. In addition to their direct effects on radionuclide transport, the THCMBR processes also influence the physical and chemical environments (e.g., temperature, fluid chemistry, biology, mechanical alteration) in the EBS, NBS, and biosphere, which in turn affect water movement, degradation of EBS components, and radionuclide transport.

The conceptual model provides a platform to describe a specific disposal system, in accordance with the PA Methodology (Figure 2-1). This is accomplished through:

- System Characterization - specification of the regions and features of the disposal system
- FEP and Scenario Analysis - identification and screening of potentially relevant FEPs and scenarios
- PA Model Construction - conceptual and numerical implementation of the FEPs and scenarios (i.e., spatial and temporal discretization, parameterization of properties including uncertainty, numerical multi-physics descriptions)

Conceptual models specific to generic representations of the salt enclosed, granite enclosed, and clay enclosed disposal options are described in Sections 3, 4, and 5, respectively. However, the development of conceptual models for generic disposal systems has challenges, as noted by Vaughn et al. (2013b):

> *The emphasis on generic repositories creates some unique challenges for safety case development and subsequent modeling of a geologic disposal system. Normally, a safety case and associated safety assessment address a specific site, a well-defined inventory, waste form, and waste package, a specific repository design, specific concept of operations, and an established regulatory environment. This level of specificity does not exist for a "generic" repository, so it is important to establish a reference case, to act as a surrogate for site/design specific information upon which a safety case can be developed. (A reference case provides) enough information to support the initial screening of FEPs and the design of models for preliminary safety assessments …*

Therefore, each of the conceptual models presented in Sections 3 through 5 is described in terms of a generic disposal system reference case. The initial focus of each of the generic reference cases is on the undisturbed scenario (e.g., performance in the absence of external events) rather than on disturbed scenarios (e.g., human intrusion, igneous activity, seismic activity). This is logical for generic repository analyses because disturbed scenarios are strongly dependent on site-specific information and regulatory considerations.

2.2 Computational Framework

The following excerpt describes the current thinking of the international PA community regarding the use of complex models and enhanced (i.e., HPC) computing environments (NEA 2012, Section 6.4):

> *The desire for more complex models is in part supported by the advances in computing power and software. Key advances during the 1990s that affect the modelling strategy are increasing computer power, and advances in software and numerical methods.*
>
> *The improvement in processor speed and memory capacity directly allows more complex calculations to be performed, involving more variables and more time steps. The increase in parallel processing capability is not yet widely exploited in repository safety assessments.*
>
> *Developments in numerical methods have been more subtle. In many respects, the increased computer power noted above has simply allowed current numerical techniques to be extended to tougher problems by brute force – i.e. allowing the model to be represented with much finer mesh spacing or time steps, and thereby avoiding numerical instability issues. However, there have been notable improvements in the numerical techniques used for discretisation and solvers, which allow for the adaptive refinement of the discretisation and therefore the assessment of more complex models.*
>
> *Another important aspect for safety assessment has been the large improvements in software visualisation methods and graphical user interfaces. This provides benefit in the preparation of input files, preparation of models and presentation of calculation results.*

Consistent with this thinking, the computational framework developed to support the enhanced generic PA modeling capability includes:

- System analysis workflow and computational capabilities (Section 2.2.1)
- Configuration management (Section 2.2.2)

2.2.1 System Analysis Workflow and Computational Capabilities

PA modeling may include deterministic and/or probabilistic analysis (NEA 2012, Section 6.3):

> *A deterministic analysis is a calculation performed with a single set of parameters, and may provide a best estimate, conservative or extreme estimate (e.g. what-if cases) of system performance. In a stochastic or probabilistic analysis, relevant parameters are simultaneously varied to address the range of their uncertainties, constrained, of course, by dependencies or correlations between these parameters. … In most safety analyses, deterministic and probabilistic calculations are now seen as complementary and both approaches are applied. Deterministic calculations are more appropriate for detailed calculations and communication purposes. Probabilistic calculations are especially appropriate to deal with parameter uncertainty. Stochastic sensitivity analyses can provide much information on the key parameters controlling the repository system behaviour.*

As outlined in Freeze and Vaughn (2012, Section 2.3), the system analysis workflow and computational capabilities control the development and execution of the integrated system PA model to support deterministic and probabilistic simulations. Specific functions include:

- Input development and pre-processing (spatial and temporal discretization, mesh generation, input parameter specification and traceability, including uncertainty)
- System model development and implementation (mathematical representations of process model FEPs and couplings, uncertainty quantification)
- Integrated system model execution (numerical representations of FEPs and couplings, data structure and matrix solvers)
- Output management and post-processing (analysis of results, visualization, sensitivity analyses)

The following open-source codes perform the core set of these functions in support of the generic repository PA modeling capability (Figure 2-4):

- DAKOTA – sensitivity analysis and uncertainty quantification
- LIME – numerical coupling of multi-physics codes
- PFLOTRAN – THC multi-physics flow and transport

Details of these codes are presented in Sections 2.2.1.1 through 2.2.1.3.

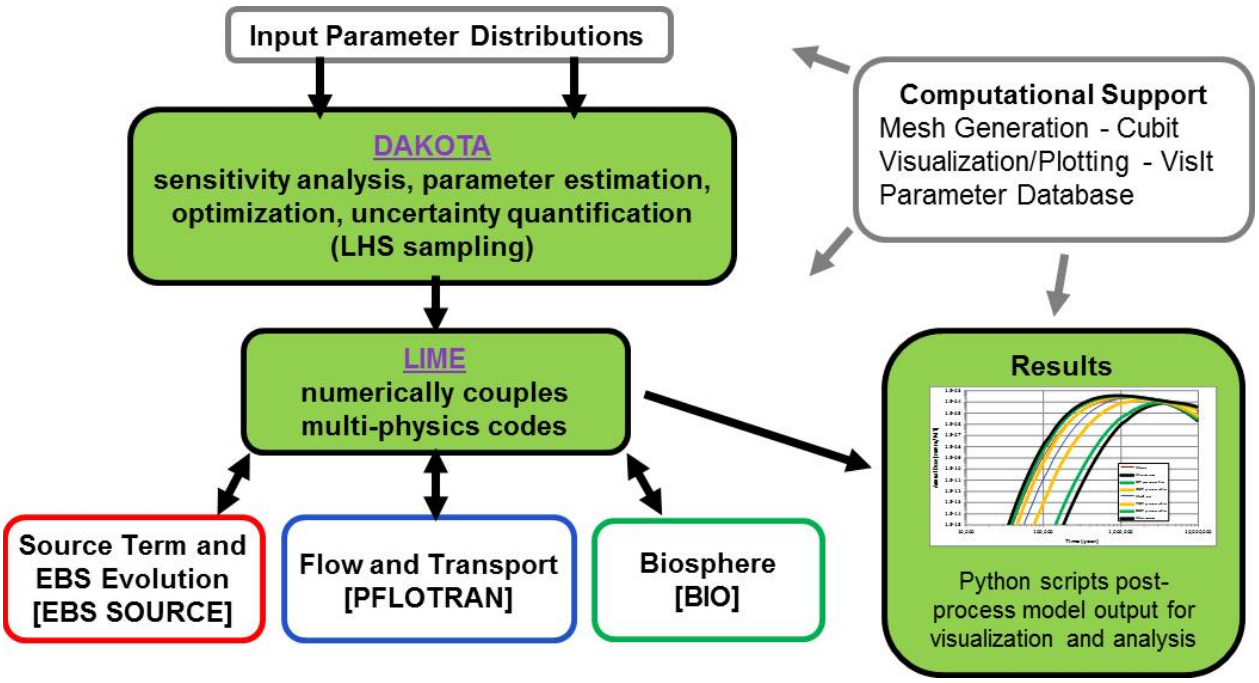

Figure 2-4. Code Integration for Enhanced PA Modeling Capability

In addition to the PFLOTRAN THC flow and transport processes, the following multi-physics code capabilities are also required:

- Source Term and EBS Evolution – An "EBS SOURCE" code to represent the multi-physics processes and the inventory, waste form degradation, and waste package degradation contributing to the radionuclide source term.
- Biosphere Transport and Receptor Uptake – A "BIO" code to represent the surface and biosphere processes contributing to the dose to a human receptor resulting from radionuclide releases from the NBS.

Details of these codes are presented in Sections 2.2.1.4 and 2.2.1.5.

As shown in Figure 2-4, the multi-physics codes (EBS SOURCE, PFLOTRAN, and BIO) are integrated to numerically represent the important coupled THCMBR processes described in Section 2.1. The EBS SOURCE code simulates the source term and EBS evolution, the PFLOTRAN code simulates EBS and NBS flow and transport, and the BIO code simulates biosphere transport and receptor uptake. The specific multi-physics model capabilities of each of these multi-physics codes are shown in Figure 2-5.

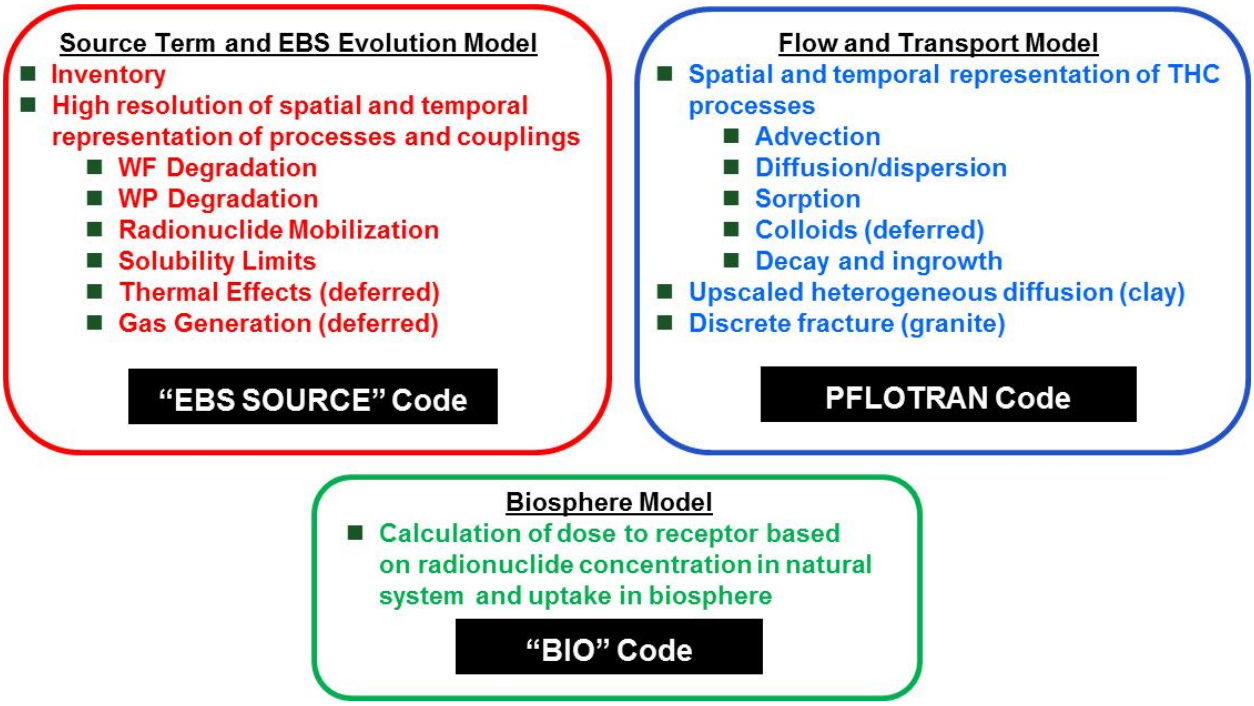

Figure 2-5. Multi-Physics Model Capabilities of the Integrated PA Codes

The computational framework includes the following supporting capabilities, also shown in Figure 2-4:

- Input Parameter Specification – Parameter database
- Mesh Generation – currently using Cubit (SNL 2013)
- Visualization – currently using VisIt (LLNL 2005)
- Scripting – Python scripts to process output data for analysis

One of the attributes of the enhanced PA modeling capability is the ability to directly integrate conceptual models of subsystem processes and couplings into the system model where necessary; this is facilitated by the HPC compatibility of the multi-physics codes. However, in some cases there will be conceptual and/or computational model advantages to relying on process model feeds or abstractions to represent some of the more complex multi-physics couplings. This type of approach is illustrated schematically in Figure 2-6, showing some potential process model codes that incorporate THCM coupling.

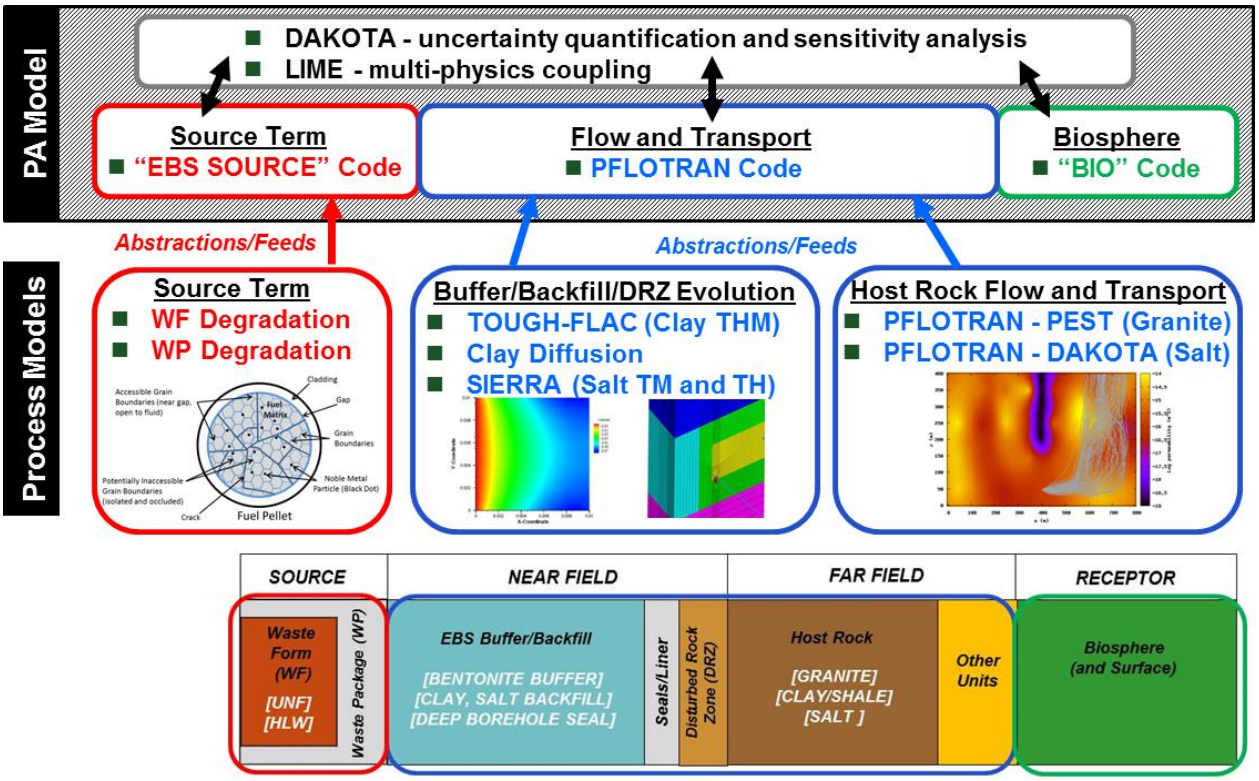

Figure 2-6. Integration of PA Model and Process Models

In the current enhanced PA modeling capability, the EBS SOURCE and BIO codes are not yet fully developed. Correspondingly, the code integration with LIME is also not yet implemented. As the conceptual model and computational frameworks evolve, the independent multi-physics EBS SOURCE and BIO codes are planned to be developed and numerically coupled to the PFLOTRAN-based flow and transport modeling capabilities using LIME.

2.2.1.1 DAKOTA

In the enhanced PA model system analysis workflow, sensitivity analysis and uncertainty quantification capabilities are provided by DAKOTA (Design Analysis toolKit for Optimization and Terascale Applications). DAKOTA (Adams et al. 2013a; Adams et al. 2013b) can be used to manage uncertainty quantification, sensitivity analyses, optimization, and calibration. Specific DAKOTA capabilities include (Figure 2-7):

- Generic interface to simulations
- Extensive library of time-tested and advanced algorithms
- Mixed deterministic / probabilistic analysis
- Supports scalable parallel computations on clusters
- Object-oriented code; modern software quality practices

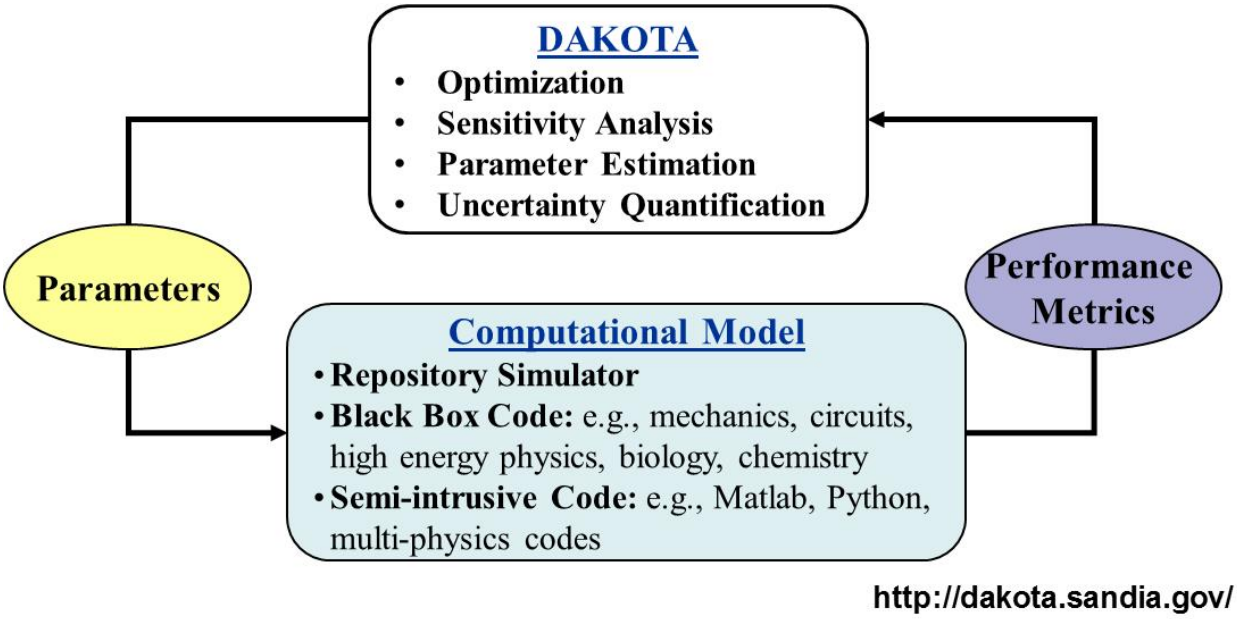

Figure 2-7. DAKOTA Code Workflow and Capabilities

2.2.1.2 LIME

In the enhanced PA model system analysis workflow, LIME (Lightweight Integrating Multi-Physics Environment) (Schmidt et al. 2011) provides a non-intrusive capability for the numerical coupling of independent multi-physics codes. Specific capabilities include (Figure 2-8):

- Combination of separate physics codes (both new and legacy/old software) with strong coupling (when needed) through non-linear solution methods (e.g., fixed point, Jacobian-Free Newton Krylov (JFNK)
- Preservation and leveraging of any specialized algorithms and/or functionality an application may provide
- Direct access to advanced solver libraries (e.g. Trilinos/NOX (Heroux et al. 2003))
- Not limited to codes written in one programming language or using a particular discretization approach (e.g., Finite Element)
- Inheritance of existing QA of legacy software

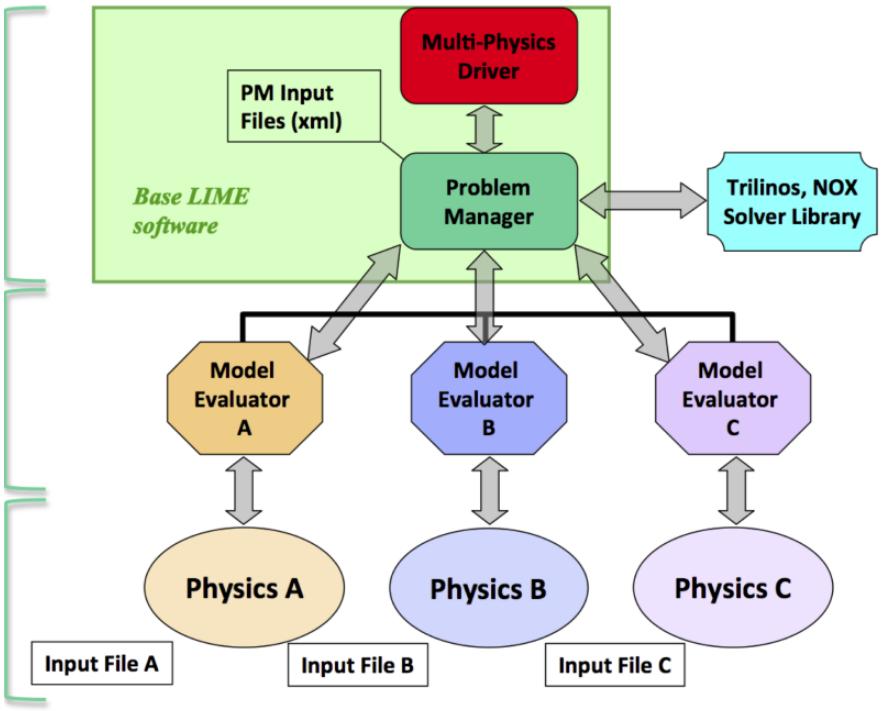

Figure 2-8. LIME Code Workflow and Capabilities

The development of LIME has been funded by the Consortium for Advanced Simulation of Light Water Reactors (CASL), a DOE Energy Innovation Hub for Modeling & Simulation of Nuclear Reactors. As part of the CASL project, LIME and DAKOTA have been coupled together with reactor multi-physics codes (Hooper et al. 2012).

As noted in Section 2.2.1, multi-physics code coupling with LIME will not be implemented until the EBS SOURCE and BIO codes are further developed.

2.2.1.3 PFLOTRAN

PFLOTRAN (Hammond et al. 2011a; Lichtner and Hammond 2012a) is an open source, reactive multi-phase flow and transport simulator designed to leverage massively-parallel high-performance computing to simulate subsurface earth system processes. PFLOTRAN has been employed on petascale leadership-class DOE computing resources (e.g., Jaguar [at Oak Ridge National Laboratory (ORNL)] and Franklin/Hopper [at Lawrence Berkeley National Laboratory (LBNL)]) to simulate THC processes at the Nevada Test Site (Mills et al. 2007), multi-phase CO_2-H_2O for carbon sequestration (Lu and Lichtner 2007), CO_2 leakage within shallow aquifers (Navarre-Sitchler et al. 2013), uranium fate and transport at the Hanford 300 Area (Hammond et al. 2007; Hammond et al. 2008; Hammond and Lichtner 2010; Hammond et al. 2011b; Lichtner and Hammond 2012b; Chen et al. 2012; Chen et al. 2013).

PFLOTRAN solves the non-linear partial differential equations describing non-isothermal multi-phase flow, reactive transport, and geomechanics in porous media. Parallelization is achieved through domain decomposition using the Portable Extensible Toolkit for Scientific Computation (PETSc) (Balay et al. 2013). PETSc provides a flexible interface to data structures and solvers that facilitate the use of parallel computing. PFLOTRAN is written in Fortran 2003/2008 and leverages state of the art Fortran programming (i.e. Fortran classes, pointers to procedures, etc.) to support its object-oriented design. The code provides "factories" within which the developer can integrate a custom set of process models and time integrators for simulating surface and subsurface multi-physics processes. PFLOTRAN employs a single, unified framework for simulating multi-physics processes on both structured and unstructured grid discretizations (i.e. there is no duplication of the code that calculates multi-physics process model functionals in support of structured and unstructured discretizations). The code requires a small, select set of third-party libraries (e.g., MPI, PETSc, BLAS/LAPACK, HDF5, Metis/Parmetis). Both the unified structured/unstructured framework and the limited number of third-party libraries greatly facilitate usability for the end user.

Specific PFLOTRAN capabilities for the simulation of generic disposal systems include:

- Multi-physics
  - Multi-phase flow
  - Multi-component transport
  - Biogeochemical processes
  - Thermal and heat transfer processes
- High-Performance Computing (HPC)
  - Built on PETSc – parallel solver library
  - Massively Parallel
  - Structured and Unstructured Grids
  - Scalable from Laptop to Supercomputer
- Modular design based on object-oriented Fortran 2003/2008 for easy integration of new capabilities

The representation of flow and transport processes with PFLOTRAN is illustrated schematically in Figure 2-9 for the near field and Figure 2-10 for the far field. These figures show the relevant flow and transport processes (consistent with Figure 2-5) and also illustrate where process model feeds or abstractions may be used to represent some of the more complex multi-physics couplings in specific disposal concepts.

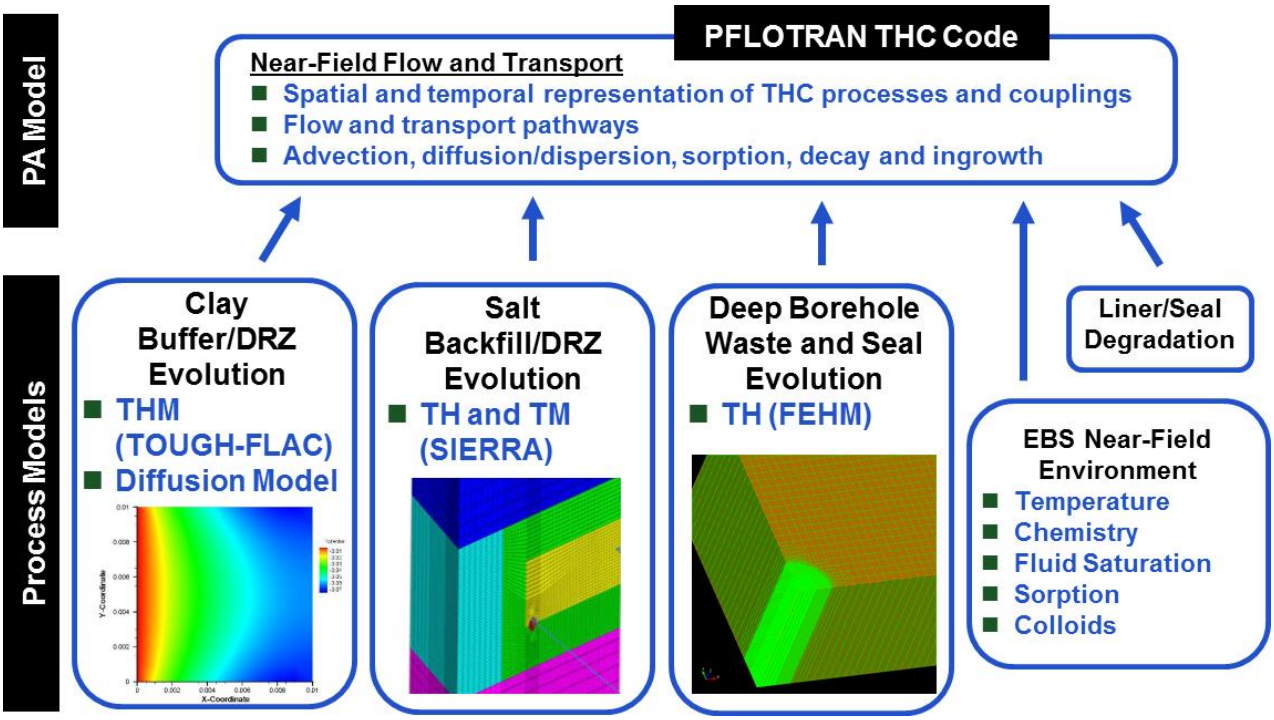

Figure 2-9. Implementation of PFLOTRAN for Near-Field Flow and Transport

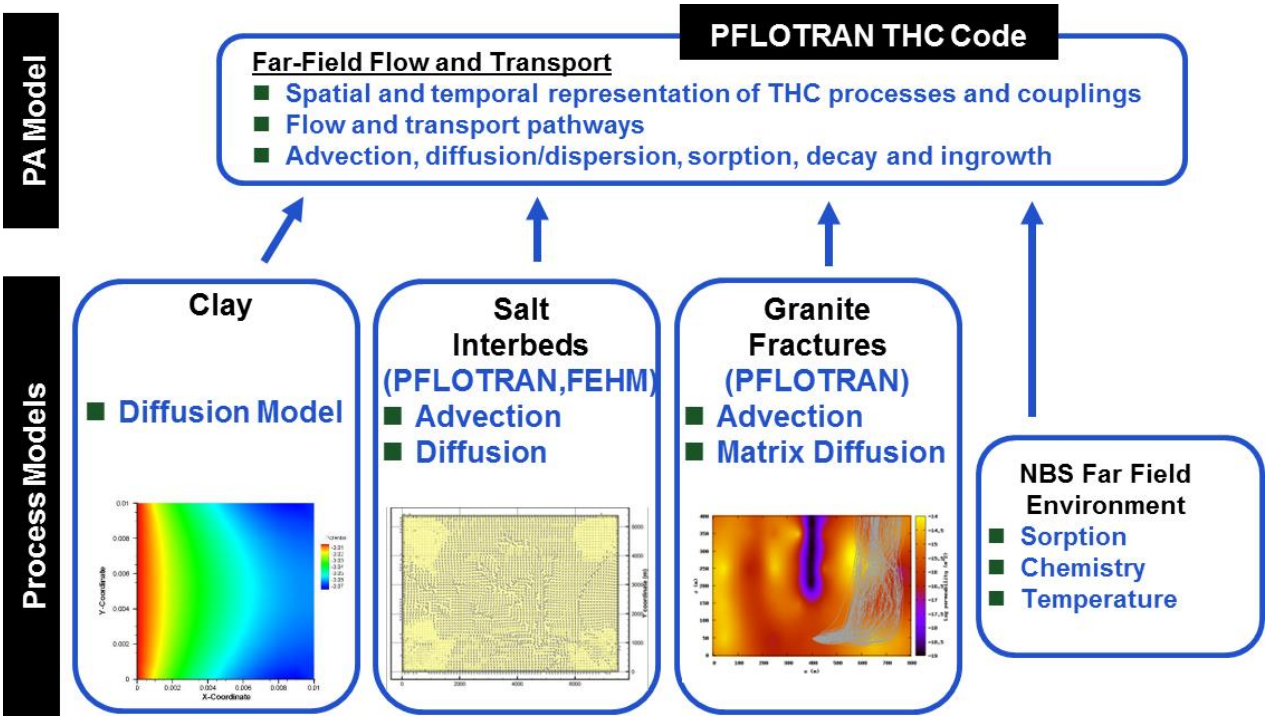

Figure 2-10. Implementation of PFLOTRAN for Far-Field Flow and Transport

2.2.1.4 Source Term and EBS Evolution

A generic disposal system model must be able to represent the inventory, waste form, and waste package degradation processes contributing to the radionuclide source term. Specific processes to be considered in a source term and EBS evolution model include (consistent with Figure 2-5):

- Waste form degradation
  - Processes and rates for degradation of UNF waste forms (e.g., cladding degradation, gap and grain boundary releases, UO_2 matrix dissolution) as a function of the EBS near-field environment
  - Processes and rates for degradation of HLW waste forms (e.g., borosilicate glass) as a function of the EBS near-field environment
- Waste package degradation
  - Processes, rates, and failure mechanisms (e.g., general and localized corrosion, stress corrosion cracking) as a function of the EBS near-field environment
  - Gas generation and consumption of water associated with waste package degradation
- Radionuclide mobilization
  - Processes for mobilization of radionuclides from degraded waste forms (e.g., alpha radiolysis, formation of a corrosion layer, colloid formation, radionuclide dissolution/precipitation and sorption)
- Radionuclide solubility limits
  - The concentrations of radionuclides dissolved in the aqueous phase may be limited by solubility. At aqueous dissolved concentrations above the solubility limits, radionuclides precipitate to a solid phase; when concentration falls below the solubility limit (e.g., due to decay and transport), the precipitate will re-dissolve up to the solubility limit.
  - Aqueous solubility is an elemental property. Solubility calculations must account for fractional contributions of all isotopes of the same element (i.e., congruent dissolution) and for isotopes that occur naturally in the geosphere.
- Radionuclide decay and ingrowth
  - Radionuclide inventory as a function of time, which includes consideration of decay in various phases (e.g., dissolved, sorbed) and ingrowth of decay chain daughter products
- EBS near-field environment
  - Processes controlling the local near-field THCMBR environment

The relationships between these processes are illustrated schematically in Figure 2-11. As noted in Section 2.2.1, the EBS SOURCE code is not yet fully developed. Therefore, for the current enhanced PA modeling capability, PFLOTRAN is used to provide a simplified representation of the source term and EBS evolution. The PFLOTRAN implementation of the EBS source is described in Section 2.2.1.4.1.

As the PA model matures, an independent EBS SOURCE code is planned to be added to the PA modeling capability (e.g., coupled via LIME). The independent EBS SOURCE code will be capable of incorporating more complexity, such as is shown in Figure 2-11.

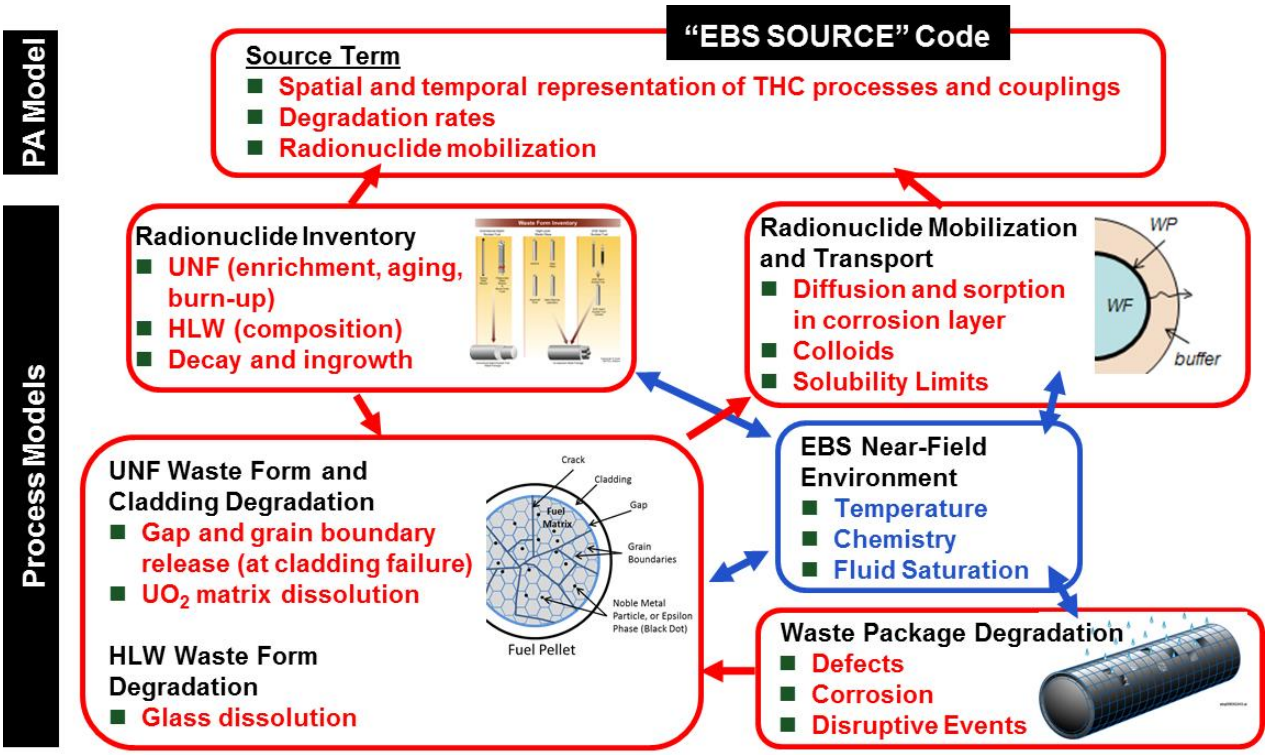

Figure 2-11. Generic Disposal System Source Term and EBS Evolution Processes

2.2.1.4.1 PFLOTRAN EBS Source Implementation

As noted in Section 2.2.1.4, a simplified representation of the source term and EBS evolution has been implemented using PFLOTRAN. The implementation uses the chemical capabilities of PFLOTRAN; the source term derives from a mineral phase (representing a UNF waste form) that kinetically degrades over time. Depending on solubility, the radionuclides released from the waste form mineral phase are then available to either enter the aqueous phase where they may be transported through the EBS, or precipitate as a secondary mineral phase. The representation of specific source term processes in PLFOTRAN is summarized below:

- Waste form degradation
  - The waste form mineral is defined to have a stoichiometry (i.e., radionuclide mole fractions) and density representative of the UNF waste form and to be unstable (i.e., it is specified to have a large dissociation constant (log *K*)). A waste form degradation rate (representative of UO_2 matrix dissolution) can then be specified by adjusting the rate of the dissociation reaction.
  - Gap and grain boundary (fast) releases and cladding degradation are not currently included in the PFLOTRAN implementation.
- Waste package degradation
  - Waste package degradation (and associated gas generation) is not included in the current PFLOTRAN implementation. Instead, waste package degradation is assumed to be instantaneous and no credit is taken for waste package performance.

- Radionuclide mobilization
  - As the waste form mineral degrades, radionuclides are released congruently to the aqueous phase where they may undergo advection, diffusion, sorption, and/or precipitation.
  - Colloid formation and processes associated with the formation of, and transport through, a corrosion layer are not included in the current PFLOTRAN implementation.
- Radionuclide solubility limits
  - Solubility limits are implemented in PFLOTRAN by defining individual secondary mineral phases for each radionuclide. A radionuclide with a dissolved concentration that reaches its solubility limit precipitates as the equilibrium secondary mineral and can re-dissolve when the dissolved concentration subsequently falls below the solubility limit.
  - Solubility limits in PFLOTRAN are defined by radionuclide rather than by element. To account for fractional contributions of different isotopes (radionuclides) of the same element, PFLOTRAN radionuclide solubility limits are calculated from elemental solubility limits by assuming that the fraction of each radionuclide of an element in the aqueous phase is the same as the fraction of each radionuclide of an element within the waste form. In reality, the radionuclide fractions in the aqueous phase will change over time and space due to decay and ingrowth and due to the different mobilities of the various radionuclides.
- Radionuclide decay and ingrowth
  - In the aqueous phase, radionuclide decay and ingrowth to daughter radionuclides are simulated using PFLOTRAN chemical reactions. Parent radionuclides are converted to daughters using a first-order forward kinetic reaction.
  - Radionuclide decay and ingrowth in the mineral phases is not included in the current PFLOTRAN implementation. This process would be important for simulation of short-lived radionuclides with slow waste form degradation rates.
- EBS near-field environment
  - In the current PFLOTRAN implementation, parameter values describing these source term processes are dependent on assumptions about the EBS near-field environment, and some of the processes (e.g., solubility) are coupled with hydrology. There is no incorporation of mechanical processes (e.g., salt creep) on the source term.

2.2.1.5 Biosphere and Receptor

The following excerpt describes the current thinking of the international PA community regarding biosphere modeling in PAs (NEA 2012, Section 6.3):

> *Significant differences exist between countries regarding the extent to which regulations allow simplified handling of the biosphere in the safety assessment. Some regulations provide specific guidance, for example, by prescribing stylised approaches for converting geosphere releases into dose, defining how to handle future climate changes, and how to address potential changes in future human behaviour. Therefore biosphere modeling varies to a large extent. In many system-level models, dose conversion factors are used, which have been derived from biosphere process-level models and provide a simple way to transfer radionuclide surface fluxes or concentrations into dose. Other system-level models implement a full biosphere model, describing radionuclide transfer between different compartments. The use of evolving landscape models is relatively recent, at least with respect to system-level models, and its utility remains to be fully explored.*

In the enhanced PA model system analysis workflow, the biosphere model is planned to be implemented using an independent BIO code (Figure 2-4 and Figure 2-5). However, as noted in Section 2.2.1, the BIO

code is not yet fully developed. As the PA model matures, the independent BIO code is planned to be added to the PA modeling capability (e.g., coupled via LIME). The independent BIO code will be capable of incorporating a number of surface and biosphere processes contributing to the dose to a human receptor resulting from radionuclide releases from the NBS (Figure 2-12). The biosphere transport and receptor uptake processes may be represented explicitly or in an abstracted fashion. In either case, the BIO code calculations are expected to only require one-way (downstream) coupling (e.g., based on radionuclide concentrations in the NBS).

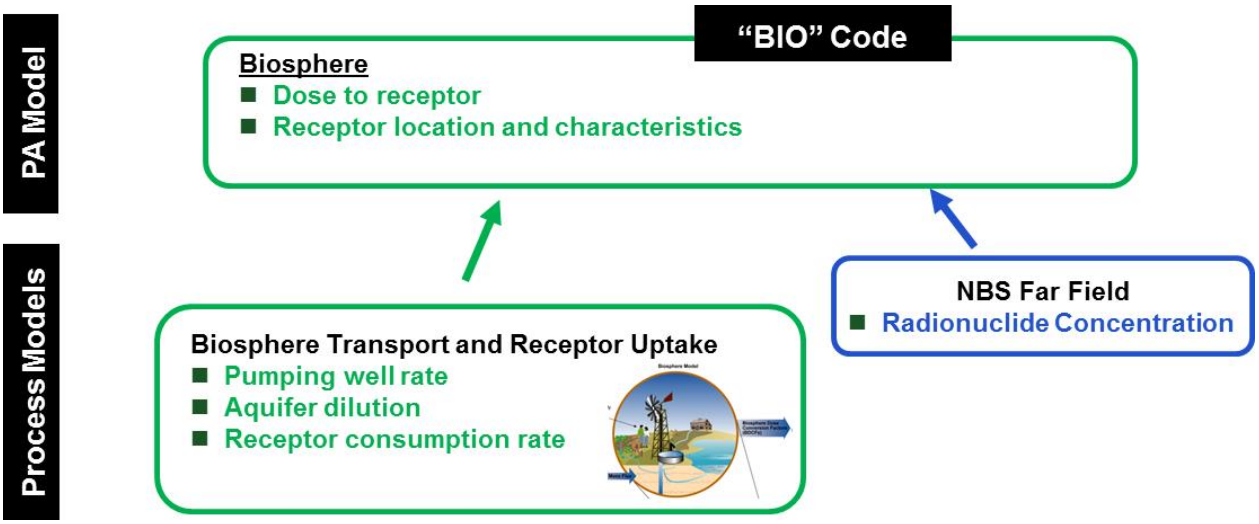

Figure 2-12. Generic Disposal System Biosphere Processes

2.2.2 Configuration Management

As outlined in Freeze and Vaughn (2012, Section 2.3), the configuration management component of the computational framework supports the following:

- Input development (parameter database, file access and storage)
- Output management (file access and storage)

For the current enhanced PA modeling capability, formal configuration management has not yet been implemented. As the PA model matures, configuration management will be formalized, as described in Vaughn et al. (2013a, Section 2.5), and will be integrated within the overall UFDC data management structure (Wang 2011). In parallel, the quality rigor level (DOE 2012a) of the code and model development will increase as the UFDC work scope advances from generic R&D to site-specific investigation and/or licensing.

The planned PA model and UFDC configuration management practices are consistent with the current thinking of the international PA community (NEA 2012, Section 6.5):

> *All modelling work is underpinned by data from a variety of sources, including laboratory experiments, field tests, large-scale experiments, site investigation, literature searches and comparisons with natural phenomena. Not all data will be obtained in the format required by the models and it is unlikely that a "complete" data set will be available for evaluating a complex system over very long times, especially when that system has not yet been built. The goal is to create a data*

set that is sufficient for the decision point for the repository system that is currently under consideration.

Some data will require processing prior to use in models. Some data will require extrapolation or interpolation because the actual data available are incomplete or do not relate to the exact conditions experienced by the repository system. Expert judgement may be combined with the available empirical data to elicit a full data set or manage the consequences of uncertainty associated with the available data, in particular the selection of probability density functions (PDFs) for certain parameters to facilitate probabilistic evaluations.

Documentation, record keeping and quality management are key requirements to the provision of information. To be useful for licensing purposes, the data must ultimately be controlled within the context of a specific project, as a controlled reference dataset.

3. GENERIC SALT DISPOSAL SYSTEM MODEL

In FY2012, a simplified salt disposal system model was developed (Vaughn et al. 2013a, Sections 3.1 and 3.5), and applied to support a generic safety case (Freeze et al. 2013c). An initial design and requirements for an enhanced PA model to support safety assessments for the disposal of high-activity waste in a mined geologic repository at a generic salt site were also documented (Sevougian et al. 2012; Vaughn et al. 2013b; Sevougian et al. 2013). The continuing development of the enhanced salt repository PA model is documented in this section.

Following the conceptual model framework described in Section 2.1 and the PA Methodology outlined in Figure 2-1, the development of a generic postclosure salt repository PA model includes:

- System Characterization – description of the disposal concept (i.e., specification of the regions and features of the disposal system) and the reference case (i.e., specification of parameter values including uncertainty quantification)
- FEP and Scenario Analysis – identification and screening of FEPs and scenarios
- PA Model Construction - development of an integrated PA model (i.e., numerical implementation of the FEPs and scenarios)
- Perform PA Calculations – Numerical HPC-based simulations of the reference case, including uncertainty and sensitivity analyses

These steps in the development of the generic salt repository model are described in the following subsections. Section 3.1 describes the salt repository disposal concept. Section 3.2 describes the generic salt repository reference case, which is informed by the disposal concept. Section 3.3 describes integrated PA model development, including preliminary FEP and scenario analysis, and presents model results for an initial demonstration of salt repository PA model capability.

3.1 Generic Salt Repository Disposal Concept

The use of salt formations for radioactive waste disposal was recognized as early as 1957 when salt was identified as a promising host rock for HLW disposal (National Academy of Sciences 1957). Specific considerations for the disposal of heat-generating nature of the waste are described in DOE (1987), Hansen and Leigh (2011), Sevougian et al. (2012), and Freeze et al. (2013c).

The Waste Isolation Pilot Plant (WIPP) is an operational salt repository for defense-generated transuranic (TRU) waste, sited in a bedded salt formation near Carlsbad, New Mexico (DOE 1996; DOE 2009). The generic disposal concept for high-activity waste is also based on a bedded salt host formation, with additional design considerations for the heat-generating nature of the waste. The high-activity waste disposal concept in bedded salt is based on a disposal concept for high-heat-generating dual-purpose canisters (DPCs) in salt described in Hardin et al. (2013, Section 4.2). The concept was originally proposed for heat-generating HLW glass (Carter et al. 2011) and extended to UNF (Hardin et al. 2012, Section 1.4.5.2). The generic salt repository disposal concept serves as the basis for the salt repository reference case described in Section 3.2.

Specific details and assumptions of the generic salt enclosed mode disposal concept include:

- Repository waste capacity of 70,000 metric tons of heavy metal (MTHM).
- Horizontal repository layout consists of excavated emplacement drifts separated by intact salt “pillars”. Drifts are laid out in pairs, separated by a central access hallway (Figure 3-1). Number of drift pairs, drift dimensions, and drift spacing are determined by total inventory, waste package size, and thermal and mechanical design considerations.

- Excavation and ground support methods are similar to those used for the WIPP. Ground support consists only of rock bolts (i.e., no liners)
- Horizontal end-to-end emplacement of waste packages in drifts. Drifts are backfilled with crushed salt immediately after waste package emplacement. Waste package spacing is determined by thermal design considerations (Figure 3-2).
- Intersections of emplacement drifts with central access hallway (i.e., drift closure seals) are backfilled or sealed. Central access hallway is backfilled.
- Shafts are used for construction, operation (e.g., waste handling), and ventilation. Shaft sealing is similar to WIPP.
- Excavated emplacement drifts are located in a relatively pure salt unit (e.g., halite) within a vertically and laterally extensive bedded salt formation. Interbeds are assumed to be clay and/or anhydrite.

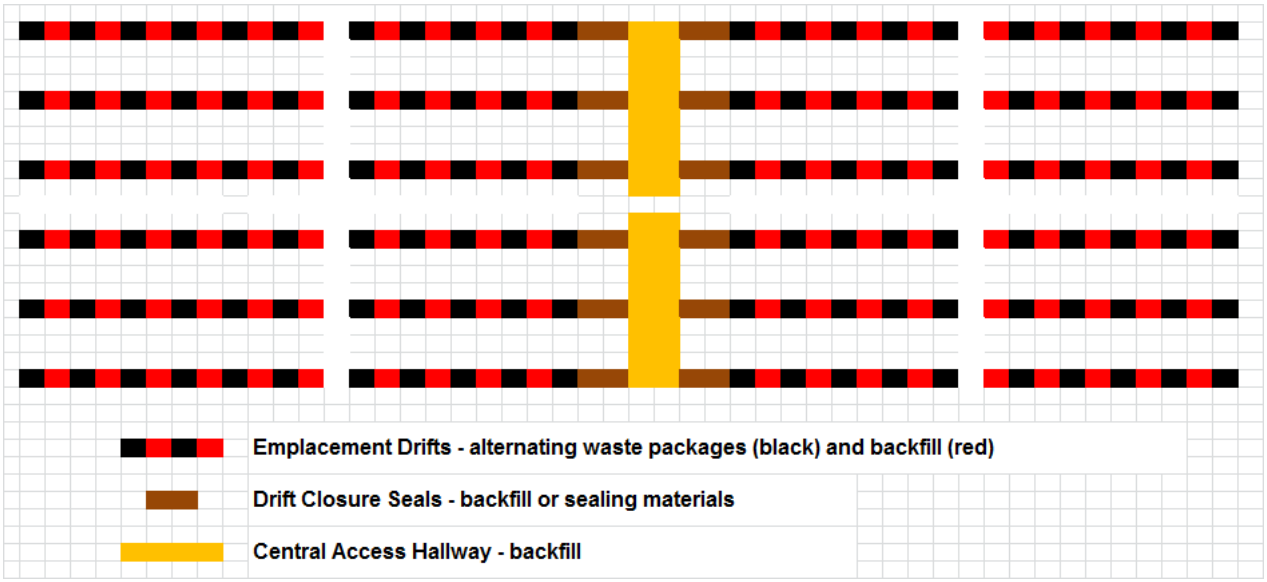

(only the portions of six pairs of emplacement drifts closest to the central access hallway are shown)

Figure 3-1. Schematic Representation of Salt Repository Layout

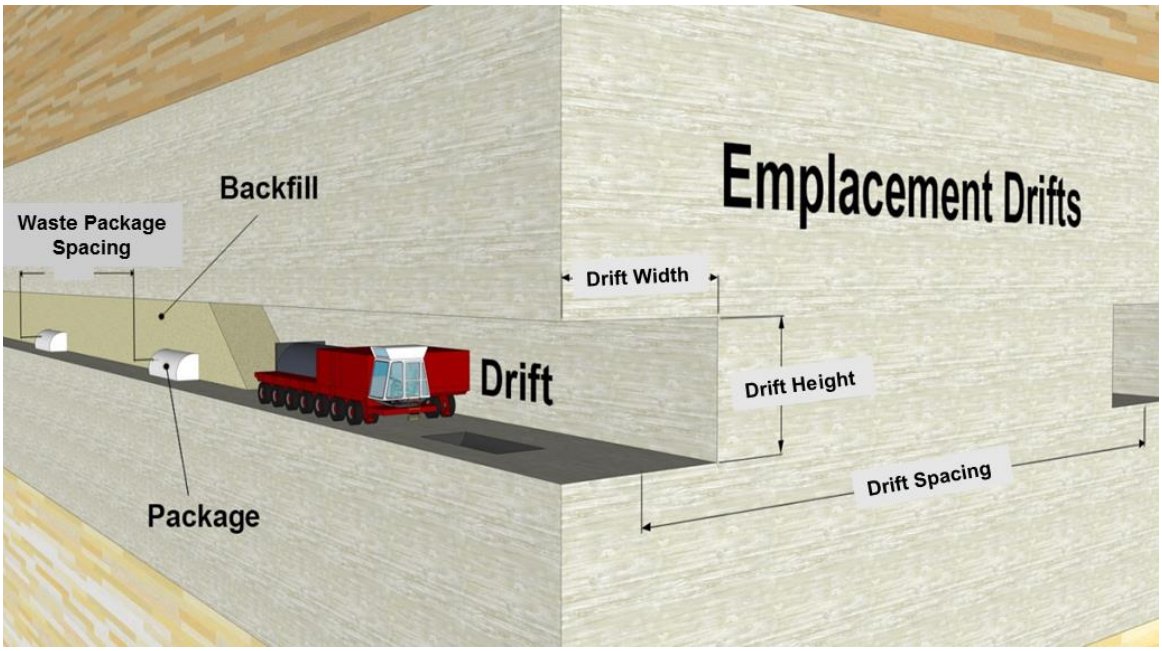

(from Hardin et al. 2013, Figure 4-3)

Figure 3-2. Schematic Illustration of an Emplacement Drift in Salt with Waste Packages and Backfill

Based on these design assumptions, the reference disposal concept includes the following regions and features (Figure 3-3):

- Engineered Barrier System: inventory, waste form, waste package, crushed salt backfill, drifts and drift seals, shafts, and shaft seals
- Natural Barrier System: DRZ, bedded salt host rock formation (intact halite and anhydrite interbed units), and surrounding geologic units (aquifers and overlying sediments)
- Biosphere: surface and receptor characteristics

Details of these regions and features are described as part of the reference case in Section 3.2.

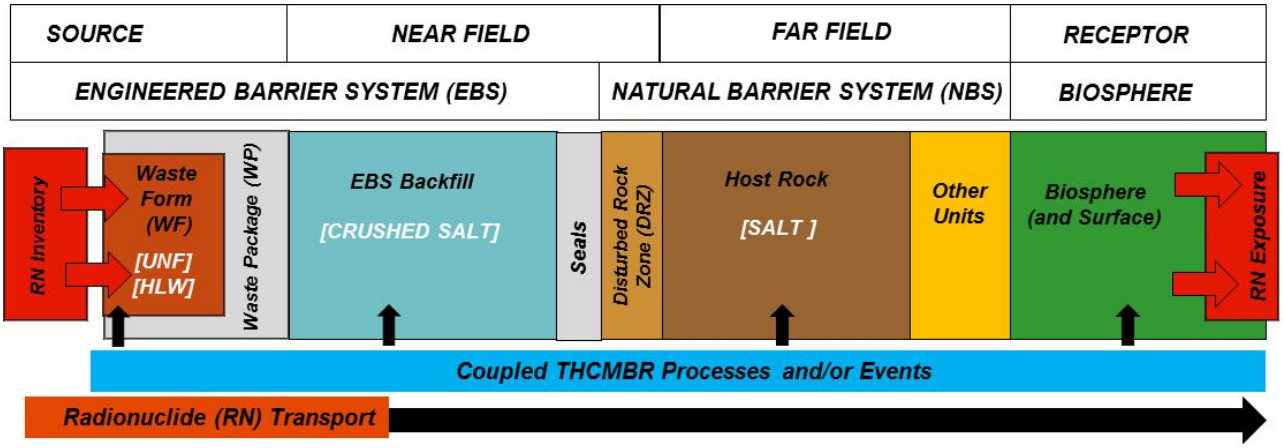

Figure 3-3. Regions and Features of a Generic Salt Repository System

The repository excavations (i.e., the emplacement drifts and shafts) must be arranged geometrically to observe certain operational, mechanical, and thermal design constraints to ensure safe preclosure and postclosure performance. Operational constraints include the dimensions of the shafts, central access hallways, and drifts to accommodate the transport and emplacement of waste packages and the associated use of readily available mining equipment. Mechanical design guidelines regarding the "extraction ratio" (defined as the mined volume to the original volume) and the pillar width-to-height ratio must be observed to ensure safe preclosure operations, i.e., to prevent drift collapse (Zipf 2001; Poulsen 2010).

Thermal constraints guide the spacing between waste packages in a drift and the spacing between adjacent drifts. For the salt repository reference case, the temperature constraint is taken to be a peak temperature of 200°C at the waste package surface (i.e., at the interface of the waste package with the salt backfill). The temperature constraint is specified to limit thermal degradation of the salt backfill and/or the salt host rock, although prior studies have also considered a peak temperature limit of 250°C (Hardin et al. 2012, Section 1.4.1). This temperature constraint can be satisfied by a combination of design factors such as: repository layout (waste package and drift spacing), inventory properties (radionuclide content, age out of reactor/decay storage time), waste package properties (size and radionuclide loading), and ventilation (e.g., see Hardin et al. 2012, Sections 1.4.2 and 1.4.5.2).

3.2 Generic Salt Repository Reference Case

The generic salt repository reference case has the following major elements:

- Waste Inventory (Section 3.2.1)
- Geologic Disposal System: Engineered Barrier System (Section 3.2.2)
- Geologic Disposal System: Natural Barrier System (Section 3.2.3)
- Biosphere (Section 3.2.4)
- Regulatory Environment (Section 3.2.5)

The descriptions in the following subsections are based on, and in some cases, updated from, the salt repository reference case in Sevougian et al. (2013, Section 2).

3.2.1 Waste Inventory

Carter et al. (2012) document the current inventory of high-activity waste in U.S. and provide projections of future waste generation under a variety of current and potential future fuel cycle alternatives. This U.S. high-activity waste inventory to be considered by the UFDC includes:

- Current and projected UNF inventory from commercial reactors (Carter et al. 2012, Section 3)
- Current and projected UNF and HLW owned and managed by DOE, including Naval UNF (Carter et al. 2012, Section 2)
- Current and projected HLW from reprocessing of UNF (Carter et al. 2012, Sections 4 through 6)
- Projected UNF and HLW from potential alternative fuel cycle alternatives (Carter et al. 2012, Sections 7 through 10)

For simplicity, the generic salt disposal reference case considers only the current and projected UNF inventory from commercial reactors, which comprises the majority of the radionuclide mass and activity of the U.S high-activity waste inventory. Under the "no replacement nuclear generation" scenario (Carter et al. 2012, Section 3.2.1), current and future UNF discharged through final shutdown of the current

reactor fleet in about 2055 will reach approximately 140,000 MTHM[1] (Carter et al. 2012, Table 3-7). This projected inventory includes 91,000 MTHM from pressurized water reactors (PWRs) (209,000 PWR used fuel-rod assemblies[2] with average initial enrichment of 4.40 wt% ^{235}U and average burn-up of 47.3 GWd/MTHM) and 49,000 MTHM from boiling water reactors (BWRs) (273,000 BWR used fuel-rod assemblies with average initial enrichment of 4.09 wt% ^{235}U and average burn-up of 45.3 GWd/MTHM). UNF inventory projections under other scenarios are higher.

As noted in Section 3.1, the reference case salt repository capacity is 70,000 MTHM. For simplicity, the entire single-repository inventory is assumed to consist of PWR UNF assemblies. Each PWR UNF assembly contains 0.435 MTHM (91,000 MTHM/209,000 assemblies). The single-repository reference case PWR inventory assumes a bounding fuel burn-up 60 GWd/MTHM. As shown in Carter et al. (2012, Figure 3-6), only about 25% of the "no replacement scenario" discharged inventory will have burn-ups between 50 and 60 GWd/MTHM, so the reference case assumption of 60 GWd/MTHM will produce a conservatively high heat loading for the repository. The isotopic composition of the reference case 60 GWd/MTHM PWR inventory assumes an initial enrichment of 4.73% and 30-year out-of-reactor (OoR) decay storage, as reported in Carter et al. (2012, Table C-1). This reference case inventory can be augmented with BWR and HLW inventories as the PA model matures.

The reference case PWR UNF inventory includes approximately 450 isotopes with a total mass of 1.44×10^6 g/MTHM and a decay heat of 1.438 kW/MT (Carter et al. 2012, Table C-1). The total mass of the PWR inventory includes actinides (dominated by ^{238}U), oxygen from the UO_2, zirconium from cladding, and other fission and activation products. In a typical PA analysis, a radionuclide screening is performed to identify a subset of radionuclides that is most important to the specific disposal system design and setting (e.g., SNL 2007). Recent generic PA analyses (e.g., Freeze et al. 2013c, Section 4) have used a subset that includes 36 radionuclides, as listed in Clayton et al. (2011, Table 3.1-1).

For the reference case, the following, smaller subset of radionuclides is considered:

- Neptunium series alpha-decay chain ($^{241}\text{Am} \rightarrow {}^{237}\text{Np} \rightarrow {}^{233}\text{Pa} \rightarrow {}^{233}\text{U} \rightarrow {}^{229}\text{Th}$)
- Uranium series alpha-decay chain ($^{242}\text{Pu} \rightarrow {}^{238}\text{U} \rightarrow {}^{234}\text{U} \rightarrow {}^{230}\text{Th} \rightarrow {}^{226}\text{Ra} \rightarrow {}^{222}\text{Rn}$)
- ^{129}I - a non-sorbing radionuclide with a long half-life

This subset of radionuclides includes: (a) ^{129}I, ^{237}Np, ^{242}Pu, and ^{226}Ra, radionuclides that are commonly important to long-term dose calculations; and (b) decay chains where daughter ingrowth may be important. Within the two decay chains, ^{233}Pa and ^{222}Rn have very short half-lives (< 30 days) and are not included in the reference case. As the PA model matures, a formal radionuclide screening will be performed and a more comprehensive set of radionuclides will be included.

The mass inventory of these selected radionuclides in a reference case PWR UNF assembly (60 GWd/MTHM burn-up, 30-year OoR, 4.73% initial enrichment) is shown in Table 3-1. The half-lives and decay constants are shown in Table 3-2.

---

[1] Carter et al. (2012) use initial or beginning of life (BOL) uranium mass (i.e., metric tons uranium (MTU)) values when reporting inventory for commercial UNF. Initial MTU and metric tons initial heavy metal (MTIHM) are the same for commercial UNF since uranium is the only heavy metal present. The difference between initial MTU and final or end of life (EOL) MTU is small (<4%) for commercial UNF because fissile uranium is less than 5% of the heavy metal. The difference between MTIHM and EOL MTHM is similarly small. (Carter et al. 2012, Section 1.7).

[2] PWR used fuel-rod assemblies contain irradiated fuel discharged from commercial PWRs. Prior to irradiation, commercial PWR fuel assemblies contain a few hundred individual fuel rods, typically arranged in a square (e.g., 14x14 to 17x17) bundle that also includes spacer materials and neutron moderators. Each individual fuel rod consists of uranium oxide (UO_2) pellets encased in a zirconium alloy (zircaloy) or stainless steel cladding tube.

Table 3-1. UNF Radionuclide Inventory for the Reference Case

Isotope	Waste inventory mass[1] (g/MTHM)	Molecular weight[2] (g/mol)	Mass fraction[2] (g / g UNF)	Mole fraction (mol / g UNF)
^{238}U	9.10×10^{5}	238.05	6.32×10^{-1}	2.66×10^{-3}
^{237}Np	1.24×10^{3}	237.05	8.61×10^{-4}	3.63×10^{-6}
^{241}Am	1.25×10^{3}	241.06	8.68×10^{-4}	3.60×10^{-6}
^{242}Pu	8.17×10^{2}	242.06	5.68×10^{-4}	2.34×10^{-6}
^{129}I	3.13×10^{2}	129.00	2.17×10^{-4}	1.69×10^{-6}
^{234}U	3.06×10^{2}	234.04	2.13×10^{-4}	9.08×10^{-7}
^{230}Th	2.28×10^{-2}	230.03	1.58×10^{-8}	6.89×10^{-11}
^{233}U	1.40×10^{-2}	233.04	9.73×10^{-9}	4.17×10^{-11}
^{229}Th	6.37×10^{-6}	229.03	4.43×10^{-12}	1.93×10^{-14}
^{226}Ra	3.18×10^{-6}	226.03	2.21×10^{-12}	9.77×10^{-15}

[1]from Carter et al. (2012, Table C-1)
[2]from Sevougian et al. (2013, Table 1)

Table 3-2. Radionuclide Half-Lives and Decay Constants

Isotope	Half-Life (yrs)	Decay Constant (s^{-1})
^{238}U	4,470,000,000	4.91×10^{-18}
^{237}Np	2,140,000	1.03×10^{-14}
^{241}Am	432.7	5.08×10^{-11}
^{242}Pu	375,000	5.86×10^{-14}
^{129}I	15,700,000	1.40×10^{-15}
^{234}U	246,000	8.93×10^{-14}
^{230}Th	75,400	2.91×10^{-13}
^{233}U	159,300	1.38×10^{-13}
^{229}Th	7,300	3.01×10^{-12}
^{226}Ra	1,599	1.37×10^{-11}

modified from Vaughn et al. (2013a, Table 3-2)

3.2.2 Geologic Disposal System: Engineered Barrier System

The description of the reference case EBS includes the following components, updated from Sevougian et al. (2013, Section 2.2):

- Waste Form (Section 3.2.2.1)
- Waste Package (Section 3.2.2.2)
- Repository Layout (Section 3.2.2.3)
- Backfill (Section 3.2.2.4)
- Seals (Section 3.2.2.5)

3.2.2.1 Waste Form

As described in Section 3.2.1, the reference case inventory is limited to PWR UNF waste. Each irradiated PWR assembly is assumed to contain 0.435 MTHM and 1.44×10^6 g/MTHM of isotopes, with mass fractions of the selected radionuclides as listed in Table 3-1. This corresponds to a total mass of 6.27×10^5 g of isotopes per PWR assembly. The PWR waste forms are assumed to be predominantly UO_2 with zircaloy cladding. UO_2 has a solid density of 10.97 g/cm^3 (Lide 1999, p. 4-94). Therefore, the solid volume of a PWR assembly can be approximated by $(6.27\times10^5$ g/assembly$)/(10.97\times10^6$ g/m$^3) = 0.057$ m^3.

Typical dimensions for unirradiated PWR assemblies are lengths of 111.8 to 178.3 in (2.84 – 4.53 m) and widths of 7.62 – 8.54 in (0.19 – 0.22 m) (Carter et al. 2012, Table A-1). Based on these dimensions, the total volume of a PWR assembly can range from about 0.10 – 0.22 m^3. The uranium loading (0.435 MTHM per assembly) is consistent with loadings, burn-ups, and enrichments of PWR assemblies listed in Carter et al. (2012, Table A-3).

The release of radionuclides from UNF includes a fast/instant fraction – predominantly from radionuclides located in the fuel and cladding gap and grain boundaries, and a slower fraction – from radionuclides released from the UO_2 matrix through dissolution/conversion of the matrix. The release of radionuclides from UNF in a typical bedded salt environment is dependent on the presence of brine and the associated near-field geochemistry. During the period when in-drift temperatures are above or near boiling), waste form degradation may be limited because it is anticipated that heat will dry out the salt, and contact between brine and the waste will be diminished (Hansen and Leigh 2011, Section 2.5.1). After this thermal period (which may persist for several hundred years, see Figure 3-4), the reference case assumption is that the near-field brine exists under chemically-reducing conditions (Clayton et al. 2011, Section 3.1.2.6). However, Hansen and Leigh (2011, Section 2.5.2) note that a range of geochemical conditions are possible.

Information on radionuclide release from UNF in chemically-reducing environments is available from SKB (2010), albeit for a granite repository. The instant release fraction is different for different radionuclides. For ^{129}I, the instant release fraction has a mean of 0.025 and a standard deviation of 0.021 (SKB 2010, Table 3-15). The fractional degradation rate of the UO_2 matrix has a best estimate of 10^{-7} yr^{-1}, a lower limit of 10^{-8} yr^{-1}, an upper limit of 10^{-6} yr^{-1}, and log-triangular distribution (SKB 2010, Table 3-21). The best estimate fractional degradation rate corresponds to a waste form half-life of 4,800,000 yrs. Although not considered in the salt reference case, HLW borosilicate glass waste forms typically have faster degradation rates.

3.2.2.2 Waste Package

A waste package for long-term disposal generally consists of a waste canister (which may contain UNF, HLW, or other waste) and a surrounding overpack. A waste canister is generally sealed permanently at the point of origin, thereby avoiding any further direct handling or exposure of the waste during

successive operations. Overpacks provide economical means to meet different requirements such as heat dissipation, impact damage limits, and corrosion resistance. Designs for overpacks (and for canister loading within the overpacks) must consider storage, transportation, and disposal issues. Overpacks for storage and transport would be re-useable, whereas those for disposal would become permanent parts of the EBS at emplacement. (Hardin et al. 2012, Section 1.4.3)

Specific functions and characteristics of a UNF waste canister are described by Hardin et al. (2012, Section 1.4.3):

> *Canisters for [UNF] provide structural integrity and support to the fuel, criticality control, heat dissipation, containment during handling and repackaging, and may provide containment after permanent disposal. These functions are met using internal features such as the basket, thermal shunts, moderator exclusion features, neutron absorbers, flux traps, and inserts or fillers. To be included, these internal features must be engineered "up front" for all storage, transport, and disposal functions, for the containers to be permanently sealed at the point of origin.*
>
> *Typical [UNF] canisters are thin-walled (e.g., 15 mm) stainless steel structures, with internal stainless steel features to hold fuel assemblies and provide strength and rigidity. Canisters may have external features such as flanges, rings, trunnions, or skirts to facilitate handling. Neutron absorbing structures can be made from borated stainless steel, or other materials with protective coatings. Moderator exclusion can be addressed in container design by incorporating filler materials, or simply limiting the size of the containers and the quantities of SNF they contain. Canisters are sealed by welding (bolted closures receive less credit in transportation safety analyses, and require more frequent inspection).*
>
> *The most common materials considered for reducing environments are carbon steel, stainless steel, copper, and titanium …. Corrosion performance of waste package materials will also be a function of temperature, ionic strength, pH, and concentrations of halide ions.*

Specific functions and characteristics of an overpack are described by Hardin et al. (2013, Section 4.2):

> *Waste package overpacks could consist of low-alloy steel (or nodular cast iron, etc.) to maintain integrity throughout repository operations, and for a period of time after emplacement. The minimum time could be on the order of 50 years to facilitate retrieval as required by current regulation … The overpack could be made of corrosion-allowance material, and robust to withstand mechanical loading by salt creep during this period. Because moisture is scarce in the salt disposal environment, corrosion of such an overpack may be limited so that containment integrity is maintained for hundreds or thousands of years.*

Based on these general considerations, the salt reference case waste package is assumed to consist of a canister, containing 12 PWR UNF assemblies, and a disposal overpack. The 12-PWR assumption derives from thermal constraints, as described in Section 3.2.2.3. The PWR UNF assemblies will be permanently sealed in stainless steel canisters that are contained in disposal overpacks made of carbon steel with welded closures. The 12-PWR waste package has length of 5.0 m and a diameter of 1.29 m (Hardin et al. (2012, Table 1.4-1). These outer dimensions include a 5.0 cm thick overpack. This overpack thickness is considered sufficient to withstand general corrosion to ensure a retrievability period of 50 years (Sevougian et al. 2013, Section 2.2.3).

Each waste package has an outer volume of 6.53 m^3 and an inner volume of 5.45 m^3. The volume of solids initially inside a 12-PWR waste package includes the UNF waste forms (12 x 0.057 m^3 = 0.68 m^3), and various structural and internals components (approximately 1.5 m^3). Therefore, the reference case initial void fraction of the waste package (including the overpack) is assumed to be 0.50 and the volume fraction of waste form in the waste package (including the overpack) is 0.104. The 12-PWR loading results in 5.225 MTHM per waste package with an initial thermal output (at 30 years OoR) of 7.5 kW per waste package.

Corrosion of the carbon steel overpack materials and the stainless steel canisters in a typical bedded salt environment is dependent on the presence of brine and the associated near-field geochemistry. As noted in Section 3.2.2.1 for waste form degradation: (a) brine may be limited during the thermal period when in-drift temperatures are above or near boiling; and (b) after the several-hundred-year thermal period, the reference case assumption is that the near-field brine exists under chemically-reducing conditions. Under these conditions, limited waste package corrosion may result in waste package integrity being maintained for hundreds or thousands of years (Hardin et al. 2013, Section 4.2). Further waste package corrosion resistance may be provided through the use of corrosion resistant materials (e.g., copper, titanium) (Hardin et al. 2013, Section 1.4.3). However, due to the possibility of waste package mechanical damage from salt creep, the reference case assumes that the waste package fails instantaneously and does not provide any barrier capability.

Future iterations of the PA model will consider the effects of non-instantaneous waste package failure and will also consider different waste canisters (e.g., HLW) and overpacks, including larger-capacity DPCs (Hardin et al. 2013).

3.2.2.3 Repository Layout

As described in Section 3.1, the repository layout must consider various operational, mechanical, and thermal design constraints. To satisfy operational and mechanical constraints, the emplacements drifts are assumed to be 4 m high by 6 m wide and the central hallway is assumed to 4 m high by 8 m wide. The repository excavations (i.e., drifts and access hallway) are assumed to be in the vertical center of relatively pure salt (halite) unit at a depth of 680 m below ground surface (Section 3.2.3).

A semi-analytical approach to determine peak waste-package surface temperature as a function of waste package size and heat output (loading), burn-up, decay storage time (age OoR), and ventilation is described in Hardin et al. (2012, Section 3 and Appendix A). For the reference case waste inventory (12-PWR waste packages with 60 GWd/MTHM burn-up and no ventilation) the peak waste package surface temperature, for an assumed 20-m by 20-m waste package spacing, is approximately 275°C for 10-year OoR waste and 130°C for 50-year OoR waste (Hardin et al. 2013, Table 4-2). Simple interpolation suggests that, for the reference case 30-year OoR aging, a 20-m by 20-m waste package spacing would approximately satisfy the peak waste package surface temperature constraint of 200°C (Section 3.1). In all cases, the peak temperatures are lower for lower burn-up (e.g., 40 GWd/MTHM) fuel.

The semi-analytical approach was also used to calculate peak temperatures for the reference case waste with a 20-m by 10-m waste package spacing (Sevougian et al. 2013, Section 2.2.1.3). With the closer spacing, OoR aging of between 50 and 70 years is required to satisfy the 200°C temperature constraint (Figure 3-4). Although this required OoR aging is longer than the 30-year OoR assumption for the reference case inventory (Section 3.2.1), the 20-m by 10-m spacing is nonetheless adopted for the salt reference case. Specifically, the reference case spacing will be 20 m between drift centers and 10 m between waste package centers in each drift. The various parameters controlling the thermal constraint and the peak temperature will be refined as the PA model matures.

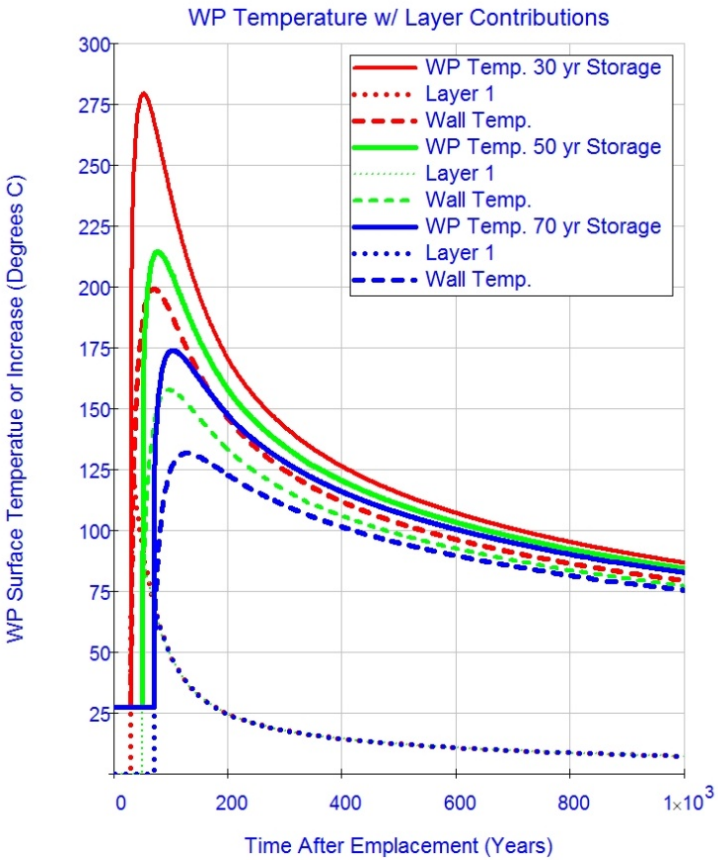

(60 GWd/MTHM 12-PWR waste packages with 20 m by 10 m spacing (from Sevougian et al. 2013, Figure 4)

Figure 3-4. Temperatures at the Waste Package Surface and Drift Wall for the Salt Repository Reference Case for Various Decay Storage Times

Based on the reference case repository layout (20 m between drift centers and 10 m between waste package centers), the overall repository dimensions can be calculated. The calculation is based on the emplacement of reference case 12-PWR UNF waste packages (with 5.225 MTHM per waste package) to a repository capacity of approximately 70,000 MTHM and emplacement drifts that each contain 80 waste packages. The resulting reference case repository dimensions are listed in Table 3-3. These dimensions correspond to the layouts shown schematically in Figure 3-1 and Figure 3-2, based on drift pairs separated by a central access hallway.

Table 3-3. Dimensions for the Salt Repository Reference Case Layout

Parameters	Value
Waste Package (WP)	
WP length (m)	5.00
WP outer diameter (m)	1.29
WP center-to-center spacing in-drift (m)	10.0
Inventory per 12-PWR WP (MTHM)	5.225
Approx. number of WPs for 70,000 MTHM	13,397.4
Emplacement Drift	
Drift height (m)	4.0
Drift width (m)	6.0
Drift center-to-center spacing (m)	20.0
Pillar width (m)	14.0
Number of WPs per drift	80
Drift seal length (m)	10.0
Drift length, including seals (m)	805.0
Central access hallway height (m)	4.0
Central access hallway width (m)	8.0
Approx. number of drifts needed for 70,000 MTHM	167.5
Repository	
Number of drift pairs (rounded up)	84
Repository length (m)	1,618.0
Repository width (m)	1,666.0
Repository Depth (m)	680.0
Total length of all drifts (m)	135,240

With a waste package length of 5.0 m and a 10 m center-to-center spacing, each 80-waste-package drift will have an alternating sequence of a 5-m long waste package and 5-m length of backfill (see Figure 3-1). At the end of the drift nearest the central access hallway, the drift seal will be 10 m long. The total number of drifts (arranged in pairs) is determined by the total inventory, and rounded up for emplacement flexibility. The total repository length includes the length of a drift pair and the central access hallway. The total repository width includes the widths of the 84 drift pairs and the separating salt pillars.

A typical repository layout also includes vertical shafts from the ground surface that intersect the excavated area (e.g., in the central access hallway) (Figure 2-2). Repository shafts may be needed during operations for a number of reasons, including: underground access for personnel and equipment, waste handling, salt handling, and ventilation. The salt disposal reference case includes a stylized representation of a single shaft that intersects the central access hallway between a drift pair. The stylized shaft is used to represent the possible effects of multiple shafts.

The design of the stylized single shaft is based on the shaft design from the WIPP (SNL 1996). Dimensions of the four WIPP shafts (salt handling, waste handling, air intake/ventilation, and exhaust) are shown in Table 3-4. Separate dimensions are given for the lower shaft – the portion in the Salado halite formation, and the upper shaft – the portion overlying the Salado formation. The stylized reference case shaft is assumed to have a cross-sectional area that is similar to combined cross-sectional area of the four WIPP shafts and a total length of 680 m from the ground surface to the depth of the excavated drifts. From Table 3-4, the combined cross-sectional area of the excavated diameters of the lower portion of the

four WIPP shafts is 85.7 m^2. This results in an effective single reference case shaft diameter of 10.45 m. Shaft seals are described in Section 3.2.2.5.

Table 3-4. Dimensions for the WIPP Shafts

	Salt Handling Shaft	Waste Handling Shaft	Air Intake Shaft	Exhaust Shaft
Upper Shaft				
Excavation diam. (m)	3.61 (11'10")	6.30-6.81 (20'8"-22'4")	6.17 (20'3")	4.78-5.08 (15'8"-16'8")
Excavation cross-sectional area (m^2)	10.2	31.2 - 36.4	29.9	17.9 - 20.3
Depth (of liner) (m)	255.6 (838.5')	247.5 (812')	248.7 (816')	257.9 (846')
Lower Shaft				
Excavation diam. (m)	3.61 (11'10")	6.10 (20')	6.17 (20'3")	4.57 (15')
Excavation cross-sectional area (m^2)	10.2	29.2	29.9	16.4
Depth (bottom) (m)	653.5 (2144')	652.9 (2142')	648.6 (2128')	654.7 (2148')

from SNL (1996, Table 4-2)

3.2.2.4 Backfill

The reference case backfill design is summarized from Sevougian et al. (2013, Section 2.2.4). The salt reference case assumes that waste packages will be emplaced on the drift floor and covered with crushed salt backfill after waste packages are emplaced. The backfill will begin consolidating as drifts and access hallways close due to creep of the salt host rock. Past field experience (DOE 2012b), supplemented by simulations, shows that backfill reconsolidates rather quickly. For example, simulations using the multi-mechanism model for creep deformation of the intact host rock (Munson et al. 1989) and a model for creep behavior of crushed salt (Callahan 1999) indicate that the reconsolidation of backfill will be mostly complete in approximately 200 years (Clayton et al. 2012).

The backfill is expected to consolidate to a condition of similar to the original intact salt host rock (Hansen and Leigh 2011, Section 2.4.1.7). A number of literature sources are available for the porosity and permeability of crushed salt backfill, as compiled in Jove-Colon et al. (2012, Part VI, Section 1.5.1); however, this is still an active area of research (Hansen et al. 2012). For the reference case, the porosity and permeability of the consolidated backfill is assumed to be the same as for the crushed-salt component of the WIPP shaft seal, which is expected to consolidate to a state close to that of the surrounding intact rock within approximately 200 years (DOE 2009, Section PA-2.1.3). Permeability and porosity values for the crushed salt seal component can be drawn from the lower portion (in the Salado halite) of the WIPP "simplified" shaft seal in the WIPP parameter database (Fox 2008) for the 2009 Compliance Recertification Application (DOE 2009).

Permeability and porosity values for the WIPP simplified shaft seal in Fox (2008) are average values for a multi-component (clay, asphalt, concrete, and crushed salt) system (James and Stein 2002). The permeability average is taken to be a harmonic mean, which means it is most strongly influenced by the lowest permeability component (i.e., the crushed salt component). The porosity average is taken to be a volume-weighted arithmetic mean. Based on the WIPP simplified shaft seal data, the reference case backfill porosity is 0.113 (Fox 2008, Table 19) and the reference case backfill log permeability (m^2) has a mean of -18.0 (1.0×10^{-18} m^2) (Fox 2008, Table 4) and a distribution as shown in Table 3-5.

Table 3-5. Cumulative Distribution of Log Permeability for the Reference Case Backfill

Value (m^2)	–20.0	–19.5	–19.0	–18.5	–18.0	–17.5	–17.0	–16.5
Percentiles	0	0.01	0.10	0.31	0.64	0.87	0.99	1

from Fox (2008, Parameter Sheet 69): Cumulative distribution of the log of intrinsic permeability for the lower portion of the WIPP simplified shaft seal from 0 to 200 years.

The permeability values for the reference case backfill in Table 3-5 correspond to the permeability of the lower portion of the WIPP "simplified" shaft seal system from 0 to 200 years. Although the reference case backfill is consolidated, the 0-to-200-year (i.e., unconsolidated) WIPP shaft seal data is considered representative. That is because the consolidation of the WIPP shaft seal is enhanced by the addition of 1 wt. % water (Hansen et al. 2012, Section 4.1.1) that might not be used in emplacement drift backfill (although decay heat could enhance the drift backfill consolidation—or at least its rate of consolidation).

3.2.2.5 Seals

Shaft and drift seals will be used to isolate the emplacement drifts and to limit water or radionuclide migration along the shafts.

The reference case shaft seal design is summarized from Sevougian et al. (2013, Section 2.2.5). The reference case shaft seal is based on the WIPP shaft seal system, a multi-component barrier consisting of clay, asphalt, concrete, and crushed salt components (James and Stein 2002, Figure 1). For the reference case, the permeability and porosity of shaft seal are assumed to be the same as for the consolidated (i.e., after 200 years) lower portion of the WIPP "simplified" shaft seal system. The reference case shaft seal porosity is 0.113 (Fox 2008, Table 19) and the reference case log permeability (m^2) has a mean of -19.8 (1.6×10^{-20} m^2) (Fox 2008, Table 4) and distribution as shown and a distribution as shown in Table 3-6.

Table 3-6. Cumulative Distribution of Log Permeability for the Reference Case Shaft Seal

Value (m^2)	–22.5	–22.0	–21.5	–21.0	–20.5	–20.0	–19.5	–19.0	–18.5	–18.0
Percentiles	0	0.02	0.08	0.17	0.31	0.53	0.70	0.87	0.97	1

from Fox (2008, Parameter Sheet 70): Cumulative distribution of the log of intrinsic permeability for the lower portion of the WIPP simplified shaft seal from 200 to 10,000 years.

The reference case drift seal is assumed to have the same properties as the backfill (Section 3.2.2.4).

3.2.3 Geologic Disposal System: Natural Barrier System

The natural barrier system (NBS) encompasses the geologic setting of the generic bedded salt repository, including the DRZ. As noted in Section 3.1, the reference case bedded salt formation is assumed to be a relatively pure salt unit (e.g., halite) within a vertically and laterally extensive bedded salt formation that includes clay and/or anhydrite interbeds. Stratigraphy and dimensions of the reference case salt repository NBS, shown in Figure 3-5, are updated from Sevougian et al. (2013, Section 2.3).

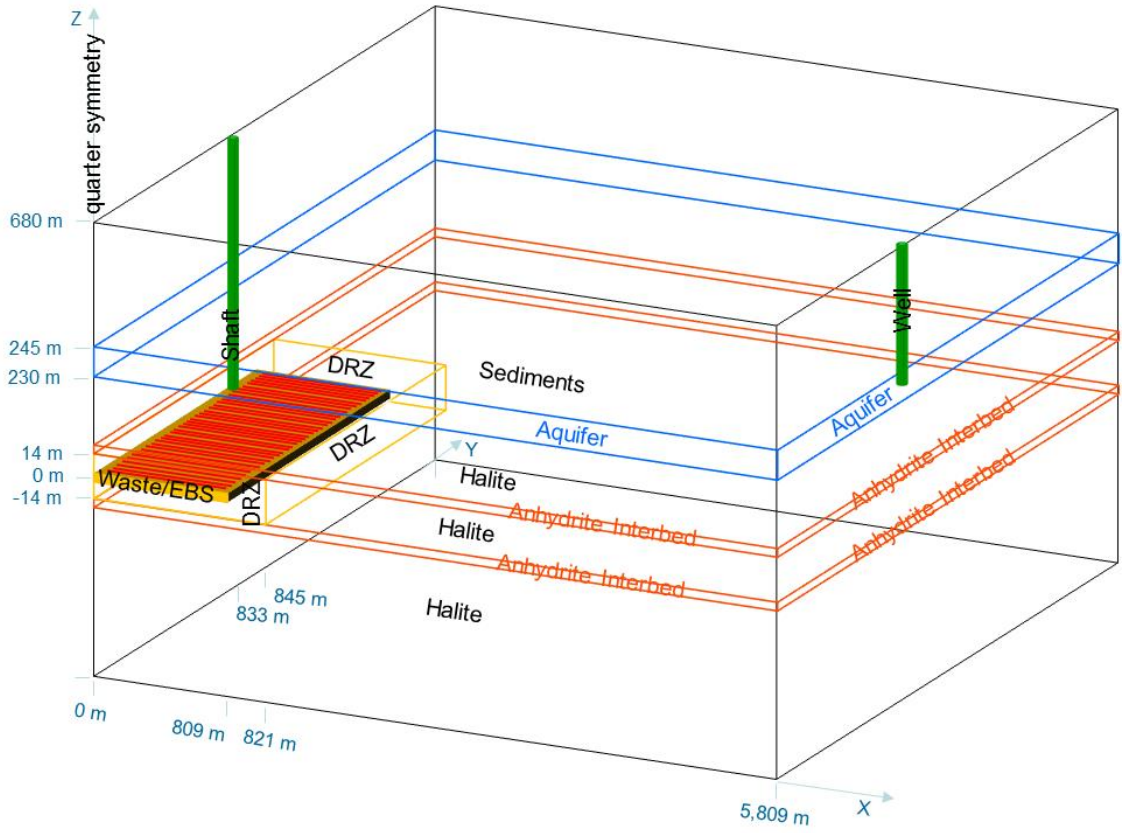

(Not to scale)

Figure 3-5. Salt Repository Reference Case Dimensions

The reference case stratigraphy draws on information and characteristics (e.g., depth, thickness, and areal extent) representative of five major bedded salt formations in the United States: Paradox Basin (Hermosa Formation), Permian Salt Basin, Michigan and Appalachian Basins (Salina Formation), Williston Basin, and Supai Basin (Sevougian et al. 2012, Table 3-1). Based on this information, the reference case assumes a depth to the top of the bedded salt formation of 450 m (with a range of approximately 300 m to 1,100 m (~1,000 to 3,600 ft)), a thickness of 460 m (with a range of approximately 75 m to 550 m (~250 to 1,800 ft)), and an areal extent of 11,618 m by 11,666 m (~135 km^2 or 52 sq. mi.). There are numerous locations throughout the Paradox, Permian, Michigan, Appalachian, and Williston Basins (but not the Supai) that have bedded salt with these ranges of depth, thickness, and areal extent, such that there are many regional and national siting options for a bedded salt repository (Sevougian et al. 2012, Section 3.2.3).

The thickness of the reference case host salt formation refers to the combined thickness of relatively pure halite and interbeds. Determination of this thickness in actual salt formations is somewhat subjective because it depends on the purity level of the halite and the tolerance for the presence of interbeds and the thickness of these interbeds. For the reference case, the 460-m-thick bedded salt host formation is assumed to consist of an alternating sequence of halite units and anhydrite interbeds that is represented by a stylized stratigraphy (Figure 3-5) consisting of: a 28-m-thick intact halite unit vertically centered at the repository horizon (i.e., at a depth of 680 m); 1-m-thick anhydrite interbeds located directly above and below the repository horizon halite unit; and intact halite units above and below the interbeds.

In addition to the halite and interbed units of the host salt formation, the reference case stratigraphy also includes an aquifer above the repository and an underlying unit that may contain regions of over-pressured fluid (i.e., a pressurized brine reservoir).

The reference case areal extent is based on the assumption (Section 3.2.5) that the distance to the biosphere (i.e., the receptor location) is 5 km from the edges of the underground excavations (defined by the repository dimensions in Table 3-3). The halite, interbed, and aquifer units of the reference case are assumed to be uniform over the lateral extent of the repository and the entire underground area encompassed by the 5-km boundary.

The geologic setting of the reference case NBS components is described further in the following subsections, updated from Sevougian et al. (2013, Section 2.3):

- Disturbed rock zone (Section 3.2.3.1)
- Host rock halite (Section 3.2.3.2)
- Host rock interbeds (Section 3.2.3.3)
- Aquifer (Section 3.2.3.4)
- Pressurized brine reservoirs (Section 3.2.3.5)
- Thermal and Chemical Environment (Section 3.2.3.6)

3.2.3.1 Disturbed Rock Zone

As described in Section 2.1, the DRZ is the portion of the host rock adjacent to the EBS that experiences durable (but not necessarily permanent) changes due to the presence of the repository. The DRZ tends to be more disturbed early in the postclosure period when thermal and excavation effects are greatest. At later times, healing tends to restore the DRZ closer to ambient conditions (i.e., similar to the undisturbed halite), particularly in a salt repository. For the reference case, the extent of the DRZ is assumed to be 3 drift diameters or about 12 meters and surrounds all sides of the excavation (Sevougian et al. 2012, Section 3.2.3.2).

The reference case DRZ porosity is assumed to be 0.0129 (Fox 2008, Table 33) and the log permeability (m^2) is assumed to be uniform over a range of –19.4 to –12.5, with a mean of -15.95 (1.1×10^{-16} m^2) (Fox 2008, Table 4 and Parameter Sheet 64).

3.2.3.2 Host Rock Halite

The host rock halite is assumed to be the relatively pure, intact halite portions (halite content > 50%) of the bedded salt formation that lie outside of the DRZ. In reality, “intact” halite contains interbeds and other seams of impurities (Section 3.2.3.3). However, as described in Section 3.2.3, the reference case host rock halite assumes the presence of a 28-m-thick intact halite unit vertically centered at the repository horizon (i.e., at a depth of 680 m) and additional thicker intact halite units above and below the anhydrite interbeds (Figure 3-5). Other interbeds and/or non-halite seams within the intact halite are assumed to be thin (less than tens of centimeters thick) and to not have an influence on the overall halite properties.

The reference case porosity for these intact halite units has a mean of 0.0182, derived from a cumulative distribution with minimum (zeroth percentile) of 0.001, a median (50^{th} percentile) of 0.01, and a maximum (100^{th} percentile) of 0.0519 (Fox 2008, Table 4 and Parameter Sheet 52). The reference case log permeability (m^2) for these intact halite units has mean of -22.5 (3.1×10^{-23} m^2) and a uniform distribution over the range of –24 to –21 (Fox 2008, Table 4 and Parameter Sheet 53)

3.2.3.3 Host Rock Interbeds

Interbeds consisting of non-halite stringers (such as anhydrite, clay, or polyhalite) with thicknesses on the order of centimeters to meters are commonly observed throughout the major U.S. bedded salt deposits. These interbeds and seams are more permeable than the surrounding halite and may become fractured as a

result of repository excavation and/or gas generation from waste degradation, thereby serving as potential preferential pathways for water seepage and/or radionuclide migration.

For the reference case, two 1-m thick anhydrite interbeds are assumed to be present, one immediately above the DRZ and one immediately below the DRZ (Figure 3-5). The reference case anhydrite interbed porosity is assumed to be 0.011 (Fox 2008, Table 31) and the log permeability (m^2) is assumed to have a Student-t distribution over a range of –21.0 to –17.1, with a mean of -18.9 (1.3×10^{-19} m^2) (Fox 2008, Table 4 and Parameter Sheet 55).

3.2.3.4 Aquifer

The generic bedded salt reference case includes an aquifer above the repository. The location and characteristics of the aquifer are important considerations because the aquifer may provide a potential pathway (directly or through a withdrawal well) to the receptor location in the biosphere.

The water in aquifers located in the vicinity of salt deposits is usually too brackish to be potable for direct human consumption, but these waters are often used to support other agricultural or ranching activities; deeper aquifers are progressively more saline (Sevougian et al. 2012, Section 3.2.3.2). However, for the reference case the water is assumed to be potable.

The reference case aquifer is assumed to be a saturated single-porosity formation in the regional groundwater basin containing the repository, located 230 m above the centerline of the repository (Figure 3-5). The aquifer is assumed to have a uniform effective thickness (water-producing interval) of 15 m (Sevougian et al. 2012, Section 3.2.3.2), a constant porosity, and a homogeneous permeability. It is assumed to behave as a porous medium with a constant regional Darcy velocity in the portion of the aquifer that might communicate with both the repository horizon and the biosphere location. As a generic approximation, the aquifer is assumed to have the properties of a dolomite, which a common water-producing unit in bedded salt formations. Dolomite units can have porosity ranging from of 0.00 to 0.20 (Freeze and Cherry 1979, Table 2.4) and log permeability (m^2) ranging from -16.0 to -12.0 (Freeze and Cherry 1979, Table 2.2). It is assumed that the water-producing reference case dolomite would have properties toward the upper end of these ranges. Representative properties for a water-producing dolomite (the Culebra dolomite overlying WIPP) are a porosity of 0.151 and a log permeability (m^2) of -13.1 (Fox 2008, Table 26). The Culebra dolomite also has a lateral hydraulic gradient for flow of approximately 0.001 (Hart et al. 2009, Figure 3-11 and Appendix C). Based on all of this information, the reference case dolomite aquifer is assumed to have a porosity of 0.15, with a range of 0.10 to 0.20, a log permeability (m^2) of -13.0, with a range of -14.0 to -12.0, and a hydraulic gradient of 0.001.

3.2.3.5 Pressurized Brine Reservoir

Pressurized brine reservoirs (i.e., in excess of depth-based hydrostatic pressure) are common in some of the larger bedded salt deposits because of the sealing properties of salt under large lithostatic loads. Because these regions, if they exist, are located outside of the repository horizon, they are not expected to influence undisturbed performance. They will be considered when the reference case is expanded to included consideration of disturbed scenarios, where such a region could be hydrologically connected to the repository via a human intrusion borehole. Properties of a representative pressurized brine reservoir are reported in Fox (2008, Table 44).

3.2.3.6 Thermal and Chemical Environment

The temperature, fluid saturation, and fluid (brine) composition in the EBS and NBS are important because they control the thermal and chemical environment in the disposal system, which in turn controls the degradation of the waste and the subsequent release and transport of radionuclides.

As noted in Section 3.2.2.3, the repository layout is designed, based on reference case waste package thermal loading, to maintain in-drift temperatures below 200°C. Figure 3-4 shows that, for the reference case waste package design and layout, in-drift temperatures should be below 100°C after about 600 years, declining to the far-field ambient temperature of 25°C. As noted in Section 3.2.2.1, the reference case assumption is that near-field brine exists under chemically-reducing conditions after this approximately 600-year thermal period. The far-field brine, which is less affected by temperature, is assumed to exist under less reducing or slightly oxidizing conditions (Clayton et al. 2011, Section 3.1.2.6).

The host rock brine composition is important because it establishes the initial chemical conditions from which the chemical environment in the repository evolves. Brine composition is site-specific and varies significantly across the different representative bedded salt formations. For the reference case, the host rock brine composition is assumed to be that of Michigan Basin Devonian Brine because it generally lies within the ranges of the other formation brines (Sevougian et al. 2012, Section 3.2.3.2). Table 3-7 summarizes important reference case brine characteristics.

Table 3-7. Reference Case Brine Composition

Characteristic	Reference Values[1]
$[Na^+]$	12,400 - 103,000 mg/l
$[Mg^{2+}]$	3,540 - 14,600 mg/l
$[K^+]$	440 - 19,300 mg/l
$[Ca^2]^+$	7,390 - 107,000 mg/l
$[SO_4^{2-}]$	0 - 1,130 mg/l
$[Cl^-]$	120,000 - 251,000 mg/l
pH	3.5 - 6.2
Specific Gravity	1.136 - 1.295
Density (kg/m^3)	1220.0[2]

[1] from Wilson and Long (1993) as summarized in Sevougian et al. (2013, Table 3-2)
[2] from Fox (2008, Table 29)

The chemical environment also influences radionuclide transport, specifically through its effect on diffusion, solubility, and sorption.

3.2.3.6.1 Diffusion

Radionuclides that are released from the waste form (either as part of the instant release fraction or by slower UO_2 matrix dissolution/conversion) are most commonly transported away from the waste package in dissolved form through advection or diffusion. Due to the low reference-case permeabilities in the salt units, diffusion is expected to be a dominant transport mechanism. Diffusive flux is a function of concentration gradient, porosity, saturation, and a diffusion/dispersivity tensor (Lichtner and Hammond 2012a, Equation 88) and can also be affected by size and charge effects and by sorption. The diffusion/dispersivity tensor is commonly represented by a hydrodynamic dispersion coefficient tensor, which combines the effects of mixing due to mechanical dispersion and of molecular diffusion in response to a concentration gradient (Freeze and Cherry 1979, Equation 9.4). The quantification of hydrodynamic dispersion requires specification of parameters controlling molecular diffusion (i.e., the bulk diffusion coefficient, which is the product of the free water diffusion coefficient and the tortuosity) and mechanical dispersion (i.e., the product of the dispersivity and the groundwater pore velocity). For the salt repository reference case, the free water diffusion coefficient is assumed to be 2.30×10^{-9} m^2/s (Cook and Herczeg 2000, Table A3), and radionuclide-specific effects (e.g., due to size and charge) are not considered. Porosity of the various material features (e.g., backfill, seals, rock units) are reported in

prior sections. Groundwater pore velocity is only significant in the aquifer (Section 3.2.3.4). For the other material-specific properties affecting diffusion, the following values are assumed to apply in all material regions: tortuosity = 1 (conservative assumption that maximizes diffusion) and longitudinal dispersivity = 1 m.

3.2.3.6.2 Solubility

The mass of any particular element that can dissolve in the local groundwater (brine) depends on the elemental solubility. If the mass of an element available for dissolution would lead to dissolved concentrations greater than the aqueous solubility, then some of the mass will precipitate and the dissolved concentration of that element will be limited. The dissolved concentrations in turn provide the radionuclide source for advection and diffusion to the surrounding EBS and NBS. Solubility limits are a function of various radionuclide and fluid (brine) properties, such as temperature, redox conditions, and pH. Solubility limits for the reference case elements are listed in Table 3-8. These reference case solubilities are for concentrated brine in a bedded salt formation at 25°C, assumed to be representative of the near-field chemically-reducing conditions (Clayton et al. 2011, Section 3.1.2.6).

Table 3-8. Solubility Limits for Reference Case Elements

Element	Uncertainty Distribution (mol/L)	Deterministic Value (mol/L)
U	Triangular Min: 4.89×10^{-8}; Max: 2.57×10^{-7}; Mode: 1.12×10^{-7}	1.12×10^{-7}
Np	Triangular Min: 4.79×10^{-10}; Max: 4.79×10^{-9}; Mode: 1.51×10^{-9}	1.51×10^{-9}
Am	Triangular Min: 1.85×10^{-7}; Max: 1.85×10^{-6}; Mode: 5.85×10^{-7}	5.85×10^{-7}
Pu	Triangular Min: 1.40×10^{-6}; Max: 1.53×10^{-5}; Mode: 4.62×10^{-6}	4.62×10^{-6}
I	No Distribution	Unlimited
Th	Triangular Min: 2.00×10^{-3}; Max: 7.97×10^{-3}; Mode: 4.00×10^{-3}	4.00×10^{-3}
Ra	No Distribution	Unlimited

from Clayton et al. (2011, Table 3.1-4)

3.2.3.6.3 Sorption

Advective and diffusive transport may be retarded by sorption of radionuclides onto solid surfaces, e.g., engineered materials, degradation products, and/or soils. For the reference case, sorption is assumed to be represented by a linear isotherm, quantified by a distribution coefficient, K_d (Freeze and Cherry 1979, Equations 9.12 and 9.13). The K_d value is a measure of the ratio of the sorbed mass (mass sorbed on the solid phase per unit mass of solid phase) to the dissolved concentration, and has units of volume aqueous phase/mass solid phase, typically reported as ml_{water}/g_{rock}. K_d values are a function of various radionuclide, fluid (brine), and rock properties. Reference case K_d values are listed in Table 3-9. These reference case K_d values are for sorption onto anhydrite in a bedded salt formation (Clayton et al. 2011, Section 3.1.2.7), and are assumed to be representative of sorption in all of the salt-containing regions in the reference case domain.

Table 3-9. Distribution Coefficients (K_d) for Reference Case Elements

Element	Uncertainty Distribution (ml/g)	Deterministic Value (ml/g)[1]
U	Uniform Min: 0.2; Max: 1.0	0.6
Np	Uniform Min: 1.0; Max: 10.0	5.5
Am	Uniform Min: 25; Max: 100	62.5
Pu	Uniform Min: 70; Max: 100	85.0
I	No Distribution	0.0
Th	Uniform Min: 100; Max: 1000	550.0
Ra[2]	Uniform Min: 1; Max: 80	40.5

[1] from Clayton et al. (2011, Table 3.1-7)
[2] from Vaughn et al. (2013a, Table C-1)

In PFLOTRAN, linear sorption is implemented using a partition coefficient, K_d^P, defined in units of mass of water in the aqueous phase/bulk volume of solid phase (kg_{water}/m^3_{rock}) (Lichtner and Hammond 2012a, Section 3.2.1). The relationship between the PFLOTRAN K_d^P (in kg/m^3) and the more traditional K_d (in ml/g) is:

$$K_d^P = K_d \ \rho_{rock}(1-n)\rho_w \cdot 10^{-3} \qquad \text{Eq. (3-1)}$$

Where ρ_{rock} is the rock solid density in kg/m^3, n is the rock porosity, and ρ_w is the density of water in the aqueous phase in kg/m^3. For the reference case, the conversion from K_d in salt (Table 3-9) to PFLOTRAN K_d^P assumes a water density of 1,000 kg/m^3, a rock solid density of 2,820 kg/m^3 (Fox 2008, Table 26), and a rock (halite) porosity of 0.0182 (Section 3.2.3.2).

3.2.4 Biosphere

As described in Section 2.2.1.5, the conceptualization of the biosphere is typically specified by regulation and can vary between different national radioactive waste disposal programs. For the salt repository reference case, the biosphere conceptualization is based on the International Atomic Energy Agency (IAEA) BIOMASS Example Reference Biosphere 1B (ERB 1B) dose model (IAEA 2003, Sections A.3.2 and C.2.6.1). The ERB 1B dose model assumes that the receptor is an individual adult who obtains drinking water from a pumping well drilled into the aquifer. In the salt repository reference case radionuclides can reach the aquifer directly via the shaft, or by upward transport through the halite. Figure 3-5 shows the shaft, aquifer, and pumping well.

Dissolved radionuclide concentrations in the aquifer are converted to estimates of annual dose to the receptor (dose from each radionuclide and total dose) using ERB 1B dose model parameters, which include the well pumping rate, the water consumption rate of the receptor, and radionuclide-specific dose conversion factors. Determination of dose model parameter values depends on the characteristics of the biosphere (e.g., climate) and the habits of the population (receptor) in that biosphere. Dose model parameters are not currently specified, but will be determined as the PA model matures.

3.2.5 Regulatory Environment

A PA model implementation typically requires certain assumptions based on the regulatory environment. The following reference case assumptions consider U.S. Environmental Protection Agency (EPA) and U.S. Nuclear Regulatory Commission (NRC) regulations (40 CFR 197 and 10 CFR 63), and address 40 CFR 191 and 10 CFR 60, where appropriate, as outlined by Sevougian et al. (2013, Section 2.5):

- The PA model will be based on a screening of FEPs for 10,000 years after repository closure, with the provision that the long-term impacts of certain disruptive events (e.g., seismicity, volcanism, and climate change) must be considered for 1,000,000 years.
- UNF and HLW are assumed to be retrievable for a period of 50 years after waste emplacement operations are initiated.
- The distance to the accessible environment (receptor location) is assumed to be 5 km.
- Annual dose will be used as a metric for repository performance for these preliminary assessments.
- The effects of human intrusion will be represented though a stylized intrusion borehole.

3.3 Application of the Salt Disposal System Model

This section describes simulation results from the application of the enhanced PA modeling capability described in Section 2 to the salt repository disposal concept and reference case described in Sections 3.1 and 3.2. Preliminary FEP analysis and scenario development, consistent with the reference case, is described in Section 3.3.1. PA model construction is described in Section 3.3.2, with PA model results presented in Section 3.3.3 for a deterministic baseline simulation, and Section 3.3.4 for probabilistic sensitivity simulations.

The simulations described in this section represent an initial demonstration of the enhanced salt repository PA modeling capability. While the results are based on representative reference case properties (Section 3.2), they are not intended to be used to evaluate the potential performance of an actual bedded salt repository.

3.3.1 Generic Salt Repository FEP and Scenario Analysis

FEP and scenario analysis methodologies are described in Freeze et al. (2013c, Section 4.2). As noted in Section 2.1 and in Sevougian et al. (2013, Section 1), the current focus of the reference case is on FEPs for undisturbed scenarios.

A list of 208 FEPs potentially relevant to a generic salt repository was compiled by Sevougian et al. (2012, Appendix A), based on a generic UFDC FEP list (Freeze et al. 2011, Appendix A). Sevougian et al. (2012, Section 3.1.2 and Appendix A) identified preliminary screening recommendations for these FEPs (e.g., included, excluded, site- and/or design-specific information needed, or further technical evaluation needed), based on a generic salt repository design and concept of operations similar to the reference case described in this report. Figure 3-6 provides a schematic illustration of the key phenomena (representative of the likely included FEPs for the reference case) identified as important to the long-term performance of a generic salt repository under undisturbed conditions.

The FEP analysis will be updated as the salt repository reference case and PA model mature. Additionally, Freeze et al. (2013d) presented a new FEP classification methodology, using a 2D matrix structure, to organize the 208 generic salt repository FEPs. The FEP matrix approach will be incorporated into the next iteration of the FEP analysis for the generic salt repository

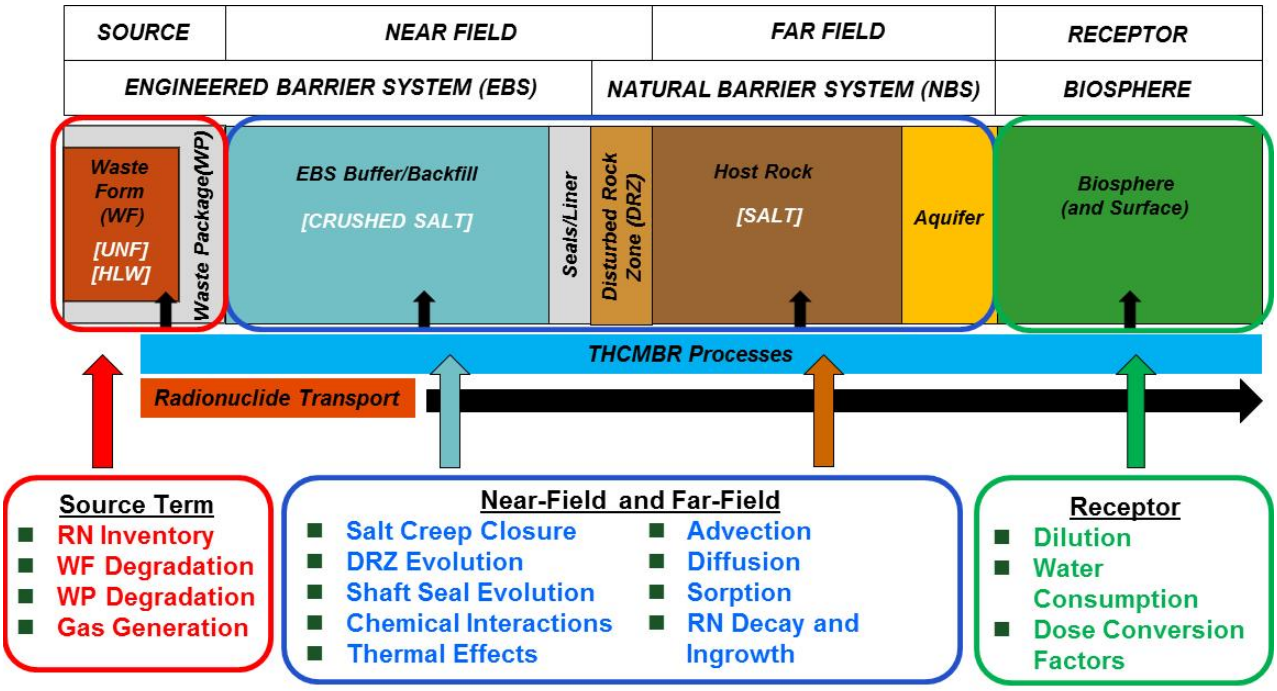

Figure 3-6. Key Phenomena for the Salt Repository Reference Case (Undisturbed Scenario)

3.3.2 Salt Repository PA Model Demonstration

The reference case salt repository is assumed to contain approximately 70,000 MTHM, distributed throughout 84 pairs of emplacement drifts (168 total drifts), where each drift is 809 m long and contains 80 waste packages of 12-PWR UNF (Table 3-3). The reference case conceptual model domain is shown schematically in quarter symmetry in Figure 3-5. In the EBS, 42 emplacement drifts, each containing waste packages, are shown (in red) along with the stylized shaft. In the NBS, the DRZ, host rock halite, anhydrite interbeds, and overlying aquifer are shown. The biosphere (receptor location) is assumed to be located at the ground surface directly above the withdrawal well, at a distance of 5,000 m laterally from the edges of the emplacement drifts.

The model of the reference case includes only a single 805 m drift containing 80 waste packages. The bottom of the model domain is a horizontal (X-Y plane) symmetry boundary imposed through the vertical center of the EBS (i.e., at elevation 0 m in Figure 3-5), and the top of the model domain is the top of the aquifer (i.e., at elevation 245 m in Figure 3-5). The resulting three-dimensional model domain is 5,809 m long (242 grid cells) in the x-direction, 20 m wide (5 grid cells) in the y-direction, and 245 m high (38 grid cells) in the z-direction, as shown in Figure 3-7 (X-Z plane, side view) and Figure 3-8 (X-Y plane, top view). The model domain includes the following regions, shown in Figure 3-7 and Figure 3-8 with their dimensions, which correspond to the EBS and NBS features described in Section 3.2: waste package (which includes the waste form); backfill; DRZ; sealed shaft; intact halite units; anhydrite interbeds; and an aquifer. The model domain also includes a portion of the central access hallway, which is assumed to be backfilled, salt pillars adjacent to the modeled drift, which are assumed to be similar to the DRZ, and a groundwater sample well, which provides dissolved radionuclide concentrations that are used as a surrogate performance indicator for dose.

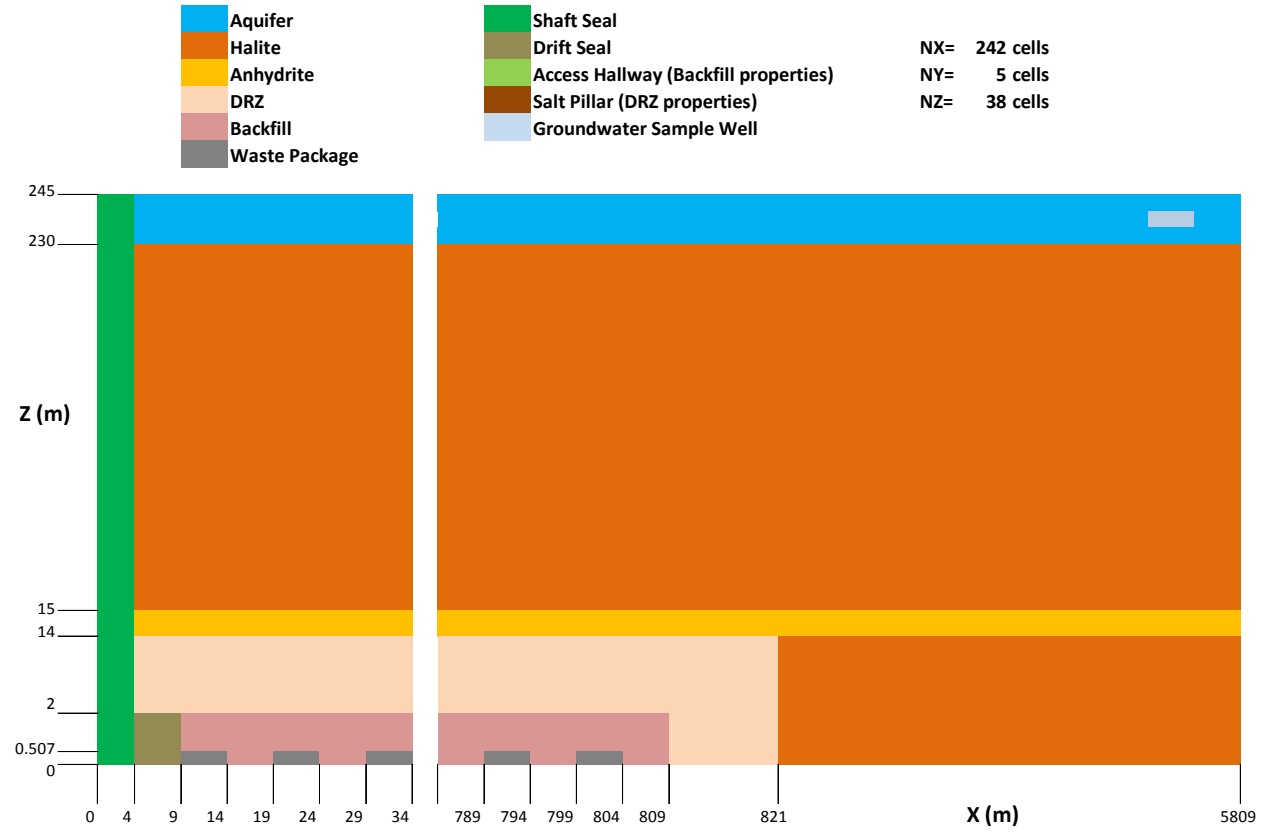

(Not to scale)

Figure 3-7. Salt Repository Reference Case Model Regions X-Z Plane

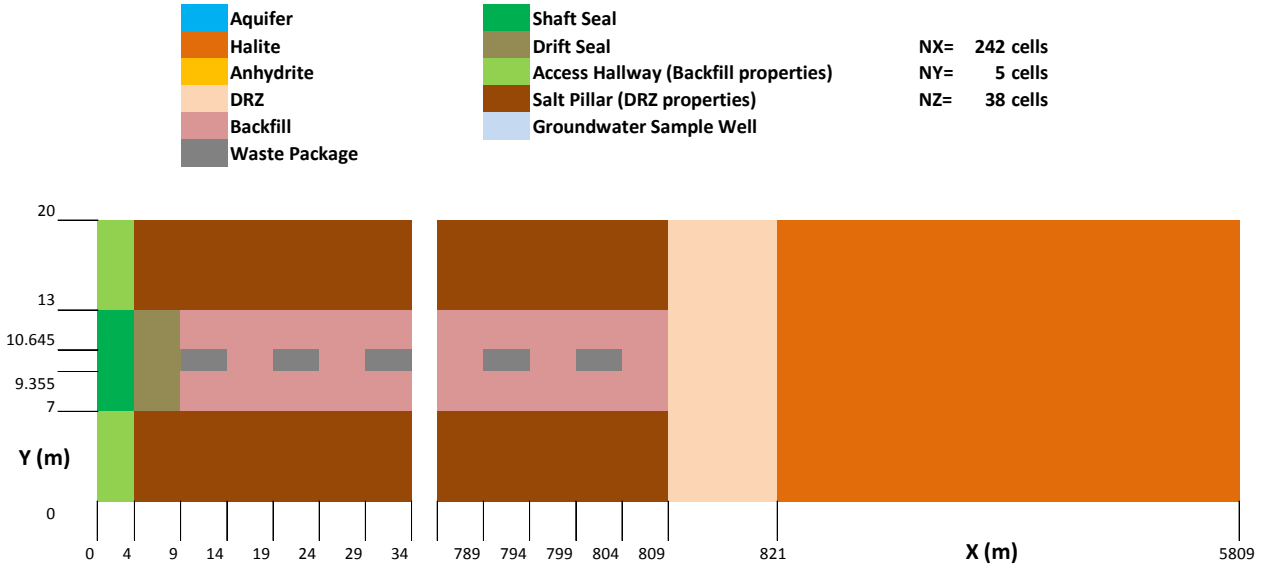

(Not to scale)

Figure 3-8. Salt Repository Reference Case Model Regions X-Y Plane

Flow boundary conditions were implemented to simulate regional groundwater flow in the X direction (west to east). Hydrostatic pressure profiles were applied along the west (x = 0 m) and east (x = 5,809 m) faces. No flow boundaries were specified along the north (y = 20 m), south (y = 0 m), and bottom (z = 0 m) faces as these are all symmetry boundaries. A no flow boundary was assumed at the top of the aquifer (z = 245 m) due the presence of an overlying confining layer. A regional hydraulic gradient of 0.001 was applied in the aquifer from west to east (Section 3.2.3.4). The initial flow conditions throughout the domain in all simulations derive from hydrostatic conditions and the regional hydraulic gradient.

Solute transport boundary conditions were specified as zero diffusive flux (concentration gradient) at the west, north, south and bottom boundaries as symmetry conditions, zero gradient on the east face as a discharge boundary, and zero flux at the top of the aquifer. The initial concentration conditions include a very low background aqueous concentration of 10^{-20} molal (mol/kg solvent) for all radionuclides, and zero secondary mineral volume fraction in all the domains except the waste emplacement drift. Initial mineral concentrations in the waste emplacement drift are specified as part of the source term.

The symmetry boundaries assigned on the west and bottom boundaries are not rigorously correct, as these are not true planes of symmetry, and zero flux at the top of aquifer does not allow diffusion from the aquifer into the overlying confining unit, thus overestimating the concentration in the aquifer. While these boundaries are not rigorously correct, they are sufficient for the purposes of the demonstration of the enhanced salt repository simulation capability at this stage.

The model domain and regions shown in Figure 3-7 and Figure 3-8 are reproduced in Figure 3-9 at a scale and orientation consistent with the model results.

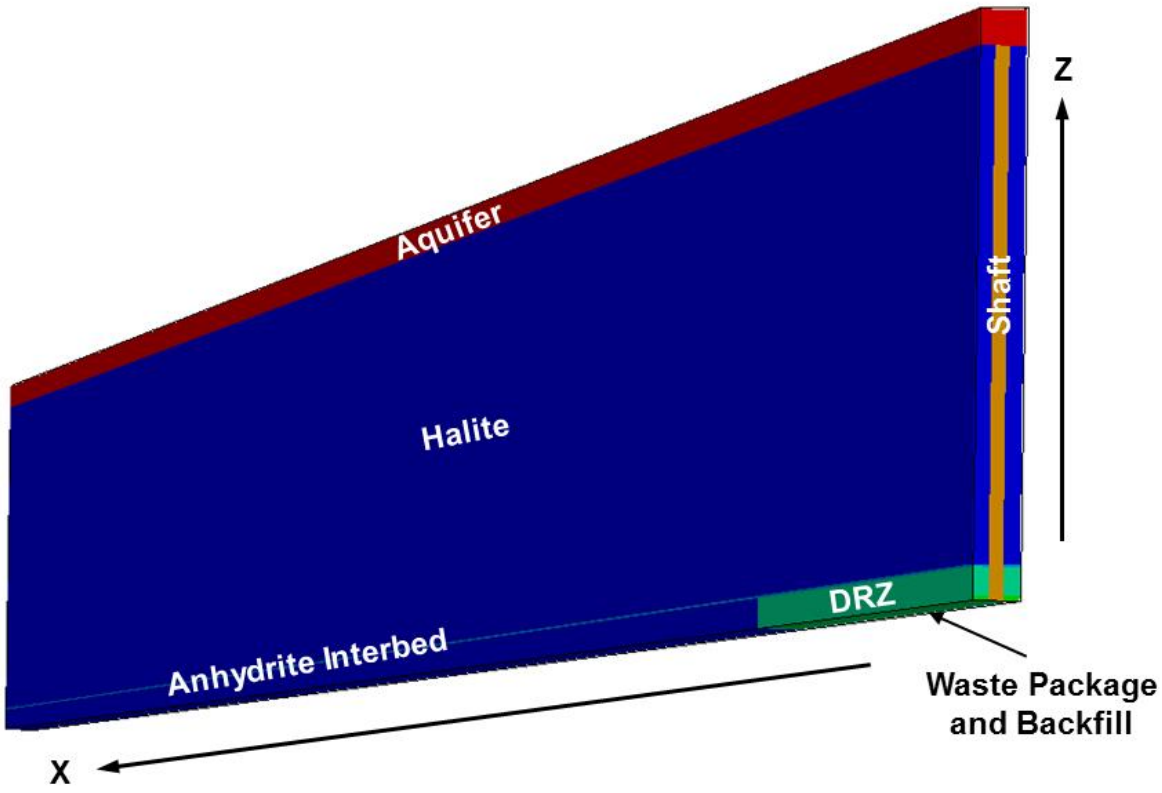

Figure 3-9. Salt Repository Reference Case Model Domain

For the deterministic simulation, the model regions were assigned reference case properties as described in Section 3.2. These are summarized in Table 3-10.

Table 3-10. Salt Repository Reference Case Deterministic Region Properties

Model Region	Permeability (m2)	Porosity	Effective Diffusion Coefficient[1] (m2/s)
Waste Package	1.00×10^{-13}	0.300	6.90×10^{-10}
Backfill	1.00×10^{-18}	0.113	2.60×10^{-10}
Shaft (sealed)	1.58×10^{-20}	0.113	2.60×10^{-10}
DRZ	1.12×10^{-16}	0.0129	2.97×10^{-11}
Halite	3.16×10^{-23}	0.0182	4.19×10^{-11}
Interbed (anhydrite)	1.26×10^{-19}	0.011	2.53×10^{-11}
Aquifer	1.00×10^{-13}	0.200	4.60×10^{-10}

[1] Effective diffusion coefficient = (Free water diffusion coefficient) x (tortuosity) x (porosity)

The implementation of the reference case in PFLOTRAN required the following deviations from the reference case:

- **Waste Package Volume –** Each of the 80 modeled waste packages is represented by a PFLOTRAN cell. Due to the bottom (z = 0 m) model symmetry boundary, each rectangular PFLOTRAN waste package cell corresponds to half of a waste package and is discretized (5.0 m x 1.29 m x 0.507 m = 3.27 m^3) to correspond to the volume of half of a cylindrical waste package (including overpack).
- **Waste Package Porosity and Permeability –** Each PFLOTRAN waste package cell was assigned a porosity of 0.30, which remained constant over the duration of the simulation. This porosity is lower than the initial porosity of 0.50 (Section 3.2.2.2) to qualitatively account for compaction of the waste package due to salt creep after closure. Each waste package cell was assigned a permeability of 1×10^{-13} m^2, representative of the degraded, compacted waste form and waste package internals.
- **Waste Package Saturation –** Each PFLOTRAN waste package cell was assumed to be fully saturated, consistent with the assumption of instantaneous waste package degradation and no gas generation.
- **Waste Form Composition –** The PFLOTRAN waste form mineral contained within each waste package cell (with a waste form volume fraction of 0.104 as per Section 3.2.2.2) was specified to have a molecular weight of 100 g/mol. The resulting initial PFLOTRAN radionuclide mole fractions (moles radionuclide per mole waste form mineral) in the waste form were calculated based on the rightmost column of Table 3-1.
- **Waste Form Degradation Rate –** The PFLOTRAN waste form mineral was assigned a very high dissociation constant (log K = 50) and an infinite solubility, ensuring that the waste form is not thermodynamically stable and that the rate of dissolution can be controlled by setting the kinetic rate of reaction. The waste form mineral was specified to have a rate constant for dissolution of 4.8×10^{-8} mol/m^2s and a specific surface area of 1 m^2/m^3. The product of the rate constant and the specific surface area (1.51 mol/m^3yr), is a constant waste form degradation rate that results in complete dissolution of the waste form in approximately 10,000 years. The waste form degradation rate represents UO_2 matrix dissolution/conversion; no instant release fraction is simulated. This simulated degradation rate is about two orders of magnitude faster than the reference case fractional rate that has a half-life of 4,800,000 years (Section 3.2.2.1). Slower constant rates are examined in the probabilistic sensitivity simulations in Section 3.3.4.

- **Radionuclide Inventory –** The modeled inventory was a subset of the 10 reference case radionuclides identified in Section 3.2.1. The reduced inventory for simulation included 5 radionuclides (the Neptunium decay chain - ^{241}Am, ^{237}Np, ^{233}U, and ^{229}Th - and ^{129}I) and 3 secondary mineral phases (^{129}I, with unlimited solubility, and ^{229}Th, with a high solubility limit, did not require secondary mineral phases because they did not precipitate). These 5 radionuclides are considered sufficient for a PA model capability demonstration.
- **Shaft Cross-Sectional Area –** In the rectangular PFLOTRAN grid, the shaft is 4 m by 6 m. However, due to symmetry only half of the shaft cross-section is modeled explicitly. Therefore, the PFLOTRAN half shaft is representative of a full shaft with a cross-sectional area of 48 m^2. The stylized reference case shaft has a cross-sectional area of 86 m^2 as per Section 3.2.2.3.
- **Drift seal –** The drift closure seal isolating the drift from the central access hallway (Figure 3-1) is modeled as a 5-m length of backfill between the shaft and the first waste package (Figure 3-7).
- **Solubility Limits –** As described in Section 2.2.1.4.1, the PFLOTRAN radionuclide solubility limits are calculated from elemental solubility limits (Table 3-8) by assuming that the fraction of each radionuclide of an element in the aqueous phase is the same as the fraction of each radionuclide of an element within the waste form. The resulting PFLOTRAN solubility limits are shown in Table 3-11. These solubilities are consistent with the assumed long-term temperature, redox conditions, and pH in the near-field regions (Section 3.2.3.6.2), but are assumed to apply throughout the model domain. This assumption is appropriate because solubility limits are most significant close to the degrading waste forms, where the dissolved concentrations are the highest. For simplicity, the solubility limits are constant for the duration of the simulation (i.e., they do not change with changing temperature or brine chemistry).

Table 3-11. PFLOTRAN Radionuclide Solubility Limits for the Salt Repository Reference Case

Radionuclide	Elemental Solubility (mol/L)	Fraction of Element in Waste Form [1]	Radionuclide Solubility Limit (mol/L)
^{241}Am	5.85×10^{-7}	0.820	4.80×10^{-7}
^{237}Np	1.51×10^{-9}	1.000	1.51×10^{-9}
^{242}Pu	4.62×10^{-6}	6.19×10^{-2}	2.86×10^{-7}
^{229}Th	4.00×10^{-3}	2.19×10^{-4}	8.76×10^{-7}
^{230}Th	4.00×10^{-3}	0.785	3.14×10^{-3}
^{233}U	1.12×10^{-7}	1.52×10^{-8}	1.70×10^{-15}
^{234}U	1.12×10^{-7}	3.32×10^{-4}	3.72×10^{-11}
^{238}U	1.12×10^{-7}	0.987	1.11×10^{-7}

[1] calculated from Carter et al. (2012, Table C-1)

- **Sorption** – As described in Section 3.2.3.6.3, sorption of radionuclides onto solid surfaces is implemented using the PFLOTRAN linear sorption partition coefficient, K_d^P, calculated from Equation 3-1. The calculated radionuclide-specific K_d^P values are representative of sorption in bedded salt units, and are assumed to apply to all model regions.

- **Aquifer Permeability and Porosity** – The aquifer is assumed to have a permeability of 1×10^{-13} m^2 and a porosity of 0.20, which is within the range of water-producing dolomite properties.
- **Biosphere –** The receptor location is assumed to be 5,000 m from the edges of the underground excavations. However, in the current salt repository demonstration simulation biosphere transport, receptor uptake, and dose calculations are not included. Instead, dissolved radionuclide concentrations calculated at the groundwater sample well location in the aquifer (at a distance of 4,900 m from the west (x = 0 m) model boundary) are used as a surrogate for dose as a repository performance indicator.

All other parameter values for the deterministic simulation are taken directly from the reference case. For the probabilistic simulations, nine parameter values were sampled, with all other parameters using deterministic values. Specific details of the sampled parameters and distributions are provided in Section 3.3.4.

The salt repository demonstration simulations were run as single phase, isothermal using PFLOTRAN "Richards" mode; governing equations are documented in Lichtner and Hammond (2012a, Sections 2 and 3). The simulations were performed on the Red Sky high-performance cluster at Sandia National Laboratories (SNL). Execution times for a simulation with 413,820 degrees of freedom (242 x 5 x 38 = 45,980 cells tracking 5 radionuclides, 1 primary mineral, and 3 secondary mineral phases) ranged between 0.5 and 3 hours, depending on the number of processors and the parameter values. For the probabilistic simulations a total of 100 realizations were run. Ten concurrent simulations each using 40 processors were run utilizing 800 cores for a total probabilistic run time (i.e., for all 100 realizations) of less than 5 hours. This indicates an average run time of about 0.5 hours for a single simulation on 40 processors. These execution times indicate that reasonably complex probabilistic 3D PA calculations (i.e., with multiple radionuclides, multiple waste packages, and multiple EBS and NBS regions) can be performed in acceptable wall clock times.

3.3.3 Deterministic Baseline Simulation Results

As noted in Section 3.2.3.6.1, the properties of the reference case result in diffusive radionuclide transport through all regions except for the aquifer. Transport includes the effects of sorption and decay and ingrowth. ^{129}I is the most mobile radionuclide because it has unlimited solubility and is non-sorbing (K_d = 0 ml/g).

Results from the deterministic simulation are shown in the form of ^{129}I dissolved concentration (reported as molality or mol/kg solvent) as a function of time and space (Figure 3-10 and Figure 3-11). ^{129}I released during waste form degradation results in high dissolved concentrations at early times in the waste package and backfill regions, which subsequently diffuses into the DRZ and halite. At about 10,000 years, the ^{129}I dissolved concentrations in the aquifer begin to exceed the background level (Figure 3-10c). After about 20,000 years, ^{129}I has been transported by advection down the length of the aquifer and is beginning to diffuse downward into the underlying halite, increasing the concentration in the halite over the entire domain (Figure 3-10d). This process continues through the duration of the simulation, resulting in dissolved ^{129}I throughout the model domain after about 200,000 years (Figure 3-10h). In this demonstration problem, the downward diffusion from the aquifer effectively homogenizes the ^{129}I dissolved concentration across the entire model domain after about 500,000 years (Figure 3-10i). However, the magnitude and timing of the downward diffusion is likely accelerated due to the solute transport boundary conditions on the top and west edges of the model.

The time history of ^{129}I dissolved concentration at the sample well location (x = 4,900 m) in the aquifer (Figure 3-11) further illustrates the diffusion process; ^{129}I dissolved concentration starts to increase from background levels after about 10,000 years and approaches a peak concentration after a few hundred thousand years.

a)

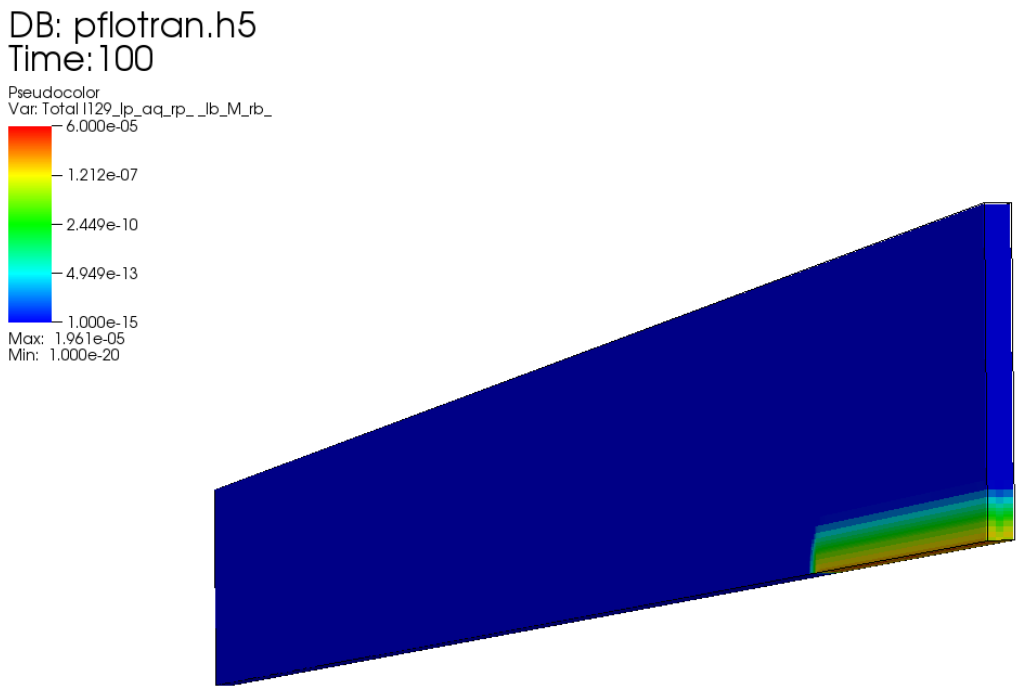

b)

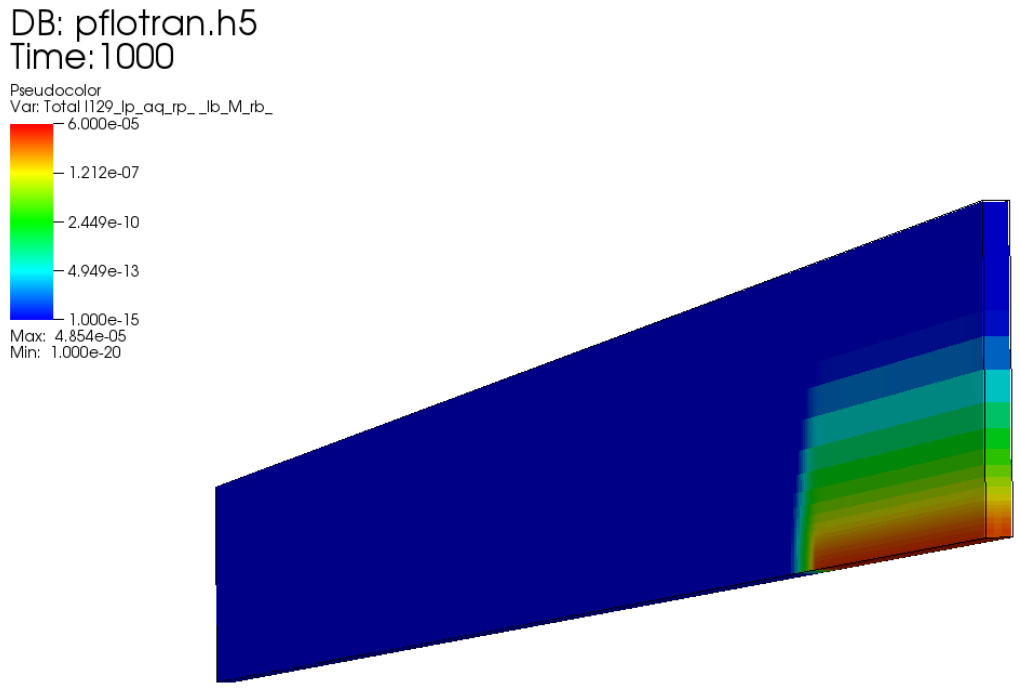

Figure 3-10. ^{129}I Dissolved Concentration at Specified Times for the Salt Repository Reference Case
a) Time = 100 years, b) Time = 1,000 years

c)

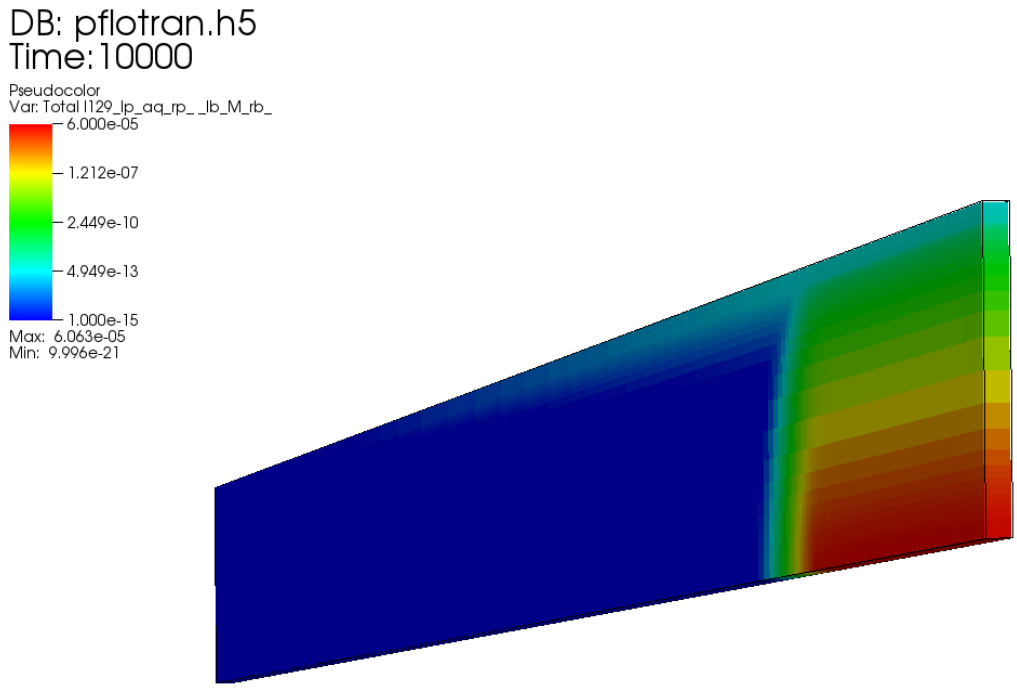

d)

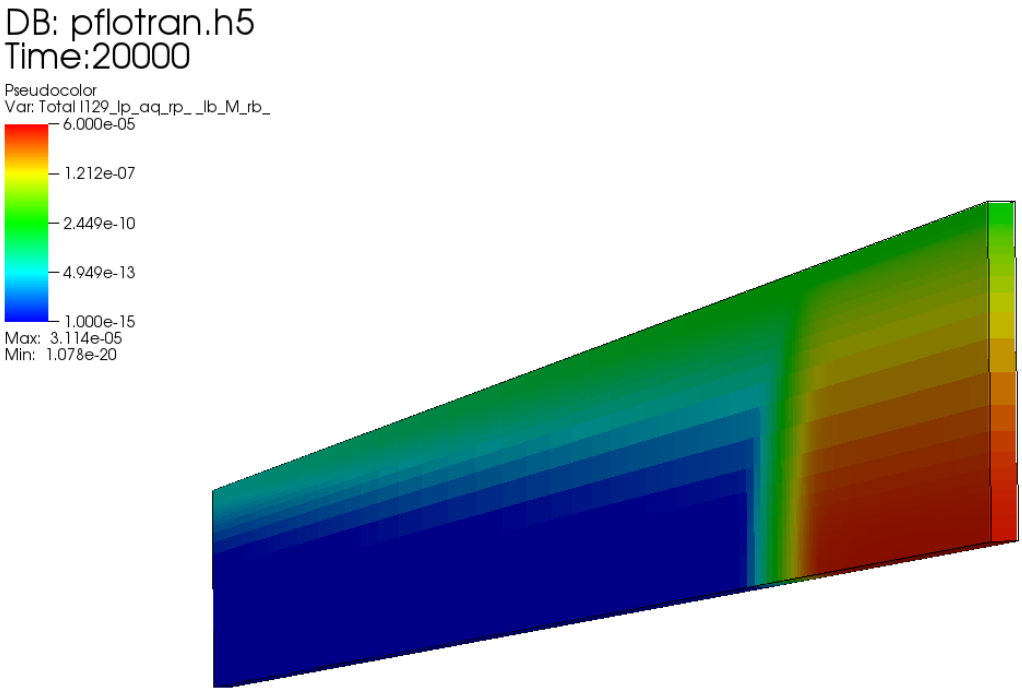

Figure 3-10. ^{129}I Dissolved Concentration at Specified Times for the Salt Repository Reference Case

c) Time = 10,000 years, d) Time = 20,000 years

e)

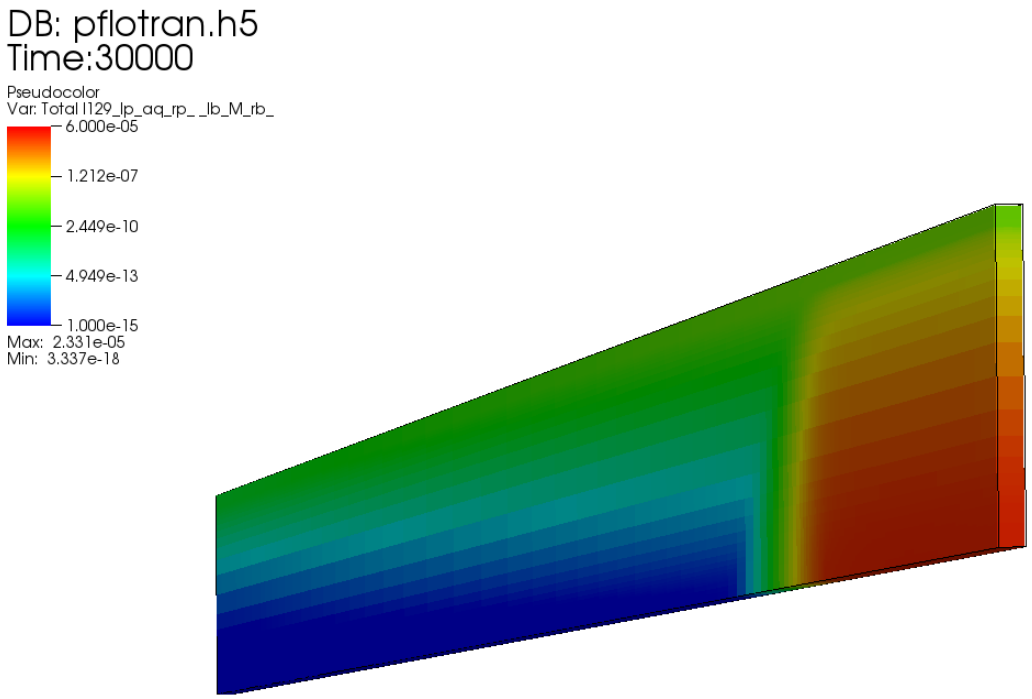

f)

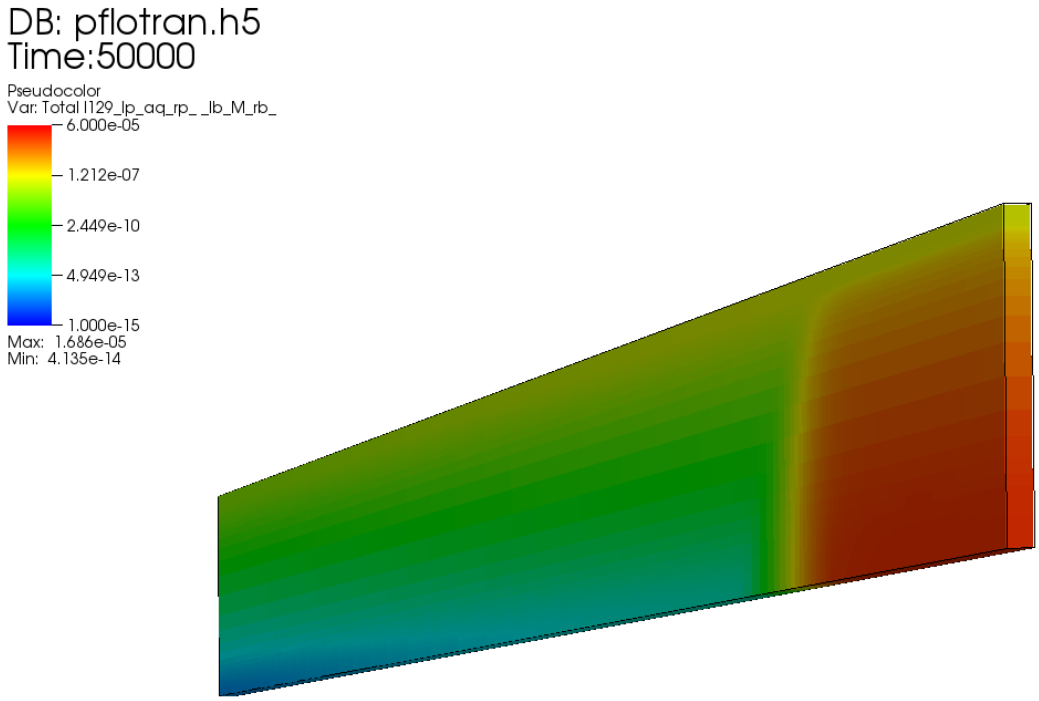

Figure 3-10. ^{129}I Dissolved Concentration at Specified Times for the Salt Repository Reference Case e) Time = 30,000 years, f) Time = 50,000 years

g)

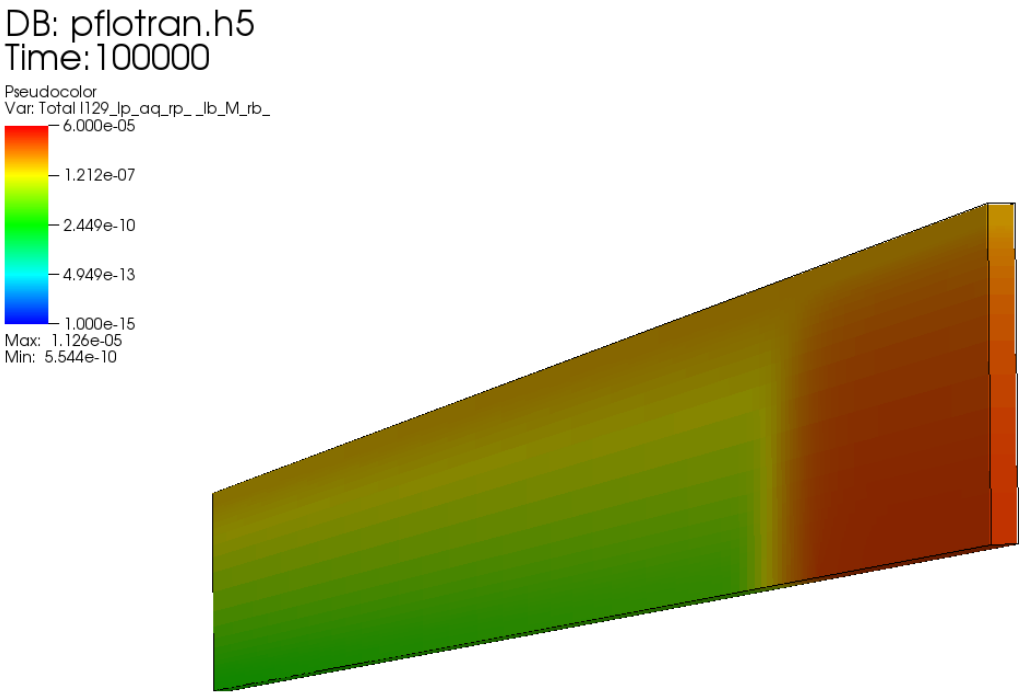

h)

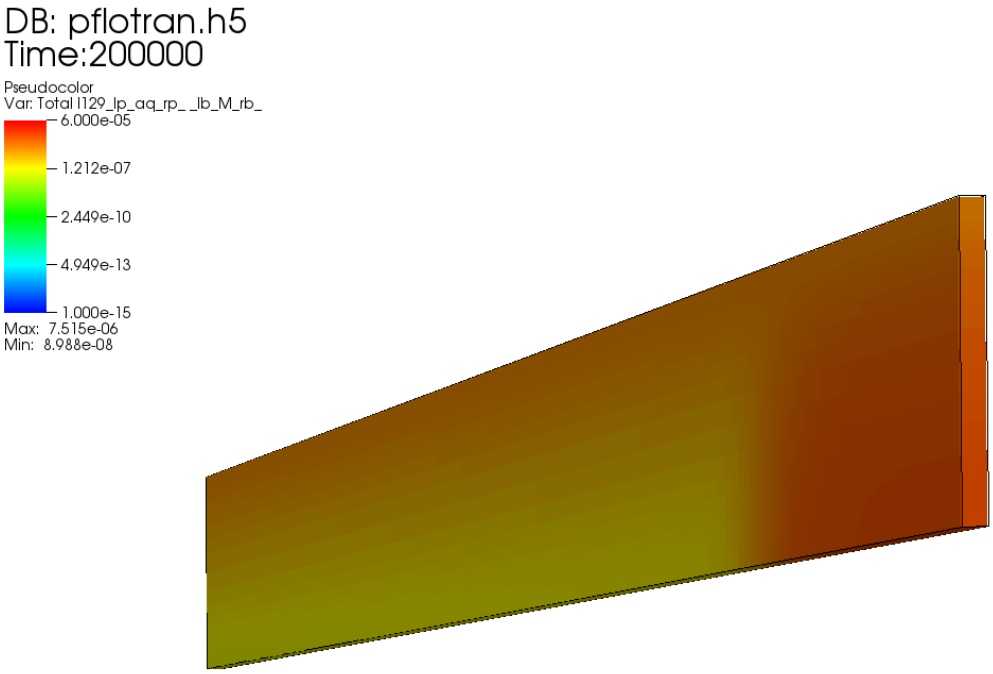

Figure 3-10. ^{129}I Dissolved Concentration at Specified Times for the Salt Repository Reference Case
g) Time = 100,000 years, h) Time = 200,000 years

i)

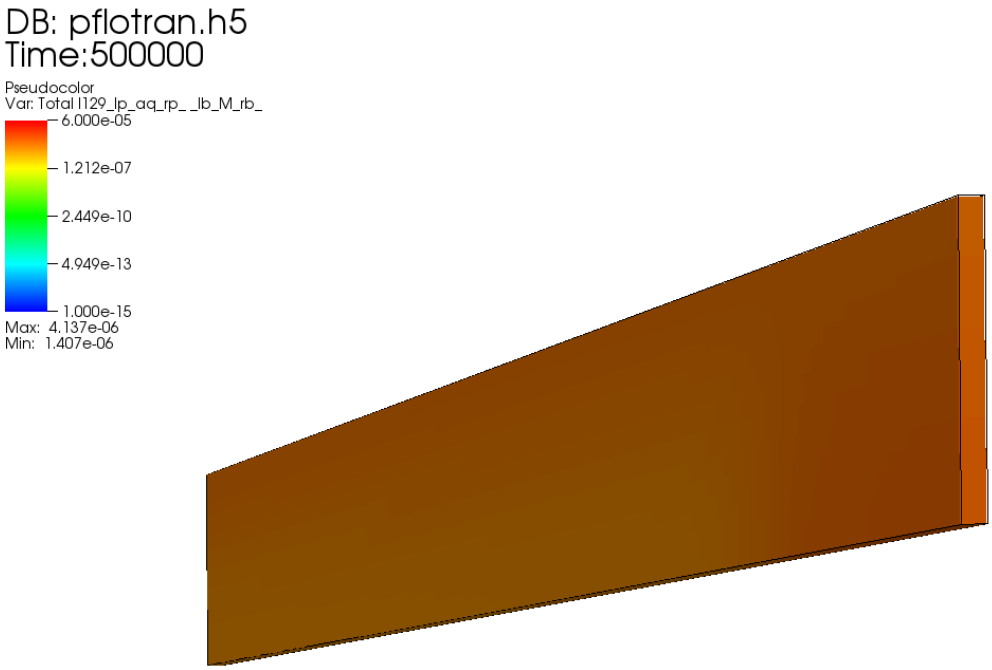

j)

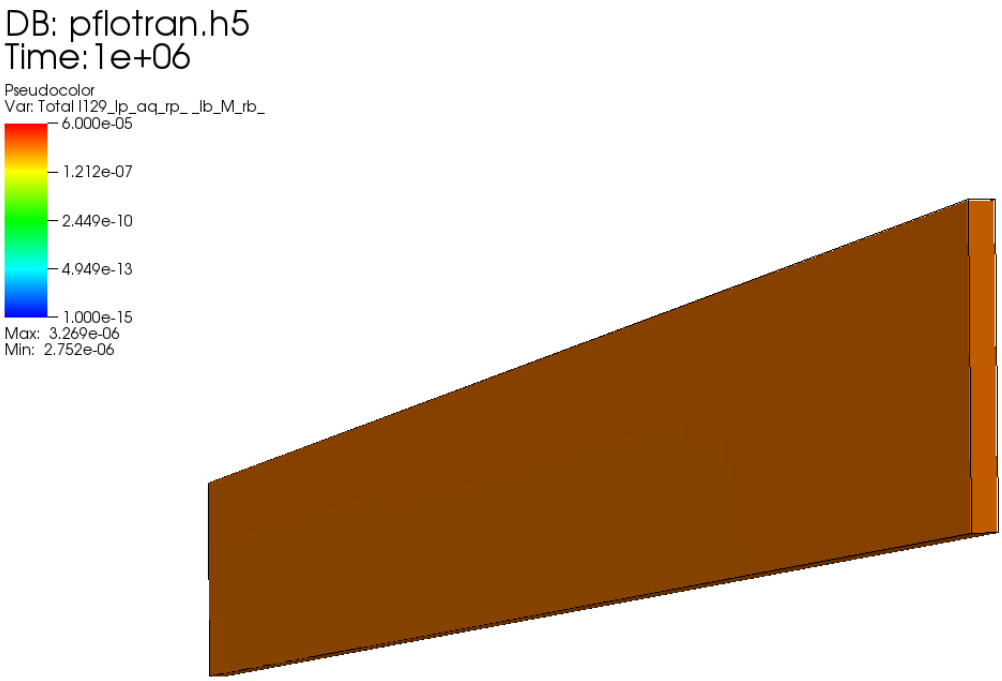

Figure 3-10. ^{129}I Dissolved Concentration at Specified Times for the Salt Repository Reference Case
i) Time = 500,000 years, j) Time = 1,000,000 years

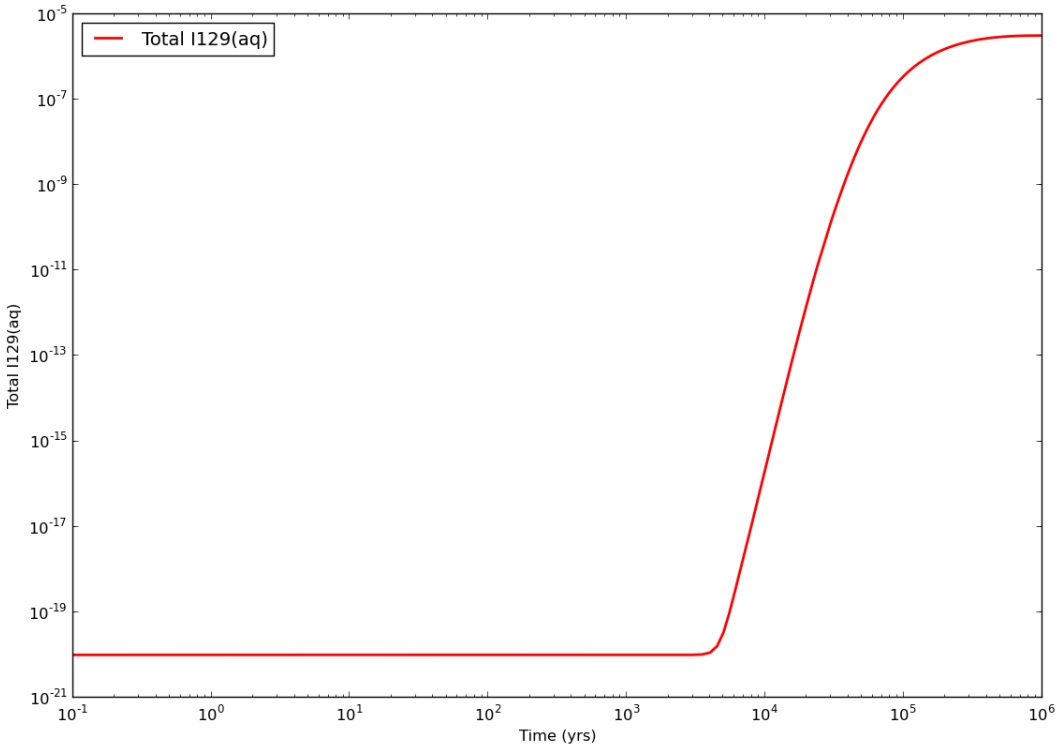

Figure 3-11. ^{129}I Dissolved Concentration in Aquifer at x=4,900 m for the Salt Repository Reference Case

Deterministic simulation results are also shown in form of ^{237}Np dissolved concentration as a function of time and space (Figure 3-12). The effects of sorption retard ^{237}Np transport, resulting in much slower transport than for ^{129}I. Preferential diffusion up the shaft is apparent (Figure 3-12c), due to the higher effective diffusion coefficient in the shaft relative to the DRZ, halite, and interbed (Table 3-10). However, by the end of simulation at 1,000,000 years, ^{237}Np has not diffused much beyond the DRZ, and has not reached the aquifer (Figure 3-12d).

a)

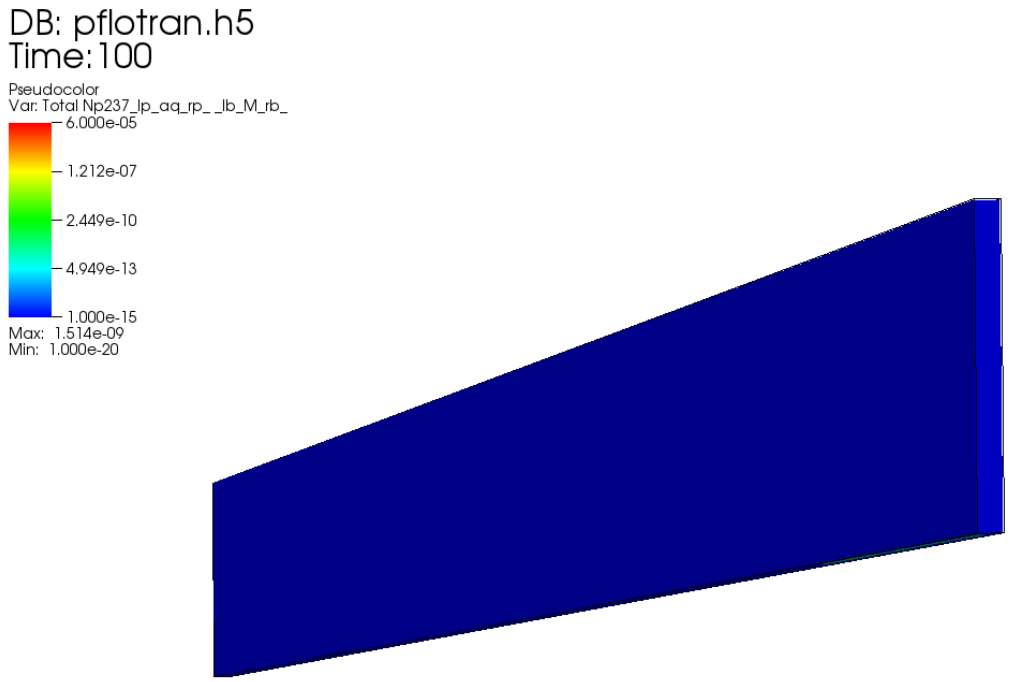

b)

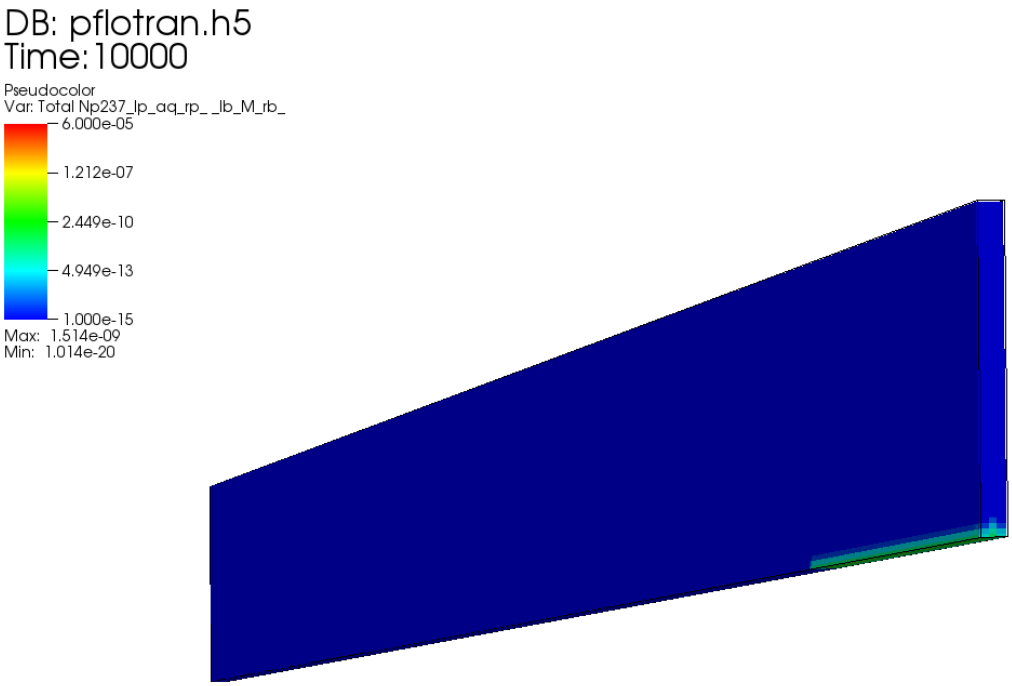

Figure 3-12. ^{237}Np Dissolved Concentration at a Specified Times for the Salt Repository Reference Case a) Time = 100 years, b) Time = 10,000 years

c)

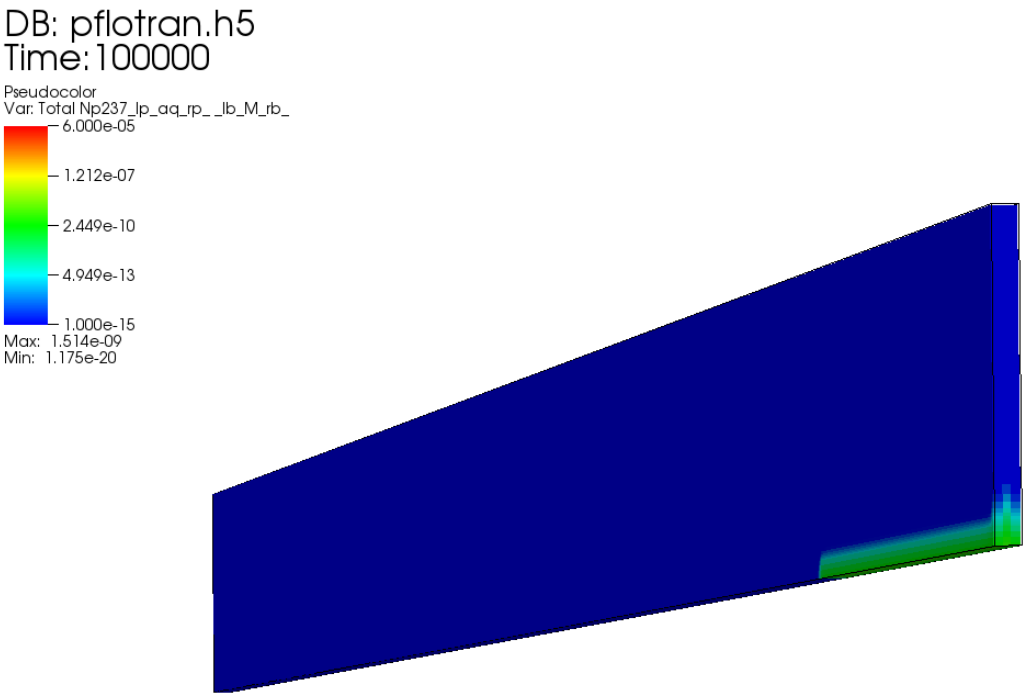

d)

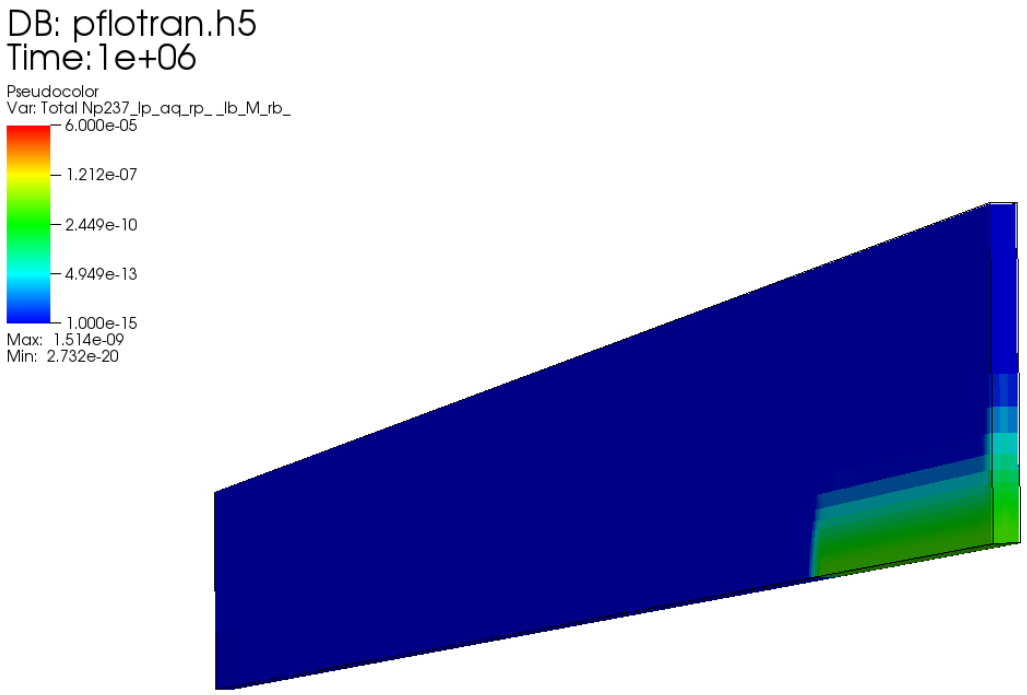

Figure 3-12. ^{237}Np Dissolved Concentration at Specified Times for the Salt Repository Reference Case

c) Time = 100,000 years, d) Time = 1,000,000 years

Figure 3-13 presents a bottom view of the model domain, showing dissolved concentration of ^{129}I and ^{237}Np at 100 years. The bottom view is rotated from the orientation of the side views shown in Figure 3-9 and Figure 3-10, and shows the bottom corner of the model domain nearest the west edge (the edge where the waste and shaft are located). In Figure 3-13, both radionuclides have high concentrations in the waste package cells; waste package cells can be distinguished from the alternating backfill cells in the Figure. The more mobile ^{129}I also has elevated concentrations in the backfill and DRZ cells.

The dissolution of the waste form mineral can be seen in Figure 3-14, which shows a bottom view of the waste form volume fraction (volume of waste form mineral/volume of waste package cell) at two different times. The waste form begins to dissolve immediately, releasing radionuclides into solution. After 100 years, the waste form volume fraction is still close to the initial volume fraction of 0.104 (Figure 3-14a). After 1,000 years, the waste form mineral has degraded to a volume fraction of about 0.09 (Figure 3-14b). By 10,000 years, the waste form has completely degraded. For radionuclides with solubility limits, secondary mineral volume fractions (i.e., precipitates) increase in the waste package cells, but secondary minerals are limited to the waste package cells throughout the simulation except for the ^{233}U secondary mineral. There is only a small mass fraction of ^{233}U present in the waste form; but the presence of ^{233}U secondary mineral outside of the waste package cells is due to ^{233}U ingrowth from ^{237}Np decay.

In addition to showing the dissolved radionuclide concentrations and waste form volume fractions, Figure 3-13 and Figure 3-14 also illustrate the 80-waste-package model fidelity. Most PA models simulate a single waste package or a stylized “lumped” waste package. However, with the HPC-enhanced PA model capability described in this report, simulations can include a detailed representation of individual waste packages.

a)

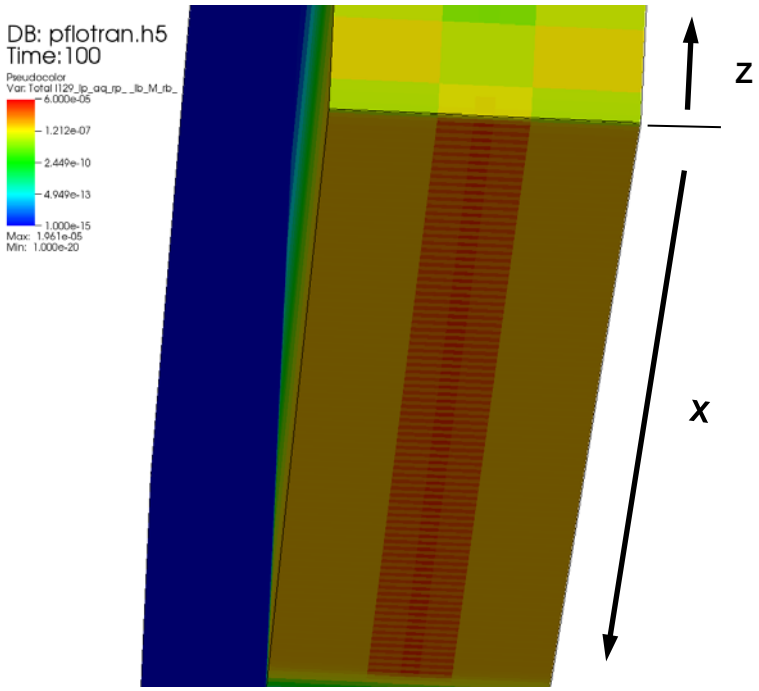

b)

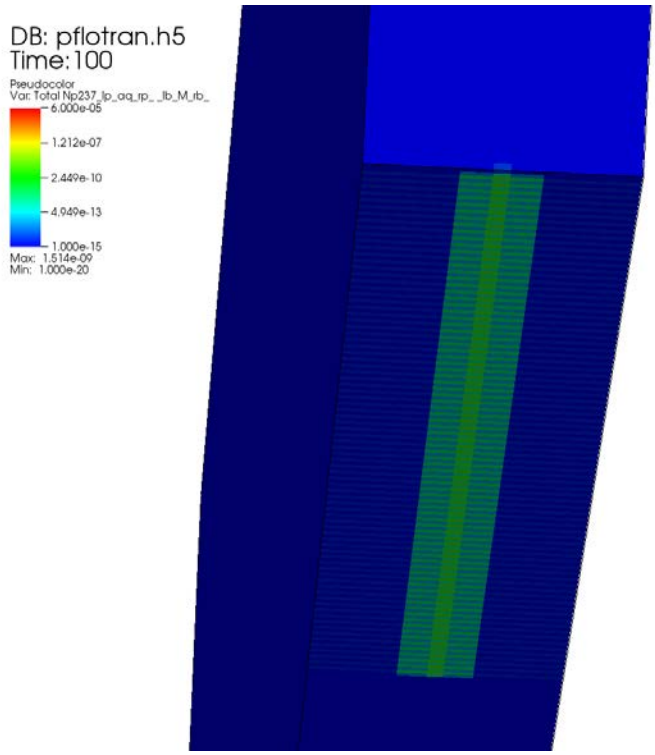

Figure 3-13. Dissolved Concentration at 100 Years for the Salt Repository Reference Case a) ^{129}I bottom view, b) ^{237}Np bottom view

a)

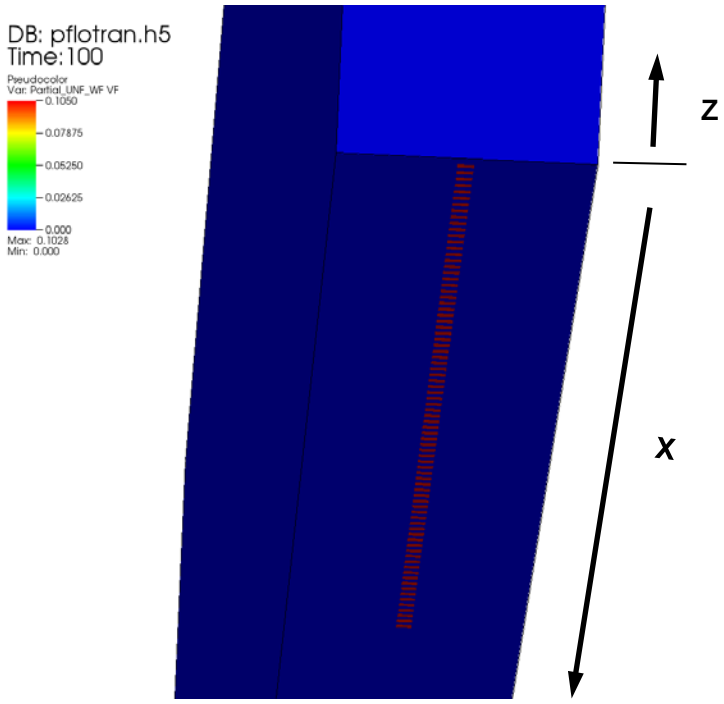

b)

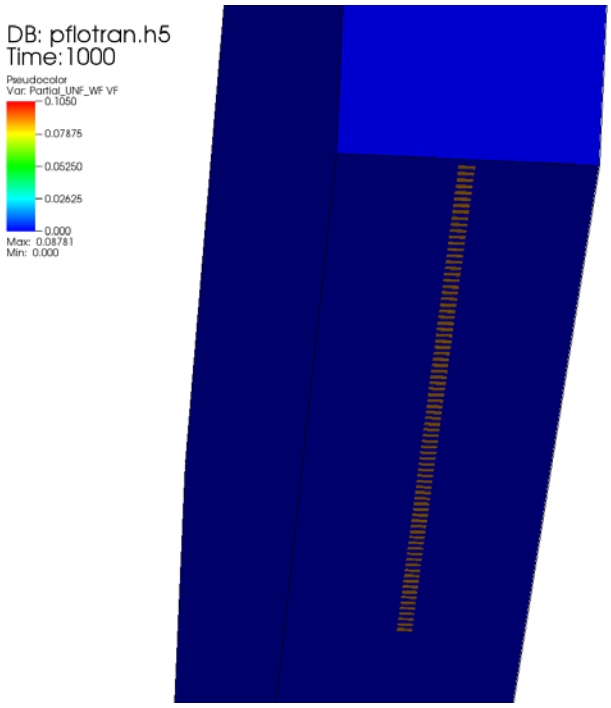

Figure 3-14. Waste Form Volume Fraction for the Salt Repository Reference Case
a) Time = 100 years, b) Time = 1,000 years

3.3.4 Probabilistic Sensitivity Simulation Results

Probabilistic simulations of the salt repository demonstration problem were carried out to further examine the enhanced PA modeling capabilities. One hundred realizations were run with parameter sampling (using Latin Hypercube Sampling (LHS)) and sensitivity analyses performed using DAKOTA. The nine parameters selected for sampling are shown in Table 3-12.

Table 3-12. Salt Repository Reference Case Probabilistic Properties

Model Parameter	Deterministic Value	Probability Range	Distribution Type
Waste Form Degradation Rate (mol/m^{2}s)	4.8×10^{-8}	1.0×10^{-12} - 1.0×10^{-8}	Log uniform
^{129}I K_d^P (kg/m^3)	0.00	0.00257 – 21.7	Log uniform
Waste Package Porosity	0.30	0.05 – 0.50	Uniform
Backfill Porosity	0.113	0.010 – 0.200	Uniform
Shaft Porosity	0.113	0.010 – 0.200	Uniform
DRZ Porosity	0.0129	0.0010 – 0.1000	Uniform
Halite Porosity	0.0182	0.0010 – 0.0519	Uniform[1]
Interbed Permeability (m^2)	1.26×10^{-19}	1.00×10^{-21} - 1.00×10^{-17}	Log uniform[2]
Aquifer Permeability (m^2)	1.00×10^{-13}	1.00×10^{-14} - 1.00×10^{-12}	Log uniform

[1] The uniform distribution is a simplification of the cumulative distribution reported in Section 3.2.3.2
2 The log uniform distribution is a simplification of the Student-t distribution reported in Section 3.2.3.3

Probabilistic results, calculated with DAKOTA, are summarized with horsetail plots of ^{129}I dissolved concentrations at the groundwater sample well location (x = 4,900 m) in the aquifer (Figure 3-15), partial rank correlations (Figure 3-16), and scatter plots (Figure 3-17).

The individual horsetail plots in Figure 3-15 suggest that there are two dominant processes controlling radionuclide transport to the sample well location in the aquifer. The first process is three-dimensional "spherical" diffusion from the waste and backfill through the DRZ, anhydrite, and halite, and subsequent advection in the aquifer. These transport processes, which are illustrated in the deterministic results in the time sequence of Figure 3-10, are evident in the realizations with an ^{129}I dissolved concentration that starts to monotonically increase after 1,000 to 10,000 years, and approaches a maximum value after about 200,000 years, similar to the concentration history in Figure 3-11. The second process is only observable in realizations that have significant advection in the anhydrite interbed (i.e., a high sampled interbed permeability). In these realizations, advective transport distributes ^{129}I along the entire length of the interbed, providing an essentially constant boundary condition for upward diffusion into the entire length of the overlying halite. Thus, subsequent ^{129}I diffusion from the halite to the overlying aquifer occurs at about the same time in all parts of the aquifer. These realizations are characterized by a rapid spike in concentration at around 10,000 years. The sawtooth peaks, and subsequent drops, in concentration give the appearance of a numerical artifact; however, they are due to rapid dissolution of the ^{129}I that diffuses upward into the aquifer at the sample well location and then is advected away through the aquifer. Further investigation of this phenomenon, and the possible associated numerical issues, are necessary.

Sensitivity of the performance metric (peak ^{129}I dissolved concentration at the sample well location in the aquifer) to each of the nine uncertain parameters, as quantified by the partial rank correlation, is shown in Figure 3-16. The most sensitive parameter is the waste form degradation rate, which controls the source concentration for diffusion. Other senstivite parameters include halite porosity and ^{129}I K_d^P, which control diffusion through the extensive halite units, and aquifer permeability, which controls advection to the

sample welll location. The low partial rank correlations for the other five parameters are statistically insignificant. The high sensitivity of the waste form degradation rate is confirmed by the scatter plots in Figure 3-17.

These sensitivity results provide preliminary insights into the important multi-physics processes and couplings controlling long-term performance for the generic reference case salt repository. However, these salt repository simulations only represent a preliminary, demonstration-scale problem. Further PA model refinement would be prudent before drawing strong conclusions regarding the relative importance of various parameters.

It is also important to note that the sensitivity indicators are dependent on the performance metric, in this case peak ^{129}I dissolved concentration at the groundwater sample well location. For example, the high sensitivity to waste form degradation rate would probably diminish if the performance metric was total mass transported to the sample well location. Similarly, the sensitivity to ^{129}I K_d^P would likely be even greater if the performance metric was time to peak concentration. However, the current objective was to test the probabilistic simulation and sensitivity analysis capability, not to perform an in-depth analysis of specific processes or parameters.

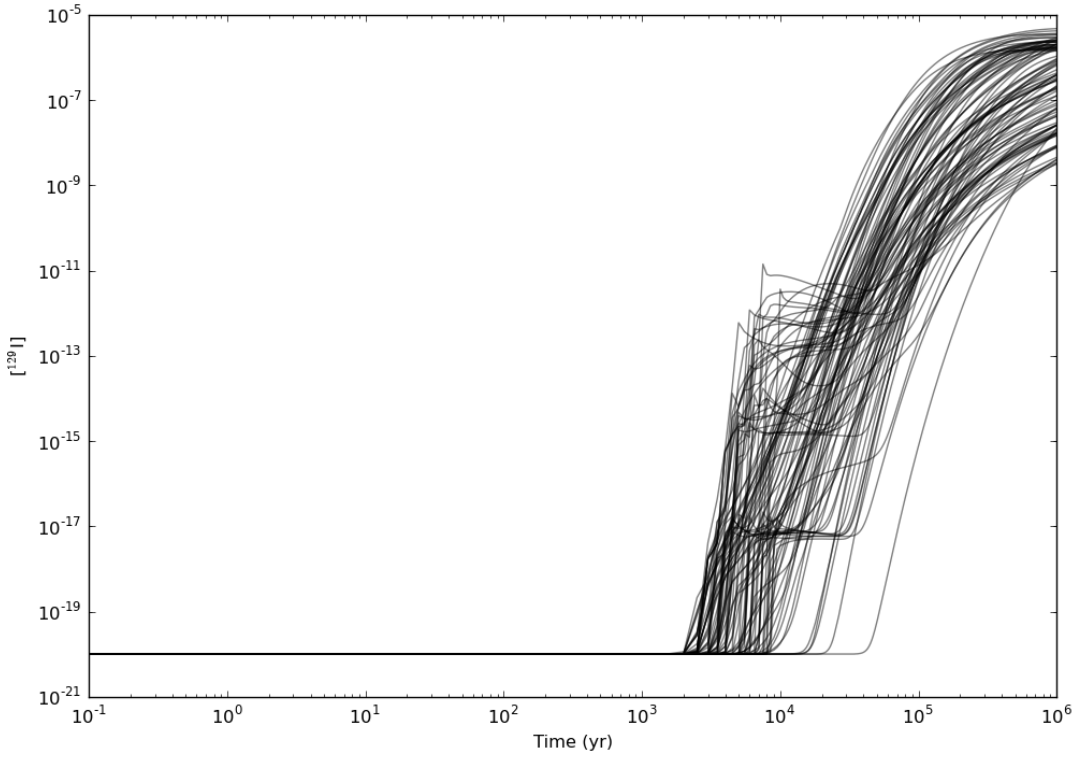

Figure 3-15. Horsetail Plot of ^{129}I Dissolved Concentration in Aquifer at x=4,900 m for the Salt Repository Reference Case

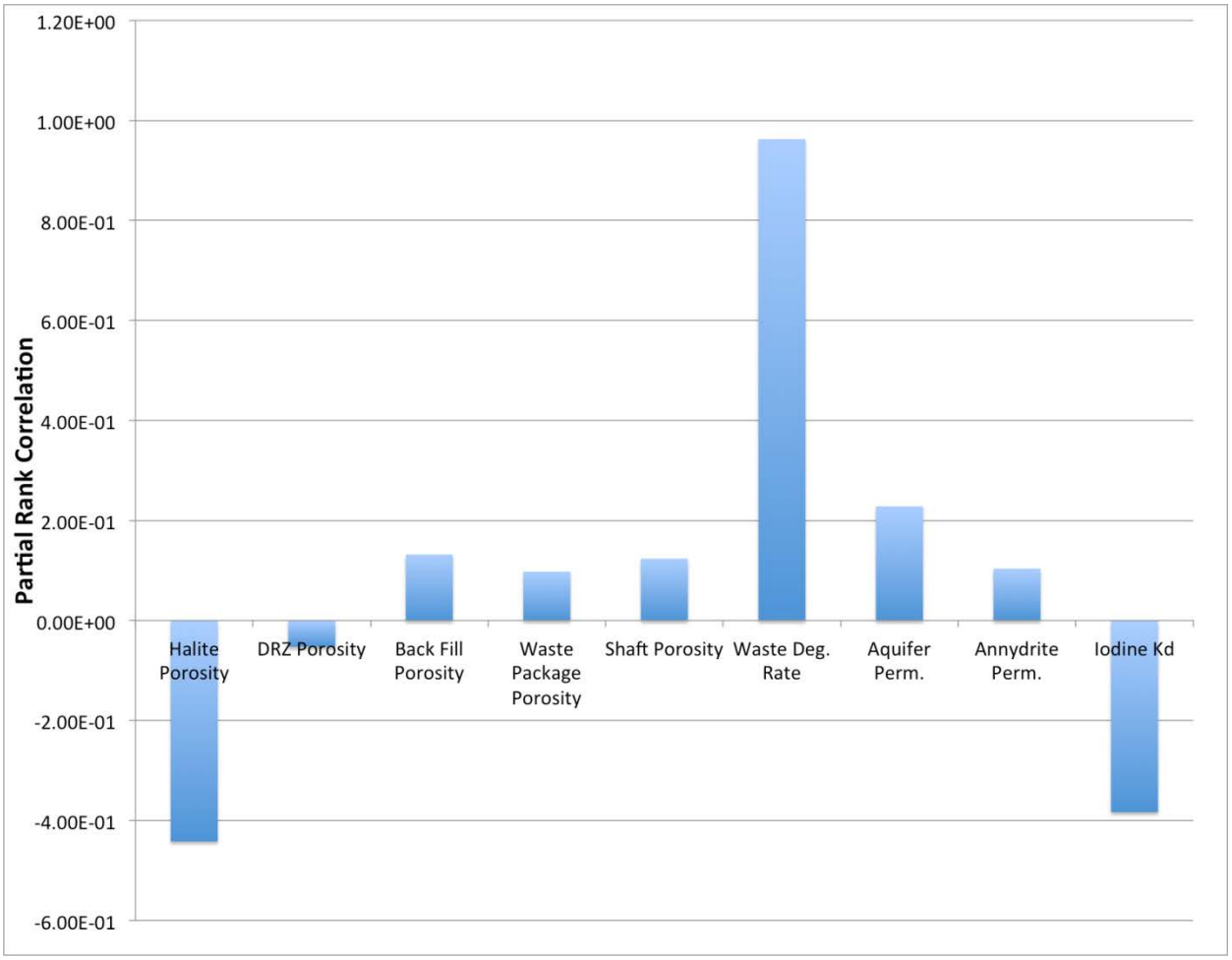

Figure 3-16. Partial Rank Correlation Analysis of Uncertain Parameters for the Salt Repository Reference Case

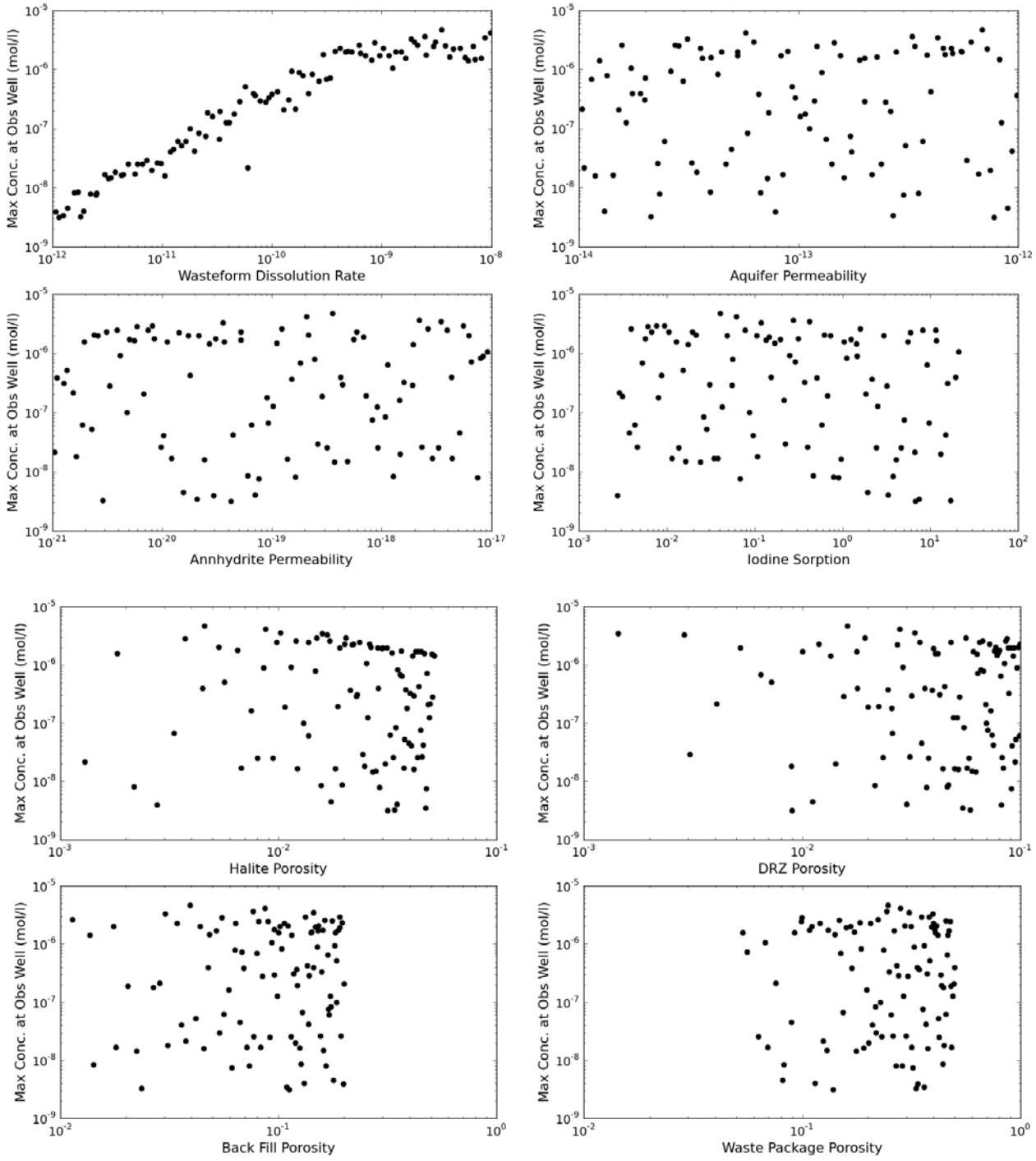

Figure 3-17. Scatter Plots of Uncertain Parameters for the Salt Repository Reference Case

4. GENERIC GRANITE DISPOSAL SYSTEM MODEL

As mentioned in Section 1.1, disposal in a granite or crystalline rock formation is one of the generic repository options being considered by the UFDC. It is important, therefore, that an enhanced PA modeling capability can incorporate the key processes and features of such a repository. A reference case for a generic granite/crystalline repository has been under development for several years (Clayton et al. 2011, Section 3.2; Mariner et al. 2011; Vaughn et al. 2013a, Section 3.2; Freeze et al. 2013c, Sections 4.2.3.2.3 and 4.2.3.3.3) and has previously been tested with an abstraction-based modeling system, using GoldSim for the source term and as the driver code for a far-field flow and transport module (Chu 2013).

To support the application of the enhanced PA modeling capability to a granite repository, the far-field hydrologic flow component of the existing granite reference case was tested in a limited parallel-computing environment (Harp et al. 2013). Initial computational testing of this far-field granite conceptual model was based on a "thin model" (effectively 2D) run on a single processor and a "thick model" (i.e., 3D) run on twelve processors. These test cases were run with the Amanzi computer code, which is the primary flow and transport module in the ASCEM framework (Freeze and Vaughn 2012, Sections 4.1.1 and 5). In FY2014, it is expected that this far-field granite reference case, described below, will be implemented in the PFLOTRAN computational framework and coupled with a representative source term model. The remainder of this section summarizes work detailed in Chu (2013) and Harp et al. (2013).

4.1 Generic Granite Repository Reference Case

The EBS portion of the granite reference case (analogous to the EBS portion of the salt repository reference case, described in Section 3.2.2) has not been developed yet for use in an HPC-based PA model but may draw upon some of the EBS properties and parameterization described by Chu (2013). However, portions of the NBS or far-field reference case design have been implemented in the HPC-capable Amanzi platform. In particular, the hydrologic properties for far-field flow, as well as the geometry of the generic simulation domain (see Chu 2013, Section 3), have been adopted, though somewhat modified, to simulate far-field flow in an HPC environment.

The granite reference case domain has a geometric layout as described by Chu (2013, Section 3), and is reproduced in two-dimensional vertical cross-section in Figure 4-1. The repository (shown in red) is located a depth of 300 m. Basic fractured rock is shown in dark gray, with an intensely fractured deformation zone shown in yellow. As described by Harp et al. (2013), simulations were performed at steady-state saturated flow conditions, driven by variations in topography. Infiltration was introduced to the top left and sloping top middle of the model (the higher-elevation green recharge zone region in Figure 4-1) as a Neumann boundary with a specified mass flux of 3.17×10^{-7} kg/s/m^2 (~10 mm/yr infiltration). Outflow was allow to discharge along the top right of the model (the lower elevation blue lake region in Figure 4-1) using a Dirichlet boundary by fixing pressure at atmospheric (~0.1 MPa). No-flow conditions were applied to all other model boundaries.

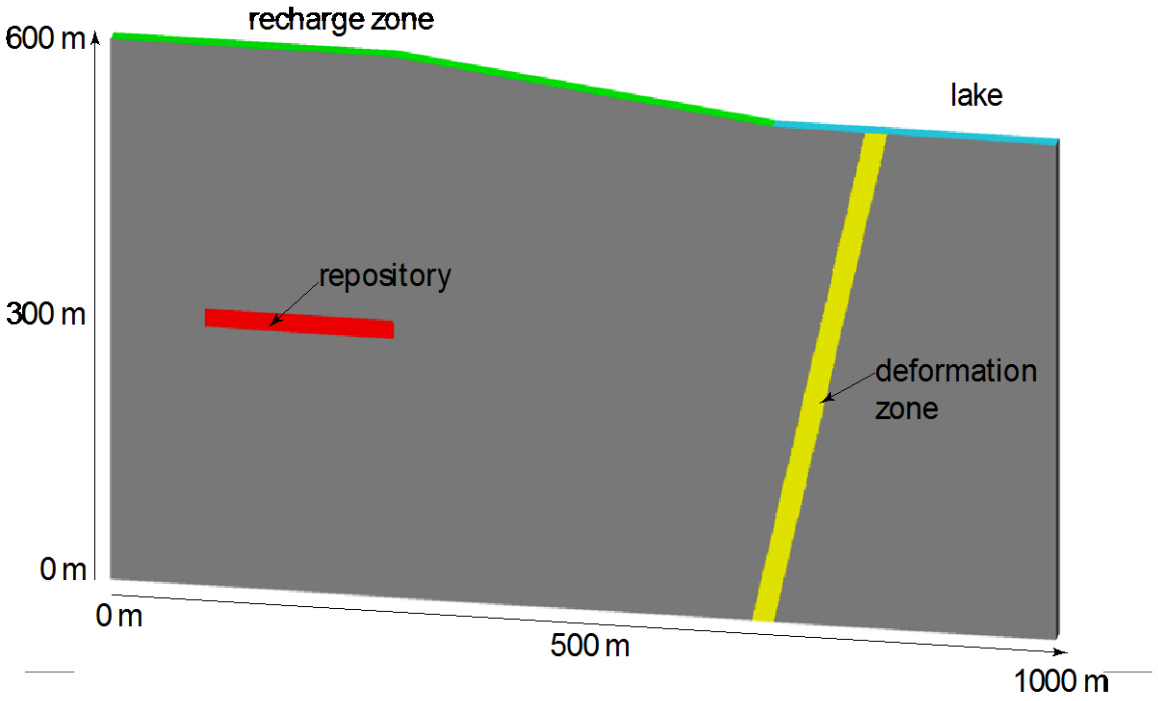

from Harp et al. 2013, Figure 1

Figure 4-1. 2D Granite Repository Reference Case Domain

Two computational grids were developed, a thin 2D model (1 m thick in the y-direction; 107,268 cells) and a thick 3D model (1,000 m thick in the y-direction; 921,085 cells). For the thin 2D model, an unconstrained, spatially-correlated permeability field was specified for the basic fractured rock, using an assumed spherical variogram with sill of 1.0 and range of 91.0 m. Permeability was uniformly distributed from 10^{-16} to 10^{-14} m^2. The deformation zone permeability was set to 10^{-14} m^2 (which is 100 times lower than the granite reference case model described in Chu (2013, Table 2)). Two cases were developed for the repository permeability, one with a high permeability of 10^{-14} m^2 and one with a low permeability of 10^{-17} m^2. Figure 4-2 shows the computational grid for the thin 2D model and Figure 4-3 shows the corresponding 2D permeability field for the high-repository-permeability case.

A cutout of the computational grid for the thick 3D model, which uses a much coarser discretization, is shown in Figure 4-4. The cutout exposes the discretization around the repository region.

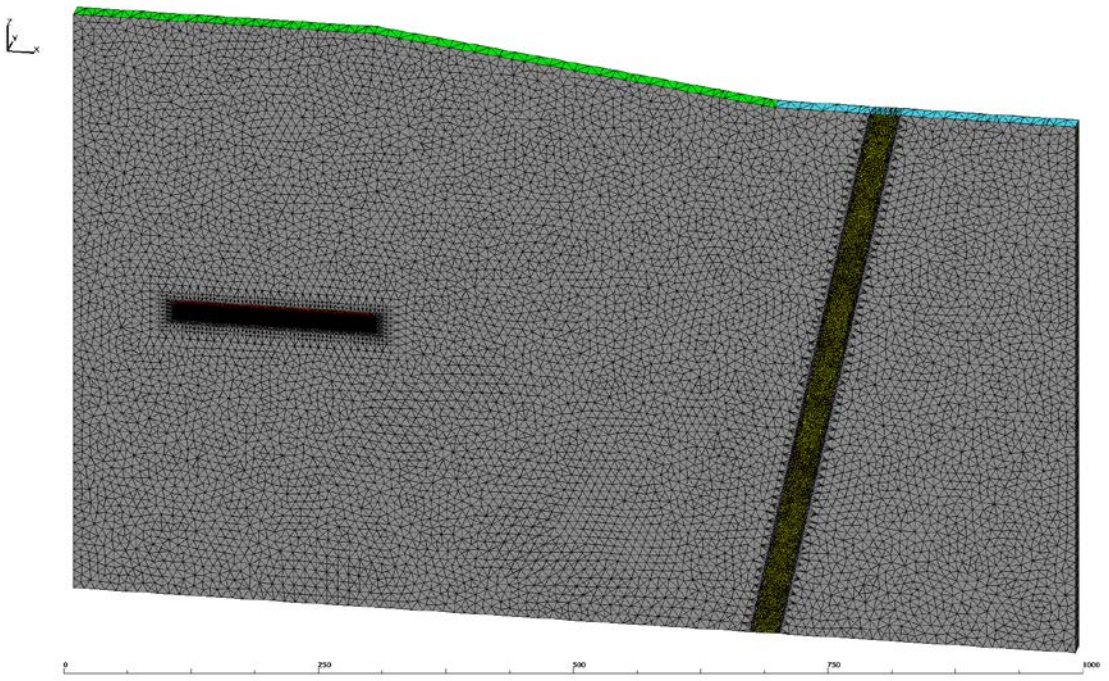

from Harp et al. 2013, Figure 2

Figure 4-2. Computational Grid for the 2D Thin Model of the Granite Repository

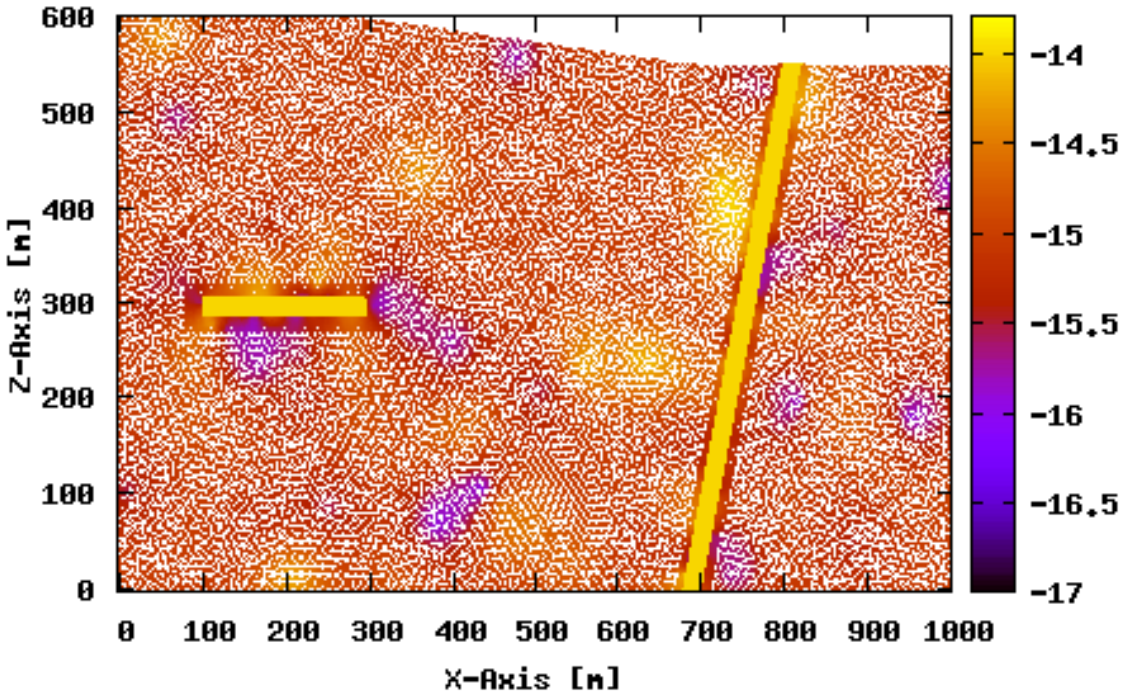

from Harp et al. 2013, Figure 3

Figure 4-3. Log Permeabilities (m^2) for the 2D Thin Model High-Repository-Permeability Case

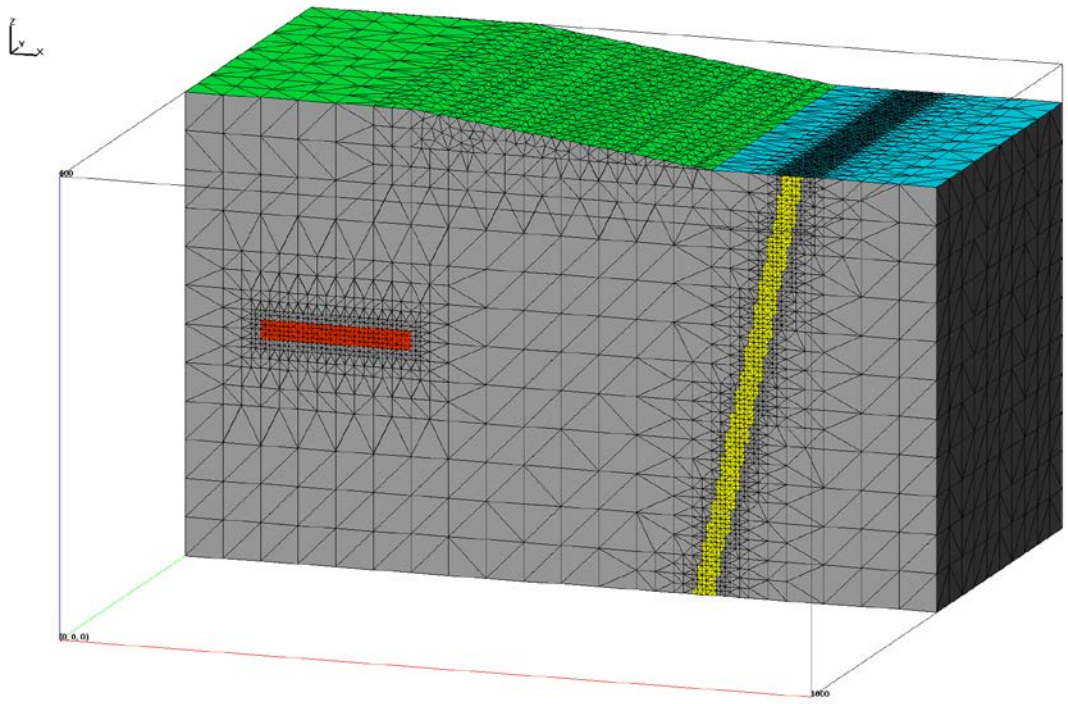

from Harp et al. 2013, Figure 5

Figure 4-4. Computational Grid for the 3D Thick Model of the Granite Repository (cut out at y=500 m)

4.2 Application of the Granite Disposal System Model

Example simulation results for the thin 2D model with high repository permeability are shown in Figures 4-5 and 4-6. Figure 4-5 shows the steady-state velocity vectors while Figure 4-6 shows the steady-state streamlines. Streamlines for the thick 3D model, with the coarser grid discretization, are shown in Figure 4-7. These results can be used as a simple comparison test for the far-field component of the PFLOTRAN-based PA model framework described in Section 2.2.1.3.

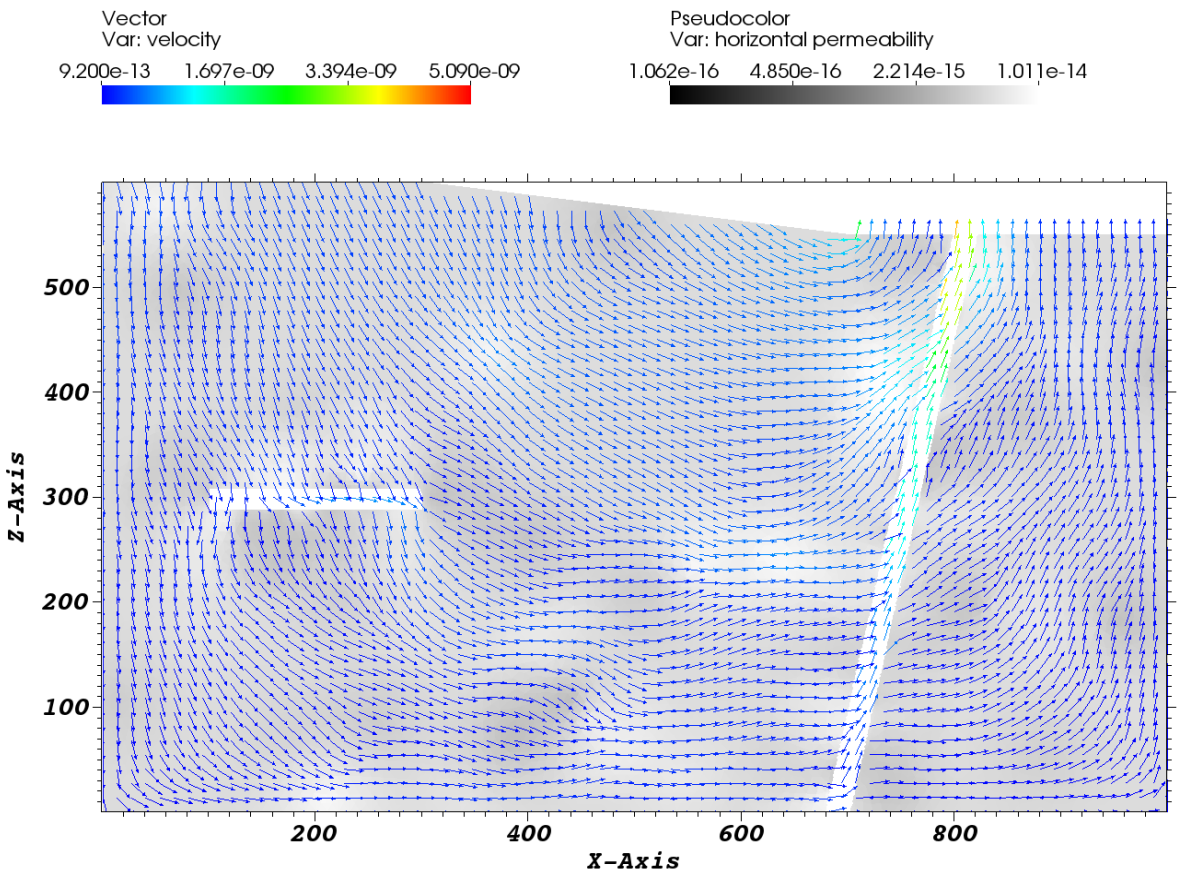

Velocity vectors (m/s) plotted over the permeability field (m^2) (from Harp et al. 2013, Figure 7A)

Figure 4-5. Velocity Vectors for the 2D Thin Model with High Repository Permeability

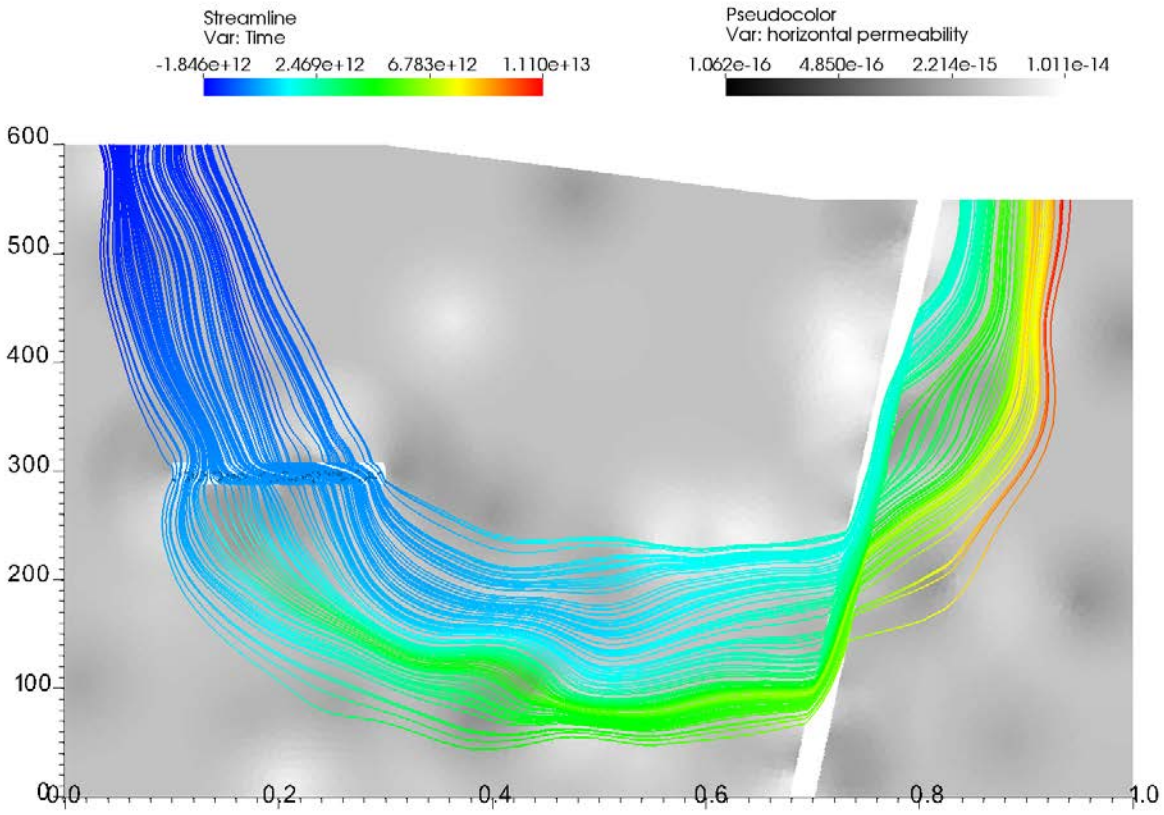

Backwards and forwards streamlines (showing seconds of travel time to or from the repository region), plotted over the permeability field (m^2) (from Harp et al. 2013, Figure 7B)

Figure 4-6. Streamlines for the 2D Thin Model with High Repository Permeability

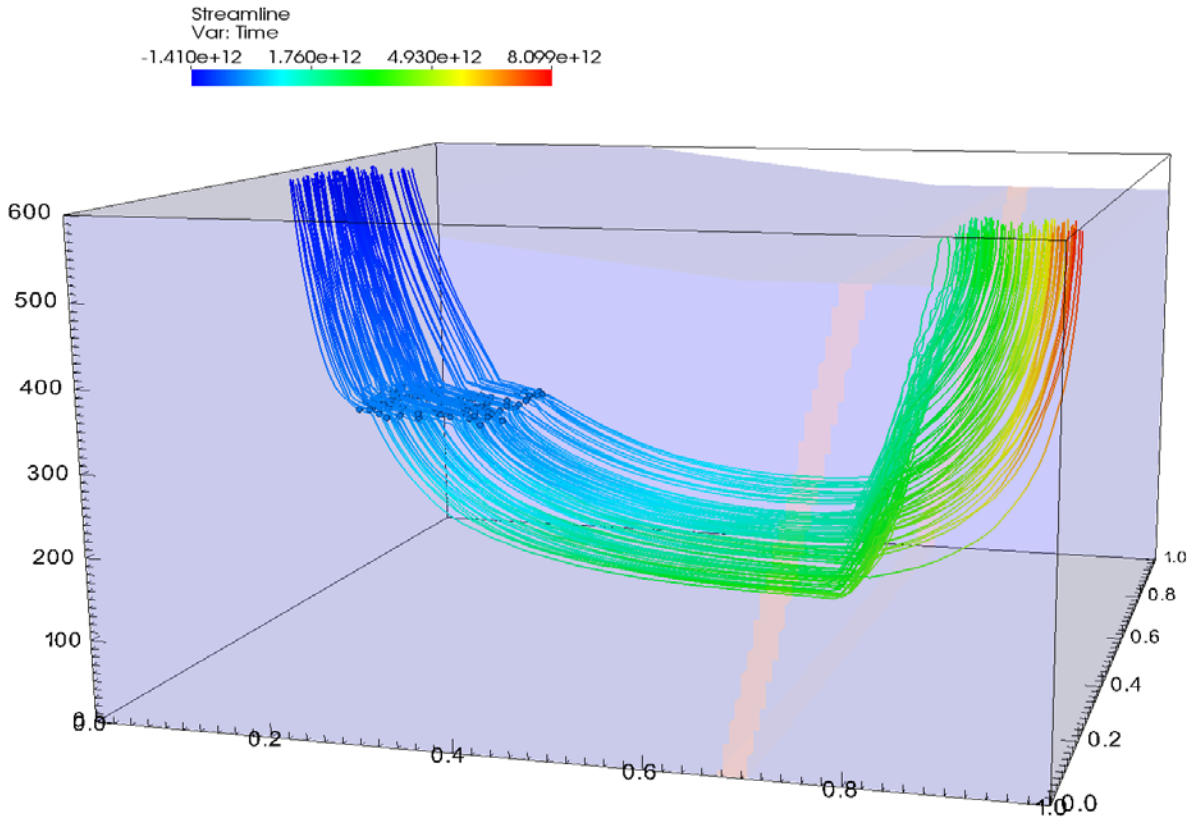

Backwards and forwards streamlines (showing seconds of travel time to or from the repository region) (from Harp et al. 2013, Figure 7B)

Figure 4-7. Streamlines for the 3D Thick Model with High Repository Permeability

5. GENERIC CLAY DISPOSAL SYSTEM MODEL

As for the generic granite repository described in Section 4, a reference case for a generic clay/shale repository has also been under development for several years (Hansen et al. 2010; Clayton et al. 2011, Section 3.3; Vaughn et al. 2013a, Section 3.3; Freeze et al. 2013c, Sections 4.2.3.2.2 and 4.2.3.3.2) and has previously been tested with an abstraction-based modeling system using GoldSim. A GoldSim-based study of large DPC-like disposal in clay has also been completed (Morris 2013).

To support the application of the enhanced PA modeling capability, the generic clay repository reference case was updated for implementation with the TOUGH2 multi-phase flow and transport code. Research included developing generic clay repository hydrogeologic parameters, investigating their effect on flow and tracer transport, and examining the effect of spatial heterogeneity on the upscaled diffusion coefficient (Bianchi et al. 2013). TOUGH2 simulations of the reference case (referred to as the base case scenario by Bianchi et al. (2013)) were conducted using a 2D representation of the repository, and a simplified unit source term. A set of ten "variant" scenarios was also simulated on the same numerical grid to investigate the influence of the DRZ properties and dimensions, as well as the effect of the vertical hydraulic gradient in the host rock (Bianchi et al. 2013, Table 3).

In FY2014, it is expected that this clay reference case can be implemented in 3D in the HPC-enhanced, PFLOTRAN-based PA modeling framework, and tested with a more realistic source term model (e.g., see Figure 2-11). The remainder of this section summarizes the clay repository reference case and flow and transport modeling described by Bianchi et al. (2013).

5.1 Generic Clay Repository Reference Case

As described by Bianchi et al. (2013), flow and transport parameters for the current version of the clay repository reference case are based on experimental data from previously published modeling studies or from published reports by national programs (i.e., the French Dossier 2005 Argile (ANDRA 2005) and the Swiss Project Opalinus Clay (Nagra 2002)). However, because of the current reference case assumes single-phase flow at fully saturated conditions, future revisions of the clay reference case may need to develop parameters related to gas flow, metal corrosion, saturation/resaturation processes, and the coupling of THM processes (Bianchi et al. 2013). Whether these new parameters will need to be explicitly included in a PA, or will instead form the basis for the initial conditions of PA simulations, depends on the outcome of future investigations.

The generic clay repository design is characterized by a vertical shaft connected to the ground surface, an operational tunnel, and a series of horizontal repository tunnels in which vitrified nuclear waste is stored. The repository tunnels are located in the middle of a deep, low permeability, clay-rich formation surrounded by two geological units, an upper and a lower formation, characterized by higher permeability and significant groundwater flow. The host rock formation is considered to be a saturated porous medium. A simplified 2D representation of the clay reference case (see Figure 5-1) includes a single horizontal tunnel, a vertical shaft, and a vertical cross section of the host rock formation. The longitudinal axis of the horizontal tunnel, which has a total length (L_T) equal to 600 m, is located at z = –50 m. The length of the model domain in the x-direction is 2,000 m, such that boundary conditions imposed at the left and right boundaries are sufficiently distant from the tunnel and the shaft. The total thickness of the host rock (t_{HR}) is 100 m, while the vertical extension of the shaft (h_S) is 50 m, from the end of horizontal tunnel to the top boundary of the host formation. In the current 2D reference case simulations, the upper and lower permeable geological units surrounding the host rock are not explicitly represented. However, these units were accounted for in the TOUGH2 simulations through boundary conditions imposed at the top and bottom boundaries of the model domain, as described in Section 5.1.1.

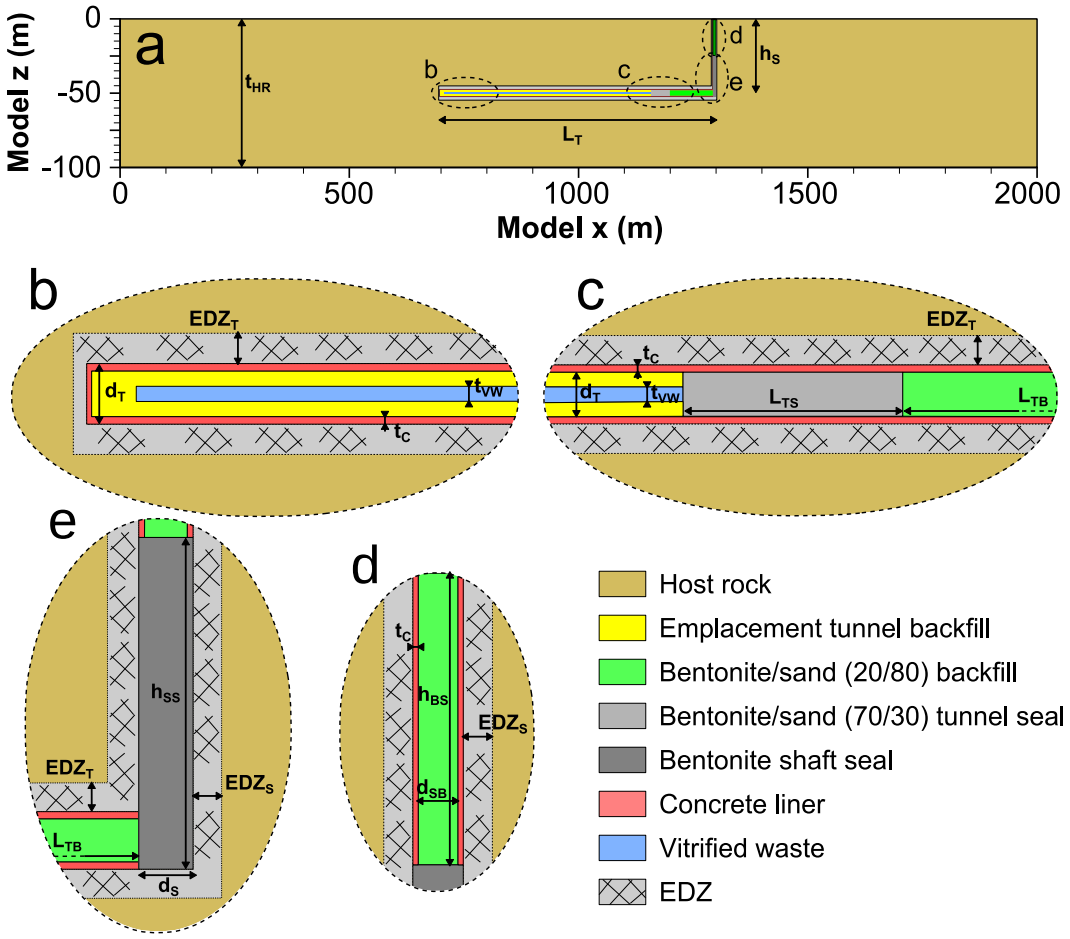

(b, c, d, and e refer to zoomed-in areas of detail of the different components. Dimensions are given in Table 5-1)

Figure 5-1. 2D Clay Repository Reference Case Domain

Figure 5-1 also shows the details of the different components of the reference case clay repository system; numerical values of their dimensions are presented in Table 5-1. The horizontal tunnel with a diameter (d_T) of 4.5 m is divided into three sections: (1) the emplacement tunnel, where vitrified waste is stored surrounded by a low-permeability backfill (Figure 5-1b), (2) an engineered barrier for sealing the emplacement tunnel (Figure 5-1c), and (3) a section filled with a backfill material different from that in the emplacement tunnel (Figure 5-1d and 5-1e). The tunnel seal has a length (L_{TS}) equal to 30 m. In the 2D conceptualization, the backfilled section of the horizontal tunnel is designed to represent a portion of the access tunnel connected with a vertical shaft. The tunnel seal and the tunnel backfill are assumed to consist of mixtures of bentonite and sand with different proportions. In particular, a 70% in volume of bentonite for the tunnel seal, and a mixture of 80% sand and 20% bentonite as tunnel backfill material, was assumed (Bianchi et al. 2013). The lower section of the shaft, which has a diameter (d_S) equal to 5.4 m, is sealed with a 30 m thick bentonite seal. The remaining section, from the top of the seal to the top of the host-rock formation, is assumed to be filled with the same bentonite/sand mixture used as backfill in the horizontal tunnel. A 0.6 m thick concrete liner is considered along the walls of this upper section of the shaft and in the horizontal tunnel. The liner is removed within the section of the shaft where the seal is emplaced. Between the undisturbed host rock and the walls of the horizontal tunnel and shaft, an EDZ is

assumed to form as a result of excavation operations (the term EDZ is used in this section rather than DRZ, consistent with the terminology in Bianchi et al. (2013)). Because experimental data show a relationship between the thickness of the EDZ and the radius of the excavations around which the EDZ had developed, two different thickness values (EDZ_T and EDZ_S in Figure 5-1) were considered, one for the EDZ around the tunnel and the other for the EDZ around the shaft.

Table 5-1. Dimension for the Clay Repository Reference Case

Dimension	Description	Value (m)
t_{HR}	Vertical thickness of the host rock formation	100
L_T	Total length of the repository in the x direction	600
h_S	Extension of the shaft between the center of the tunnel and the top of the host rock	50
d_T	Repository tunnel diameter	4.5
t_C	Thickness of the concrete liner	0.6
t_{VW}	Thickness of the vitrified waste	0.9
L_{TS}	Length of the tunnel seal	30
L_{TB}	Length of the tunnel backfill	100
h_{SS}	Height of the seal in the shaft	30
d_S	Shaft diameter	5.4
d_{SB}	Thickness of the backfill in the shaft	1.2
h_{BS}	Extension of backfill in the shaft	20.9

from Bianchi et al. (2013)

5.1.1 Initial and Boundary Conditions

For groundwater flow simulations of the clay reference case, specified head values were imposed at the top and bottom boundaries of the simulated domain, while no-flow boundary conditions were applied at the boundaries located at x = 0 m and x = 2,000 m. For the reference case and nine of the ten variant scenarios considered, the initial conditions for the transient flow simulations are represented by steady-state conditions according to the hydraulic gradient in the vertical direction. One variant scenario had initial conditions not representative of hydrostatic equilibrium, since it was intended to represent an overpressured system. The flow field at the beginning of a set of transport simulations was calculated from the flow model after a simulated time equal to 150 years. This time was chosen to represent the duration of both the construction and operational stages of the repository.

Transport simulations used a simplified source term, represented by an instantaneous release of iodine (^{129}I), and the results were analyzed in terms of relative concentrations, rather than absolute values. The ^{129}I was assumed to have no sorption (i.e., K_d = 0 ml/g) and a diffusion coefficient of 1.08×10^{-9} m^2/s (Bianchi et al. 2013).

5.1.2 Material and Flow Properties

As noted by Bianchi et al. (2013), permeability enhancement in the EDZ can result in preferential flow and transport pathways from the waste region to the biosphere. Therefore, the appropriate conceptual model and parameterization of the EDZ is one of the most important aspects of the clay reference case. Sensitivity to the EDZ conceptual model and parameterization was examined with eight of the ten variant scenarios simulated with TOUGH2. However, the reference case scenario is a dual porosity approach: "since it can provide a more realistic representation of the flow field in the fractures and microfissures." Permeability in the fracture continuum of this dual porosity model (k_f) is defined somewhat arbitrarily by relating it to an assumed permeability of an equivalent single continuum model (k_{eq}) via an arithmetic average, where f is the equivalent continuum fracture porosity (assumed to be 1% in the reference case), i.e., the fraction of total flow volume associated with fracture permeability:

$$k_{eq} = k_m(1-f) + k_f f \qquad \text{Eq. (5-1)}$$

The reference case assumes a vertical hydraulic gradient, determined by the difference in hydraulic head between the values imposed at upper and lower boundaries of the flow model, equal to 1 m/m. This value is consistent with the hydraulic conditions of the Opalinus Clay (Nagra 2002). Hydrogeological parameter values assigned to the host rock and the repository components are listed in Table 5-2. These values are based on, and similar to, those used in previously published performance assessment models of radioactive waste repositories in clay-rich formations (Bianchi et al. 2013). For example, the host-rock permeability is within the range of permeability values measured in clay-rich formations currently under investigation as potential host rock for geological disposal, such as the Callovo-Oxfordian Argillites (e.g., ANDRA 2005) and the Opalinus Clay (e.g., Nagra 2002). The thicknesses of the EDZ around the horizontal tunnel (EDZ_T in Figure 5-1) and the shaft (EDZ_S) were chosen to be equal to 1.2 times the radius of the corresponding excavation. This value is comparable with observations conducted at the Mont Terry Rock Laboratory in the Opalinus Clay (Bossart et al. 2004). As mentioned above, for the definition of the dual-porosity system in TOUGH2, the fractures were assumed to occupy 1% of the volume of the TOUGH2 mesh elements representing the EDZ. By assuming a single-continuum permeability (k_{eq}) equal to 1×10^{-18} m^2 (20 times higher than the undisturbed host rock permeability), the calculated equivalent permeability of the fracture domain using Equation 5-1 is equal to 9.505×10^{-17} m^2.

Table 5-2. Clay Repository Reference Case Input Parameters

Hydrogeological Setting			
Parameter			***Value***
Initial hydraulic gradient along the z direction			1
Hydraulic head at the top of the host rock formation			350 m
Hydraulic head at the bottom of the host rock formation			450 m
Hydrogeological Parameters			
Material	***Permeability[1] (m^2)***	***Porosity***	***Compressibility (Pa^{-1})***
Host rock formation	5×10^{-20}	0.12	9.7×10^{-10}
Emplacement tunnel backfill	1×10^{-17}	0.30	1.0×10^{-9}
Bentonite/sand (20/80) backfill	1×10^{-16}	0.30	1.0×10^{-9}
Bentonite/sand (70/30) tunnel seal	5×10^{-19}	0.30	1.0×10^{-9}
Bentonite shaft seal	1×10^{-20}	0.40	1.0×10^{-9}
Concrete liner	1×10^{-17}	0.20	6.7×10^{-10}
Vitrified waste	1×10^{-19}	0.20	5.0×10^{-10}
EDZ[2]	1×10^{-18}	0.14	9.7×10^{-10}
Dual-Porosity Parameters for the EDZ			
Parameter			***Value***
Volume fraction of fractures			0.01
Fracture permeability			9.505×10^{-17} m^2
Thickness of the EDZ			
EDZ_T: thickness of the EDZ in the tunnel ($1.2 \times 0.5\ d_T$)			2.4 m
EDZ_S: thickness of the EDZ in the shaft ($1.2 \times 0.5\ d_S$)			3.3 m

[1] Horizontal permeability. The vertical permeability is assumed 10 times lower than the horizontal permeability.
[2] Effective permeability.

from Bianchi et al. (2013)

5.2 Application of the Clay Disposal System Model

Based on the 2D simulation results with TOUGH2, Bianchi et al. (2013) made some observations regarding the importance of accurately conceptualizing the flow and diffusive transport models for the clay repository reference case, as well as the associated parameterization of the model parameters in the various simulation domains, such as the EDZ and host rock. These observations indicate the importance of uncertainty characterization both for parameters and conceptual models.

Comparisons between the flow fields generated with a single effective continuum approach versus the dual porosity approach show the influence of the conceptual model on the simulated fracture flow in the EDZ. In particular, the EDZ plays a major role in establishing an important horizontal component of groundwater flow in the horizontal tunnel in all the scenarios where it is represented by a dual-porosity system. In these scenarios, flow is convergent toward the horizontal tunnel, and the pathlines, which initially cut through the waste emplacement tunnel, tend to be parallel to the horizontal tunnel within the EDZ. On the other hand, when the EDZ is treated as a single equivalent continuum, it does not represent a preferential flow path, and flow lines go through the EDZ with little disturbance. This discrepancy between results obtained with different modeling approaches may have significant implications for the performance assessment of a geological disposal system, because the role of the EDZ as preferential flow path might be underestimated if it is simply modeled as a single continuum.

The observed behavior with the more realistic dual porosity approach is potentially unfavorable for the postclosure safety of the geological disposal system, since the main groundwater flow path near the waste zone is through the EDZ associated with tunnels and shafts, rather than through the lower permeability undisturbed host rock. Thus, the groundwater flow tends to bypass the tunnel and shaft seals in the more realistic dual porosity conceptual model, suggesting that healing of the EDZ may be important for long-term containment.

Other observations for the clay repository reference case include (Bianchi et al. 2013):

- Error propagation concepts were effectively applied to develop analytical expressions for estimating the uncertainty of the previously developed model for upscaling the diffusion coefficient (*D*) in heterogeneous clay-rich formations. These expressions allow estimating the variance in the upscaled *D* as a result of the uncertainty related to the statistics of the laboratory-scale *D* measurements (i.e., mean and variance).
- Simulations showed that radionuclide transport behavior is driven by molecular diffusion in the undisturbed host rock and mostly by advection in the EDZ for the parameter values assumed for the reference case. Transport is mostly diffusive in the engineered components of the repository, even though the advective component can be relevant in the backfilled sections of the horizontal tunnel and the shaft.
- The type of transport behavior and the importance of the advective component in the EDZ are sensitive to the type of modeling approach employed. In particular, when the fractures and the rock matrix in the EDZ are simulated with a dual-porosity approach, the velocity of radionuclide transport is on average twice as fast as when the EDZ is treated as a single continuum. On the other hand, if the EDZ permeability is assumed to heal (back to undisturbed host rock permeability), transport is dominated by molecular diffusion in almost the totality of the simulated domain.
- The ambient hydraulic gradient and the presence of overpressures in the host rock were also found important for determining the type of behavior in the simulated domain and in the EDZ. In particular, results showed that the presence of overpressured zones in the host rock, as typically observed in clay-rock formations in sedimentary basins, can significantly increase the importance of advection and consequentially transport velocity, due to locally higher hydraulic gradients, even in systems in which the regional hydraulic gradient is low.

6. SUMMARY AND CONCLUSIONS

This report describes an enhanced PA modeling and analysis capability that takes advantage of HPC environments to simulate the important THCMBR multi-physics phenomena and couplings associated with the radionuclide source term, EBS, and NBS of a geologic repository for UNF and HLW. The HPC-based enhanced PA modeling capability was demonstrated with deterministic and probabilistic analyses of a bedded salt repository reference case.

The capability demonstration includes a baseline deterministic simulation and a set of 100 probabilistic simulations for sensitivity analysis. The PFLOTRAN-based multi-physics included representations of the coupled processes of waste degradation, radionuclide mobilization, fluid flow, and radionuclide transport (advection, dispersion, diffusion, sorption, and radionuclide decay and ingrowth) through the EBS and the bedded salt formation to a groundwater sample well location in the aquifer.

The simulation results provide preliminary insights into the important multi-physics processes and couplings controlling long-term performance for the generic reference case salt repository. However, the salt repository simulations only represent a preliminary, demonstration-scale problem. Further salt PA model refinement would be prudent before drawing strong conclusions regarding the relative importance of various parameters.

The HPC environment enabled reasonable run times for the set of 100 probabilistic simulations of the coupled radionuclide source term and flow and transport equations. The application of HPC solutions to the modeling of these integrated phenomena is a significant advancement in PA modeling capability in that it allows the important multi-physics couplings to be represented directly, rather than through simplified abstractions. It also allows for complex representations of the source term, such as the 80-waste-package model fidelity in the demonstration problem.

In addition to the enhanced PA model demonstration for the salt repository, reference cases were also developed for generic granite and clay repositories. Far-field flow and transport simulations were performed for these reference cases as a preliminary demonstration of their compatibility with an enhanced PA model. Implementation of these two reference cases in the PFLOTRAN-based enhanced PA modeling framework is planned for FY2014, along with refinements to the salt repository PA model.

7. REFERENCES

Adams, B.M., M.S. Ebeida, M.S. Eldred, J.D. Jakeman, L.P. Swiler, W.J. Bohnhoff, K.R. Dalbey, J.P. Eddy, K.T. Hu, D.M. Vigil, L.E. Baumann, and P.D. Hough 2013a. *Dakota, a Multilevel Parallel Object-Oriented Framework for Design Optimization, Parameter Estimation, Uncertainty Quantification, and Sensitivity Analysis, Version 5.3.1+ User's Manual.* SAND2010-2183, Updated May 22, 2013. Sandia National Laboratories, Albuquerque, NM. (http://dakota.sandia.gov/)

Adams, B.M., M.S. Ebeida, M.S. Eldred, J.D. Jakeman, L.P. Swiler, W.J. Bohnhoff, K.R. Dalbey, J.P. Eddy, K.T. Hu, D.M. Vigil, L.E. Baumann, and P.D. Hough 2013b. *Dakota, a Multilevel Parallel Object-Oriented Framework for Design Optimization, Parameter Estimation, Uncertainty Quantification, and Sensitivity Analysis, Version 5.3.1+ Theory Manual.* SAND2011-9106, Updated May 22, 2013. Sandia National Laboratories, Albuquerque, NM. (http://dakota.sandia.gov/)

ANDRA (Agence Nationale pour la gestion des Déchets Radioactifs) 2005. *Dossier 2005 Argile: Evaluation of the Feasibility of a Geological Repository in an Argillaceous Formation*. ANDRA Report Series. ANDRA, Paris, France

Arnold. B.W., P.V. Brady, S.J. Bauer, C. Herrick, S. Pye and J. Finger 2011. *Reference Design and Operations for Deep Borehole Disposal of High-Level Radioactive Waste*. SAND2011-6749. Sandia National Laboratories, Albuquerque, NM.

Balay S., J. Brown, K. Buschelman, V. Eijkhout, W.D. Gropp, D. Kaushik, M.G. Knepley, L. Curfman McInnes, B.F. Smith and H. Zhang 2013. *PETSc Users Manual*, ANL-95/11 – Revision 3.4, Argonne National Laboratory, Argonne IL.

Bianchi, M., H.H. Liu, and J. Birkholzer 2013. *Diffusion Modeling in a Clay Repository: FY13 Report*, FCRD-UFD-2013-000228, U.S. Department of Energy, Office of Nuclear Energy, Used Fuel Disposition Campaign, Washington, DC.

Bossart P., T. Trick, P.M. Meierand, and J.C. Mayor 2004. "Structural and hydrogeological Characterization of the excavation-disturbed zone in the Opalinus Clay (Mont Terri Project, Switzerland)". *Applied Clay Science* 26, pp. 429– 448.

Brady, P.V., B.W. Arnold, G.A. Freeze, P.N. Swift, S.J. Bauer, J.L. Kanney, R.P. Rechard, and J.S. Stein 2009. *Deep Borehole Disposal of High-Level Radioactive Waste.* SAND2009-4401. Sandia National Laboratories, Albuquerque, NM.

Callahan, G.D. 1999. *Crushed Salt Constitutive Model*. SAND98-2680. Sandia National Laboratories, Albuquerque, NM.

Carter, J.T., F. Hansen, R. Kehrman, and T. Hayes 2011. *A Generic Salt Repository for Disposal of Waste from a Spent Nuclear Fuel Recycle Facility*. SRNL-RP-2011-00149 Rev. 0. Savannah River National Laboratory, Aiken, SC.

Carter, J. T., A. J. Luptak, J. Gastelum, C. Stockman, and A. Miller 2012. *Fuel Cycle Potential Waste Inventory for Disposition*. FCRD-USED-2010-000031, Rev. 5. U.S. Department of Energy, Office of Used Nuclear Fuel Disposition, Washington, DC.

Chen, X., H. Murakami, M. Hahn, G.E. Hammond, M.L. Rockhold, J.M. Zachara and Y. Rubin 2012. "Three-Dimensional Bayesian Geostatistical Aquifer Characterization at the Hanford 300 Area using Tracer Test Data", *Water Resources Research*, 48, doi:10.1029/2011WR010675.

Chen, X., G. Hammond, C. Murray, M. Rockhold, V. Vermeul and J. Zachara 2013. "Applications of Ensemble-based Data Assimilation Techniques for Aquifer Characterization using Tracer Data at Hanford 300 Area", *Water Resources Research*, 49, doi:10.1002/2012WR013285.

Chu, S. 2013. *Status Report on Reference Case for Generic Disposal System Modeling in Granite*, FCRD-UFD-2013-000235, LA-UR-13-26365, Los Alamos National Laboratory, Los Alamos, NM.

Clayton, D., G. Freeze, T. Hadgu, E. Hardin, J. Lee, J. Prouty, R. Rogers, W.M. Nutt, J. Birkholzer, H.H. Liu, L. Zheng, and S. Chu 2011. *Generic Disposal System Modeling – Fiscal Year 2011 Progress Report.* FCRD-USED-2011-000184, SAND2011-5828P. U.S. Department of Energy, Office of Nuclear Energy, Used Fuel Disposition Campaign, Washington, DC.

Clayton, D.J., J.G. Arguello Jr., E.L. Hardin, F.D. Hansen, and J.E. Bean 2012. "Thermal-Mechanical Modeling of a Generic High-Level Waste Salt Repository" in *SALTVII, 7th Conference on the Mechanical Behavior of Salt.* SAND2012-2741C. Paris, France. April 16-19, 2012. (www.saltmech7.com)

Cook, P. and A.L. Herczeg 2000. *Environmental Tracers in Subsurface Hydrology*, Kluwer Academic Publishers, Norwell, MA.

DOE (U.S. Department of Energy) 1987. *Site Characterization Plan Conceptual Design Report for a High-Level Nuclear Waste Repository in Salt, Horizontal Emplacement Mode.* DOE/CH/46656-14 (2 volumes). U.S. Department of Energy, Washington, DC.

DOE (U.S. Department of Energy). 1996. *Title 40 CFR Part 191 Compliance Certification Application for the Waste Isolation Pilot Plant.* DOE/CAO-1996-2184 (21 volumes). U.S. Department of Energy, Carlsbad Area Office, Carlsbad, NM. (http://www.wipp.energy.gov/library/CRA/BaselineTool/Documents/Appendices/SEAL%20A.PDF)

DOE (U.S. Department of Energy) 2008. *Yucca Mountain Repository License Application Safety Analysis Report.* DOE/RW-0573, Revision 1. U.S. Department of Energy, Washington, DC. (http://www.nrc.gov/waste/hlw-disposal/yucca-lic-app/yucca-lic-app-safety-report.html#1)

DOE (U.S. Department of Energy) 2009. *Title 40 CFR Part 191 Subparts B and C Compliance Recertification Application for the Waste Isolation Pilot Plant*. DOE/WIPP 09-3424. U.S. Department of Energy, Carlsbad Area Office, Carlsbad, NM.

DOE (U.S. Department of Energ) 2012a. *Fuel Cycle Technologies Quality Assurance Program Document, Revision 2*. Effective Date 12/20/2012. U.S. Department of Energy, Office of Nuclear Energy, Fuel Cycle Technologies, Washington, DC.

DOE (U.S. Department of Energy) 2012b. *Waste Isolation Pilot Plant Geotechnical Analysis Report, Volumes 1 and 2*. July 2010 – June 2011. DOE/WIPP-12-3484. U.S. Department of Energy

Fox, B. 2008. *Parameter Summary Report for CRA-2009, Revision 0,* WIPP:1.2.5:PA:QA-L:547488, Sandia National Laboratories, Carlsbad, NM.

Freeze, R.A. and J.A. Cherry 1979. *Groundwater*, Prentice-Hall, Englewood Cliffs, NJ.

Freeze, G., P. Mariner, J.A. Blink, F.A. Caporuscio, J.E. Houseworth, and J.C. Cunnane 2011. *Disposal System Features, Events, and Processes (FEPs): FY11 Progress Report.* FCRD-USED-2011-000254. SAND2011-6059P. Sandia National Laboratories, Albuquerque, NM.

Freeze, G. and P. Vaughn 2012. *Development of an Advanced Performance Assessment Modeling Capability for Geologic Disposal of Nuclear Waste: Methodology and Requirements.* SAND2012-10208. Sandia National Laboratories, Albuquerque, NM.

Freeze, G., P. Gardner, P. Vaughn, S.D. Sevougian, P. Mariner, and V. Mousseau 2013a. *Performance Assessment Modeling of a Generic Salt Disposal System: Annotated Outline.* FCRD-UFD-2013-000219. SAND2013-6183P. Sandia National Laboratories, Albuquerque, NM.

Freeze, G., P. Gardner, P. Vaughn, S.D. Sevougian, P. Mariner, and V. Mousseau 2013b. *Evaluation of Advanced Performance Assessment Modeling Frameworks: Annotated Outline.* FCRD-UFD-2013-000218. SAND2013-6913P. Sandia National Laboratories, Albuquerque, NM.

Freeze, G., M. Voegele, P. Vaughn, J. Prouty, W.M. Nutt, E. Hardin, and S.D. Sevougian 2013c. *Generic Deep Geologic Disposal Safety Case.* FCRD-UFD-2012-000146 Rev. 1, SAND2013-0974P. Sandia National Laboratories, Albuquerque, NM.

Freeze, G., S.D. Sevougian, and M. Gross 2013d. *Safety Framework for Disposal of Heat-Generating Waste in Salt: Features, Events, and Processes (FEPs) Classification.* FCRD-UFD-2013-000191. SAND2013-5220P. Sandia National Laboratories, Albuquerque, NM.

Hammond, G., P. Lichtner, and C. Lu 2007. "Subsurface multiphase flow and multicomponent reactive transport modeling using high performance computing", in *Journal of Physics: Conference Series 78*, pp. 1-10.

Hammond, G.E., P.C. Lichtner, R.T. Mills, and C. Lu 2008. "Toward petascale computing in geosciences: application to the Hanford 300 Area", in *Journal of Physics Conference Series*, 125, 012051 doi:10.1088/1742-6596/125/1/012051.

Hammond, G.E. and P.C. Lichtner 2010. "Field-Scale Modeling for the Natural Attenuation of Uranium at the Hanford 300 Area using High Performance Computing", *Water Resources Research*, 46, W09527, doi:10.1029/2009WR008819.

Hammond, G.E., P.C. Lichtner, C. Lu, and R.T. Mills. 2011a. "PFLOTRAN: Reactive Flow and Transport Code for Use on Laptops to Leadership-Class Supercomputers", in F. Zhang, G.T. Yeh, and J. Parker (ed.) *Groundwater Reactive Transport Models*, Bentham Science Publishers.

Hammond, G.E., P.C. Lichtner and M.L. Rockhold 2011b. "Stochastic Simulation of Uranium Migration at the Hanford 300 Area", *Journal of Contaminant Hydrology*, v120-121, pp. 115-128, doi:10.1016/j.jconhyd.2010.04.005.

Hansen, F.D., E. L. Hardin, R.P. Rechard, G. A. Freeze, D.C. Sassani, P.V. Brady, C.M. Stone, M.J. Martinez, J.F. Holland, T. Dewers, K.N. Gaither, S.R. Sobolik, and R.T. Cygan 2010. *Shale Disposal of U.S. High-Level Radioactive Waste.* SAND2010-2843, Sandia National Laboratories, Albuquerque, NM.

Hansen, F. D. and C .D. Leigh 2011. *Salt Disposal of Heat-Generating Nuclear Waste.* SAND2011-0161, Sandia National Laboratories, Albuquerque, NM.

Hansen F. D., S. J. Bauer, S. T. Broome, and G. D. Callahan 2012. *Coupled Thermal-Hydrological-Mechanical Processes in Salt: Hot Granular Salt Consolidation, Constitutive Model and Micromechanics.* FCRD-USED-2012-000422, SAND2012-9893P. Sandia National Laboratories, Albuquerque, NM.

Hardin, E., T. Hadgu, D. Clayton, R. Howard, H. Greenberg, J. Blink, M. Sharma, M. Sutton, J. Carter, M. Dupont, and P. Rodwell 2012. *Repository Reference Disposal Concepts and Thermal Load Management Analysis.* FCRD-UFD-2012-000219 Rev. 2. U.S. Department of Energy, Office of Used Nuclear Fuel Disposition, Washington, DC.

Hardin, E. L., D. J. Clayton, R. L. Howard, J. M. Scaglione, E. Pierce, K. Banerjee, M. D. Voegele, H. R. Greenberg, J. Wen, T. A. Buscheck, J. T. Carter, T. Severynse, and W. M. Nutt 2013. *Preliminary Report on Dual-Purpose Canister Disposal Alternatives (FY13).* FCRD-UFD-2013-000171 Rev. 0, U.S. Department of Energy, Office of Used Nuclear Fuel Disposition, Washington, DC.

Harp, D., S. Chu, T. A. Miller, and S. Painter 2013. *Generic Disposal System Modeling Using Amanzi: Generic Granite Repository Example.* LA-UR-13-26043. Los Alamos National Laboratory, Los Alamos, NM.

Hart, D.B., R.L. Beauheim, and S.A. McKenna 2009. *Analysis Report for Task 7 of AP-114: Calibration of Culebra Transmissivity Fields*. WIPP:1.4.1.1:TD:QA-L:RECERT:541153, Sandia National Laboratories, Carlsbad, NM.

Heroux, M., R. Bartlett, V. Howle, R. Hoekstra, J. Hu, T. Kolda, R. Lehoucq, K. Long, R. Pawlowski, E. Phipps, A. Salinger, H. Thornquist, R. Tuminaro, J. Willenbring, and A. Williams 2003. *An Overview of Trilinos.* SAND2003-2927, Sandia National Laboratories, Albuquerque, NM.

Hooper, R., R. Schmidt, R., and K. Belcourt 2012. "LIME: Software for Robust & Flexible Multiphysics Coupling", SAND2012-5628C, presented at *2012 SIAM Annual Meeting CP14: Simulation*, Minneapolis, MN, July 2012.

IAEA (International Atomic Energy Agency) 2003. *Reference Biospheres for Ssolid Radioactive Waste Disposal*. IAEA-BIOMASS-6. International Atomic Energy Agency, Vienna, Austria.

IAEA (International Atomic Energy Agency) 2007. *IAEA Safety Glossary: Terminology Used in Nuclear Safety and Radiation Protection, 2007 Edition*. STI/PUB/1290. International Atomic Energy Agency, Vienna, Austria.

James S. and J. Stein 2002. *Analysis Plan for the Development of a Simplified Shaft Seal Model for the WIPP Performance Assessment*, AP-094 Rev. 0, December 11, 2002. Sandia National Laboratories, Carlsbad NM.

Jove-Colon C.F., J.A. Greathouse, S. Teich-McGoldrick, R.T. Cygan, T. Hadgu, J.E. Bean, M.J. Martinez, P.L. Hopkins, J.G. Argüello, F.D. Hansen, F.A. Caporuscio, M. Cheshire, S.S. Levy, M.K. McCarney, H.R. Greenberg, T.J. Wolery, M. Sutton, J. Rutqvist, C.I. Steefel, J. Birkholzer, H.H. Liu, J.A. Davis, R. Tinnacher, I. Bourg, M. Holmboe, and J. Galindez 2012. *Evolution of Generic EBS Design Concepts and Process Models: Implications to EBS Design Optimization,* FCRD-USED-2012-000140, SAND2012-5083P. Sandia National Laboratories, Albuquerque, NM.

Lichtner, P.C. and G.E. Hammond 2012a. *Quick Reference Guide: PFLOTRAN 2.0 (LA-CC-09-047) Multiphase-Multicomponent-Multiscale Massively Parallel Reactive Transport Code*. DRAFT LA-UR-06-7048. December 8, 2012. Los Alamos National Laboratory, Los Alamos, NM.

Lichtner, P.C. and G.E. Hammond 2012b. "Using High Performance Computing to Understand Roles of Labile and Nonlabile U(VI) on Hanford 300 Area Plume Longevity", *Vadose Zone Journal*, v11, n2, doi:10.2136/vzj2011.0097.

Lide, D.R., ed. 1999. *CRC Handbook of Chemistry and Physics*, CRC Press, Boca Raton, FL.

LLNL (Lawrence Livermore National Laboratory) 2005. *VisIt User's Manual, Version 1.5, October 2005.* UCRL-SM-220449. Lawrence Livermore National Laboratory, Livermore, CA. (www.visitusers.org)

Lu, C. and P.C. Lichtner 2007. "High resolution numerical investigation on the effect of convective instability on long term CO2 storage in saline aquifers", *Journal of Physics Conference Series*, 78, doi:10.1088/1742-6596/78/1/012042.

Mariner, P. E., J. Lee, E. L. Hardin, F. D. Hansen, G. A. Freeze, A. S. Lord, B. Goldstein, and R. H. Price 2011. *Granite Disposal of U.S. High-Level Radioactive Waste.* SAND2011-6203, Sandia National Laboratories, Albuquerque, NM.

Meacham, P.G., D.R. Anderson, E.J. Bonano, and M.G. Marietta 2011. *Sandia National Laboratories Performance Assessment Methodology for Long-Term Environmental Programs: The History of Nuclear Waste Management.* SAND2011-8270, Sandia National Laboratories, Albuquerque, NM.

Mills, R., C. Lu, P.C. Lichtner, and G. Hammond 2007. Simulating Subsurface Flow and Transport on Ultrascale Computers using PFLOTRAN, *Journal of Physics Conference Series*, 78, 012051 doi:10.1088/1742-6596/78/1/012051.

Morris, E. 2013. *Clay Generic Disposal System Model – Sensitivity Analysis for 32 PWR Assembly Canisters.* FCRD-UFD-2013-000390. U.S. Department of Energy, Office of Used Nuclear Fuel Disposition, Washington, DC.

Munson, D.E., A.F. Fossum, and P.E. Senseny 1989. *Advances in Resolution of Discrepancies between Predicted and Measured WIPP In-situ Room Closures*, SAND88-2948. Sandia National Laboratories, Albuquerque, NM.

Nagra (Nationale Genossenschaft für die Lagerung Radioaktiver Abfälle) 2002. *Project Opalinus Clay: Safety Report. Demonstration of Disposal Feasibility for Spent Fuel, Vitrified High-Level Waste and Long-Lived Intermediate Level Waste (Entsorgungsnachweis).* Nagra Technical Report NTB 02-05, Wettingen, Switzerland.

National Academy of Sciences 1957. *The Disposal of Radioactive Waste on Land: Report of the Committee on Waste Disposal of the Division of Earth Sciences*. Publication 519. National Research Council, National Academy of Sciences.

Navarre-Sitchler, A., R.M. Maxwell, E.R. Siirila, G.E. Hammond and P.C. Lichtner 2013. "Elucidating geochemical response of shallow heterogeneous aquifers to CO_2 leakage using high-performance computing: implications for monitoring CO_2 sequestration", *Advances in Water Resources*, v53, pp. 45-55, doi:10.1016/j.advwatres.2012.10.005.

NEA (Nuclear Energy Agency) 2012. *Methods for Safety Assessment of Geological Disposal Facilities for Radioactive Waste: Outcomes of the NEA MeSA Initiative.* NEA No. 6923. Organisation for Economic Co-operation and Development, Nuclear Energy Agency.

NRC (U.S. Nuclear Regulatory Commission) 1999. *Regulatory Perspectives on Model Validation in High-Level Radioactive Waste Management Programs: A Joint NRC/SKI White Paper*. NUREG-1636. U.S. Nuclear Regulatory Commission, Washington, DC.

NRC (U.S. Nuclear Regulatory Commission) 2003. *Yucca Mountain Review Plan*. NUREG-1804, Revision 2. Office of Nuclear Material and Safeguards, Washington, DC.

NWTRB (U.S. Nuclear Waste Technical Review Board) 2011. *Technical Advancements and Issues Associated with the Permanent Disposal of High Activity Wastes, Lessons Learned from Yucca Mountain and Other Programs*. June 2011.

Poulsen, B. A. 2010. "Coal pillar load calculation by pressure arch theory and near field extraction ratio", in *International Journal of Rock Mechanics & Mining Sciences*, Vol. 47 (2010) pp. 1158–1165, (www.elsevier.com/locate/ijrmms)

Schmidt, R., N. Belcourt, R. Hooper, and R. Pawlowski 2011. *An Introduction to LIME 1.0 and its Use in Coupling Codes for Multiphysics Simulations.* SAND2011-8524. Sandia National Laboratories, Albuquerque, NM.

Sevougian, S.D., G.A. Freeze, M.B. Gross, J. Lee, C.D. Leigh, P. Mariner, R.J. MacKinnon, and P. Vaughn 2012. *TSPA Model Development and Sensitivity Analysis of Processes Affecting Performance of a Salt Repository for Disposal of Heat-Generating Nuclear Waste*. FCRD-UFD-2012-000320 Rev. 0, U.S. Department of Energy, Office of Used Nuclear Fuel Disposition, Washington, DC.

Sevougian, S.D., G.A. Freeze, P. Vaughn, P. Mariner, and W.P. Gardner 2013. *Update to the Salt R&D Reference Case*. FCRD-UFD-2013-000368, SAND2013-8255P. Sandia National Laboratories, Albuquerque, NM.

SKB (Svensk Kärnbränslehantering AB) 2010. *Data Report for the Safety Assessment SR-Site*. Technical Report TR-10-52. Swedish Nuclear Fuel and Waste Management Co., Stockholm, Sweden.

SNL (Sandia National Laboratories) 1996. *Waste Isolation Pilot Plant Shaft Sealing System Compliance Submittal Design Report*. SAND96-1326/1. Sandia National Laboratories, Albuquerque, NM.

SNL (Sandia National Laboratories) 2007. *Radionuclide Screening*. ANL-WIS-MD-000006 REV 02, U.S. Department of Energy, Office of Civilian Radioactive Waste Management, Las Vegas, Nevada.

SNL (Sandia National Laboratories) 2013. *Cubit 14.0 User Documentation.* Sandia National Laboratories, Albuquerque, NM. (https://cubit.sandia.gov)

Vaughn, P., G. Freeze, J. Lee, S. Chu, K.D. Huff, W.M. Nutt, T. Hadgu, R. Rogers, J. Prouty, E. Hardin, B. Arnold, E. Kalinina, W.P. Gardner, M. Bianchi, H.H. Liu, and J. Birkholzer 2013a. *Generic Disposal System Model: Architecture, Implementation, and Demonstration.* FCRD-UFD-2012-000430 Rev. 1, SAND2013-1539P. Sandia National Laboratories, Albuquerque, NM.

Vaughn, P., S. D. Sevougian, E. L. Hardin, P. Mariner, and M. B. Gross. 2013b. "Reference Case For Generic Disposal of HLW and SNF in Salt," in *Proceedings of the 2013 International High-Level Radioactive Waste Management Conference*, Albuquerque, NM, April 28 – May 2, 2013, American Nuclear Society, La Grange Park, IL. (www.ans.org)

Wang Y. 2011. *Integration Plan for Used Fuel Disposition (UFD) Data Management.* FCRD-USED-2011-000386. Sandia National Laboratories, Albuquerque, NM.

Wilson, T. P. and D. T. Long 1993. "Geochemistry and isotope chemistry of Michigan Basin brines: Devonian formations," *Applied Geochemistry,* Vol. 8, pp. 81-100.

Zipf K.R. 2001. "Towards pillar design to prevent collapse of room-and-pillar mines," in *Proceedings of the 108th Annual Exhibition Meeting, Soc. Min. Metall. Explor.*
(http://www.cdc.gov/niosh/mining/ UserFiles/works/pdfs/tpdtp.pdf)